AP1000 TECHNICAL REPORT REVIEW

Response to Request For Additional Information (RAI)

RAI Response Number: RAI-SRP3.7.1-SEB1-11
Revision: 4

Question:

The staff requests that Westinghouse provide additional figures in Section 5.2 TR-115, to include all location/direction combinations presented in the Section 5.1 figures, and to provide a cross-reference between the corresponding 5.1 and 5.2 figures.

Additional Request (Revision 2):

More data, i.e., HRHF response spectra for 5 locations on the basemat (4 locations at 4 corner and center) comparison of coherent at 5 nodes, 25 samples of incoherent and average of 25 incoherent response spectra.

Additional Request (Revision 3):

A. Westinghouse will revise analysis to correct boundary conditions of rigid beams to solid elements in the NI20 SASSI model.
B. Westinghouse will evaluate the need of modifying the transition shell to brick interface.
C. Review interpolation function for NI20 SASSI model.
D. Reanalysis of seismic response will correct/clarify values and results will be re-issued as a new revision to RAI-SRP3.7.1-SEB1-11.

Additional Request (Revision 4)

Westinghouse is requested to update figures provided as part of previous revisions that are changed as a result of the revised responses.

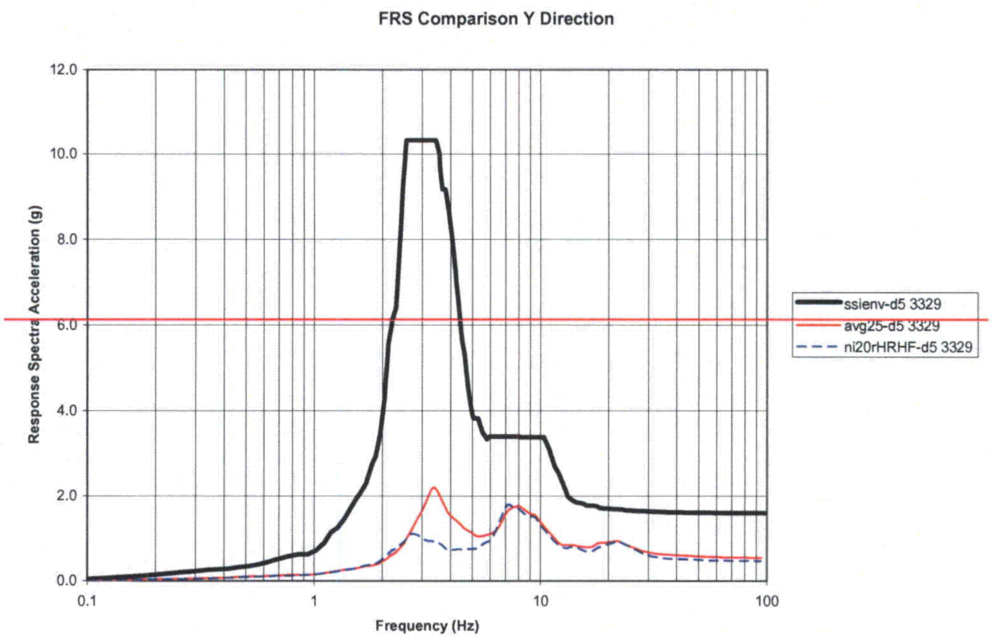

~~RAI-SRP3.7.1-SEB1-11-21: SCV Near Polar Crane Y-Dir~~

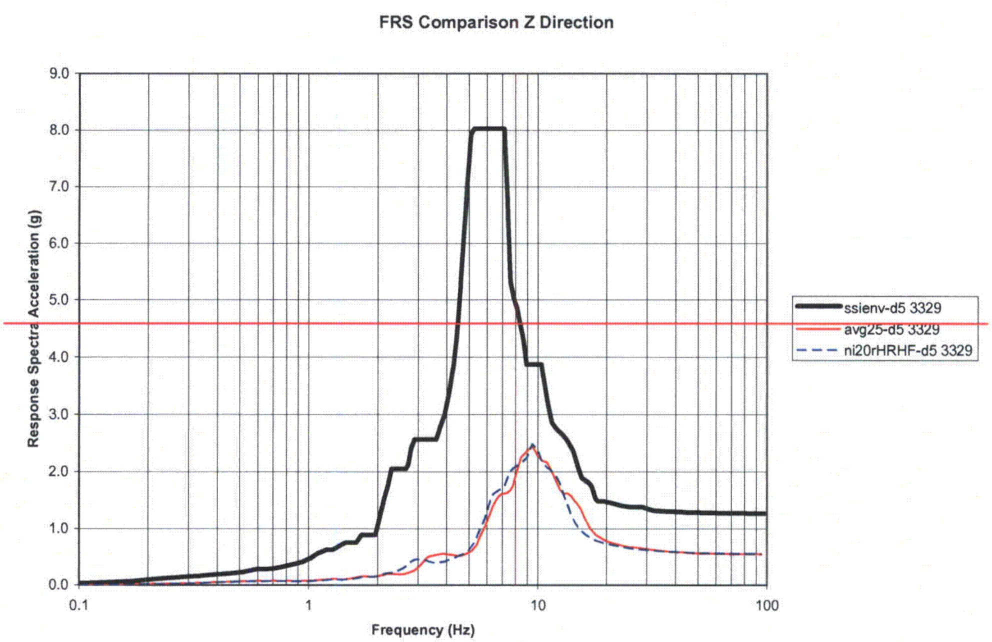

~~RAI-SRP3.7.1-SEB1-11-22: SCV Near Polar Crane Z-Dir~~

Westinghouse Response ~~(Revision 2)~~:

The figures provided in Section 5.1 are for comparison of NI10 and NI20 models. The time histories are different from that used in the HRHF evaluation documented in TR-115 as discussed in the Westinghouse response to RAI-SRP3.7.1-SEB01-07. No reduction for incoherency was considered. A representative group of HRHF floor response spectra were developed at locations considered susceptible to the high frequency response for comparison to the CSDRS floor response spectra. Some of these locations are the same or close to those given in Section 5.1. It would not be useful to add additional figures in Section 5.2 since the locations chosen are considered sufficient for comparison. A cross-reference between corresponding 5.1 and 5.2 figures cannot be given since different time histories are used.

In response to the NRC's request to supplement Section 5.2 in the TR-115 during May 19-23, 2008, Westinghouse has provided incoherent and coherent comparison response spectrum for the nodal locations presented in TR-115 Section 5.1. These spectra are presented below in Figure RAI-SRP3.7.1-SEB1-11-1 to RAI-SRP3.7.1-SEB1-11-9 (5% damping).

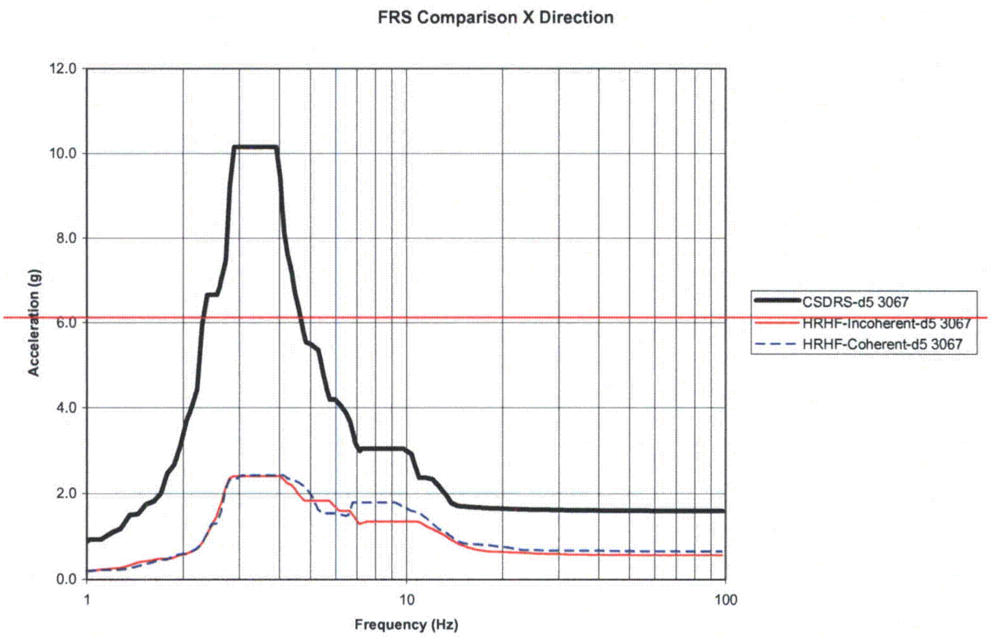

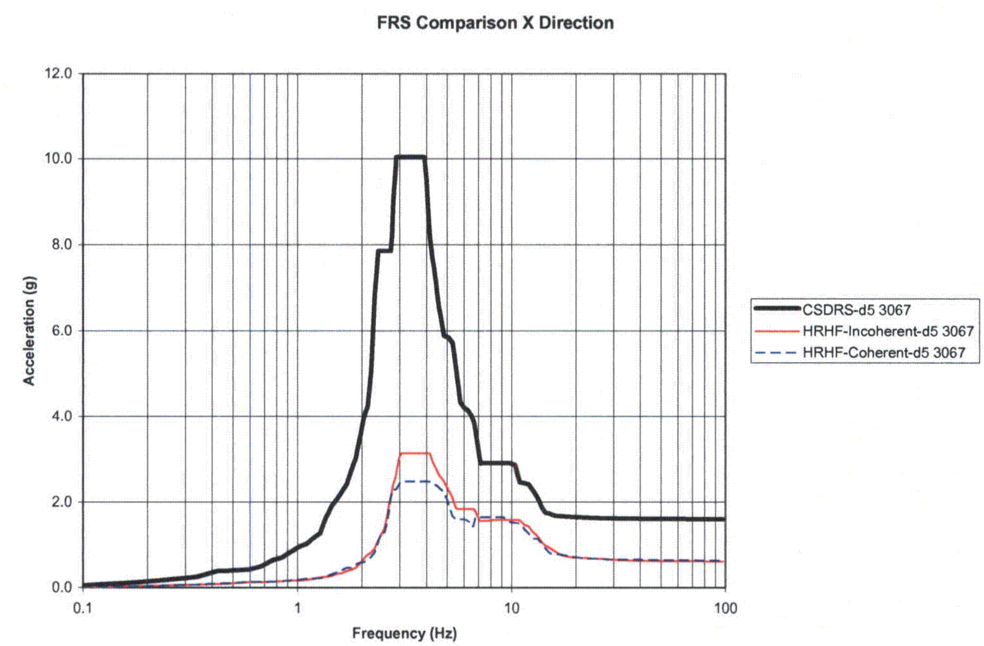

RAI-SRP3.7.1-SEB1-11-1: Seismic Response Spectra on roof of Shield Building X-Direction

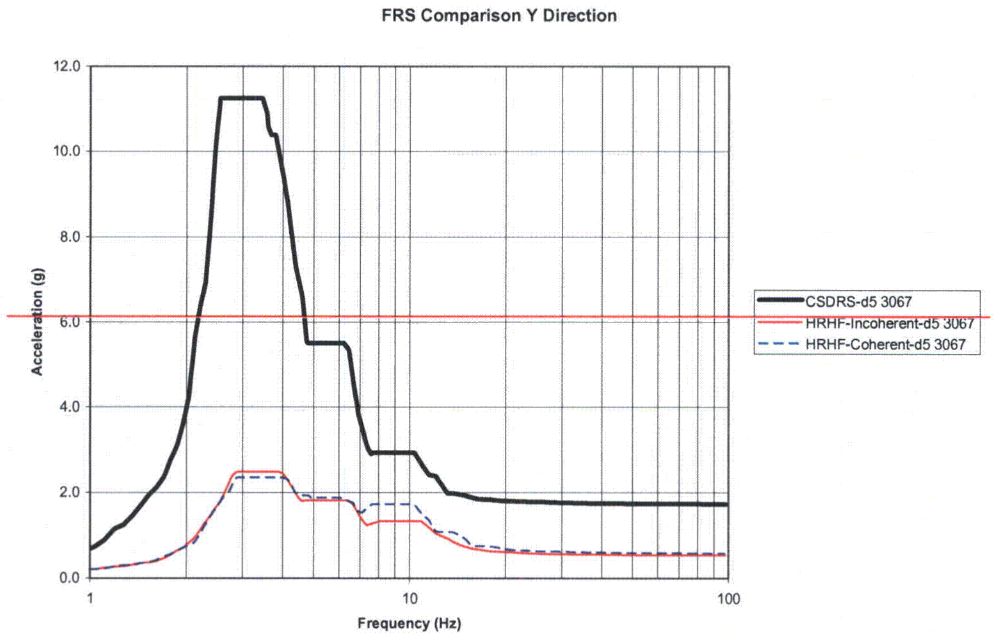

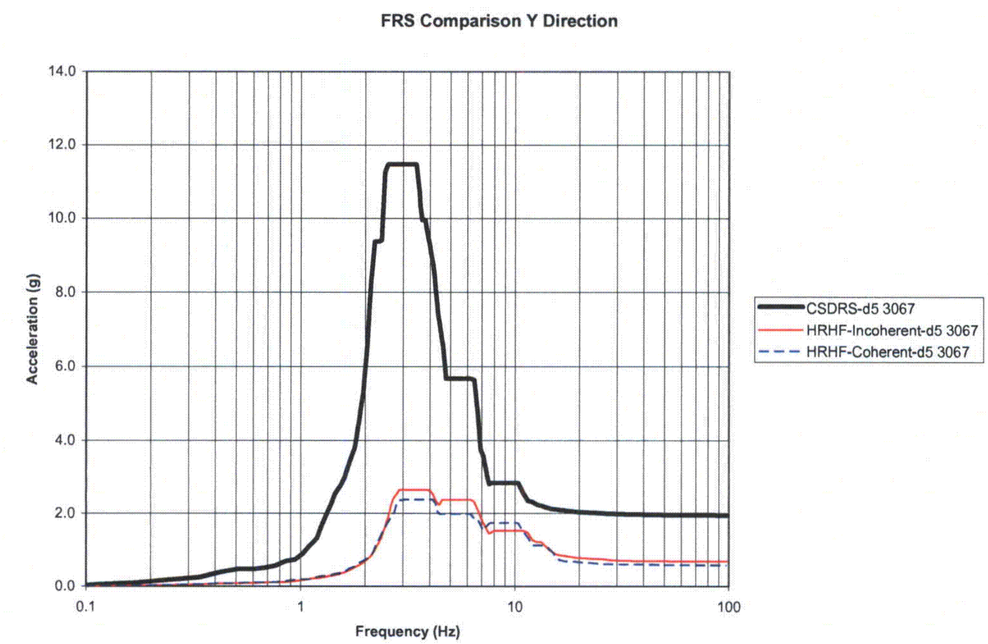

RAI-SRP3.7.1-SEB1-11-2: Seismic Response Spectra on roof of Shield Building Y-Direction

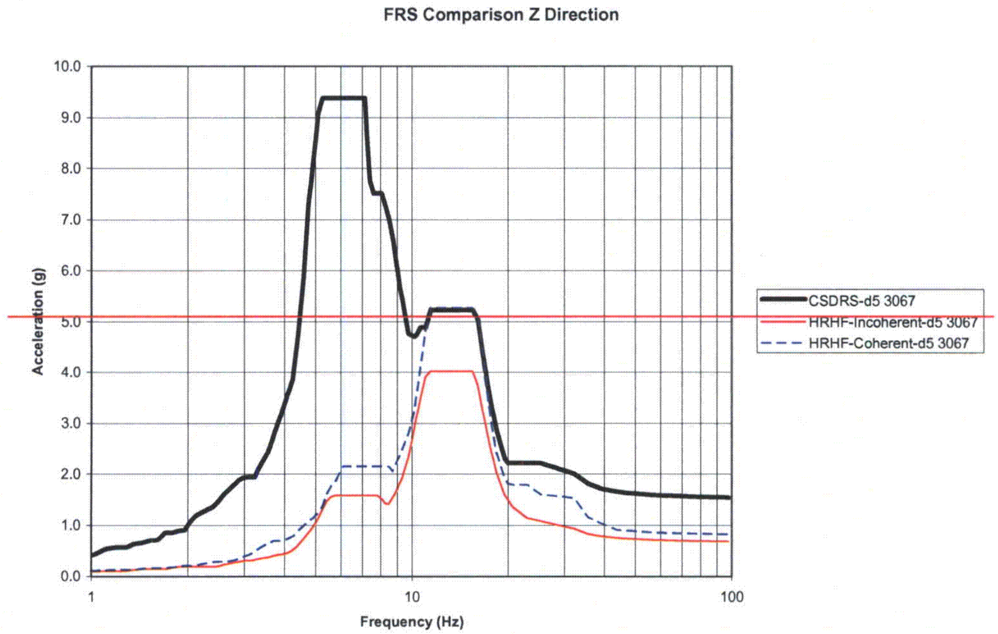

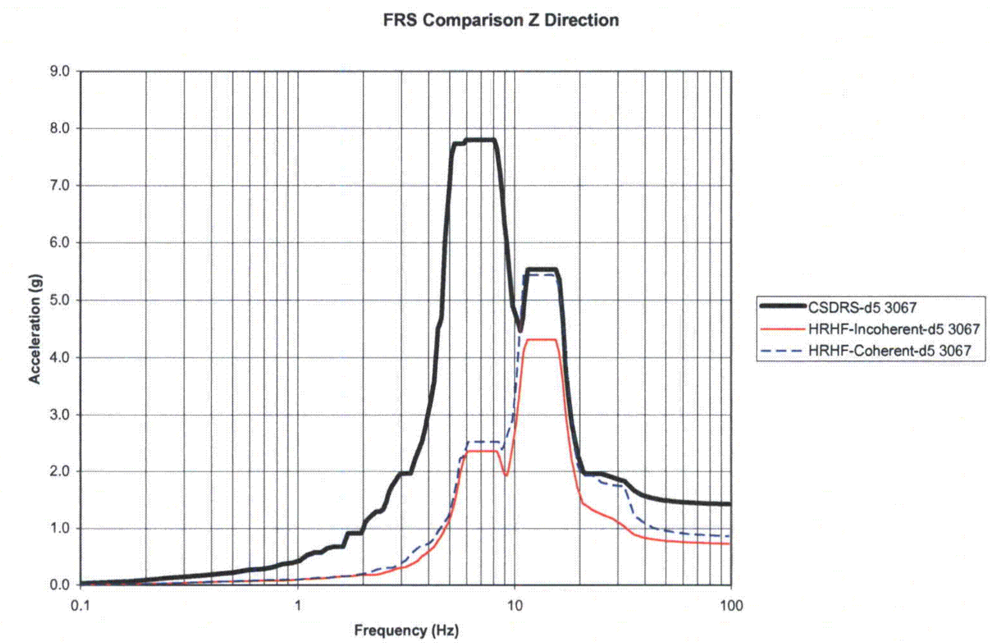

RAI-SRP3.7.1-SEB1-11-3: Seismic Response Spectra on roof of Shield Building Z-Direction

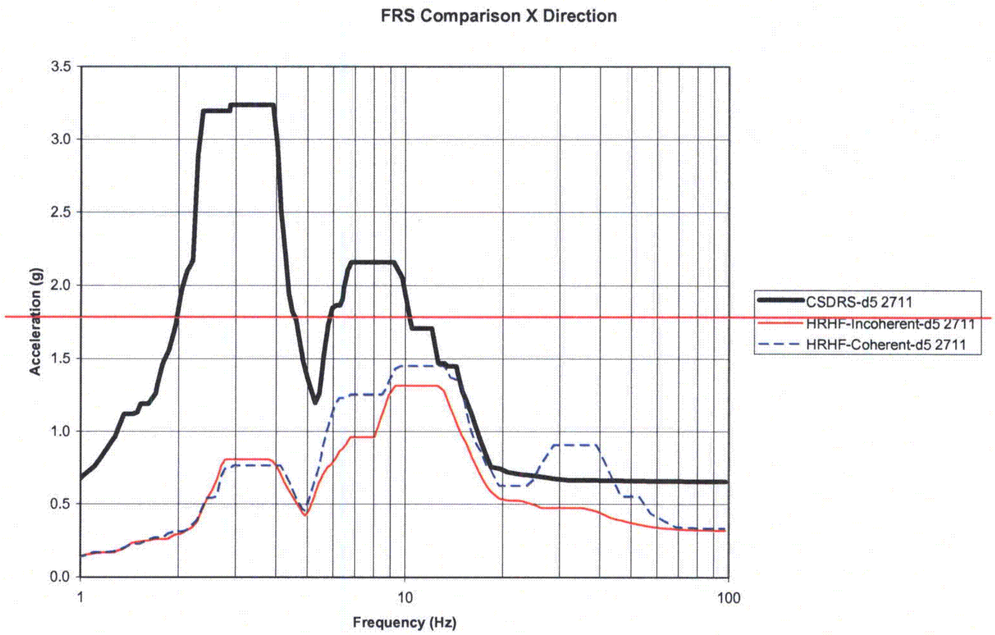

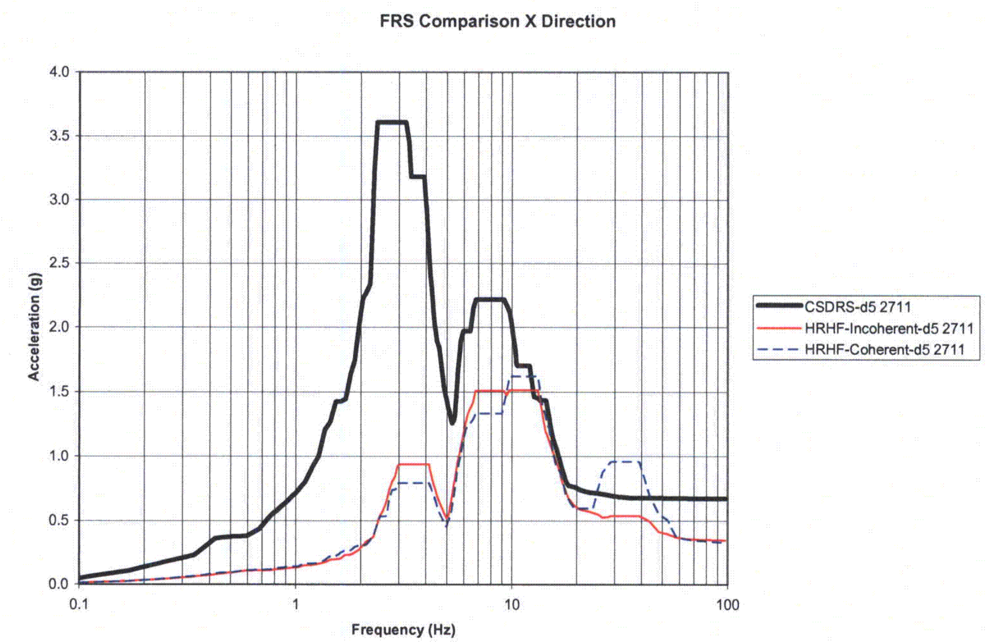

RAI-SRP3.7.1-SEB1-11-4: Seismic Response Spectra for West Side of Shield Building X-Direction

FRS Comparison Y Direction

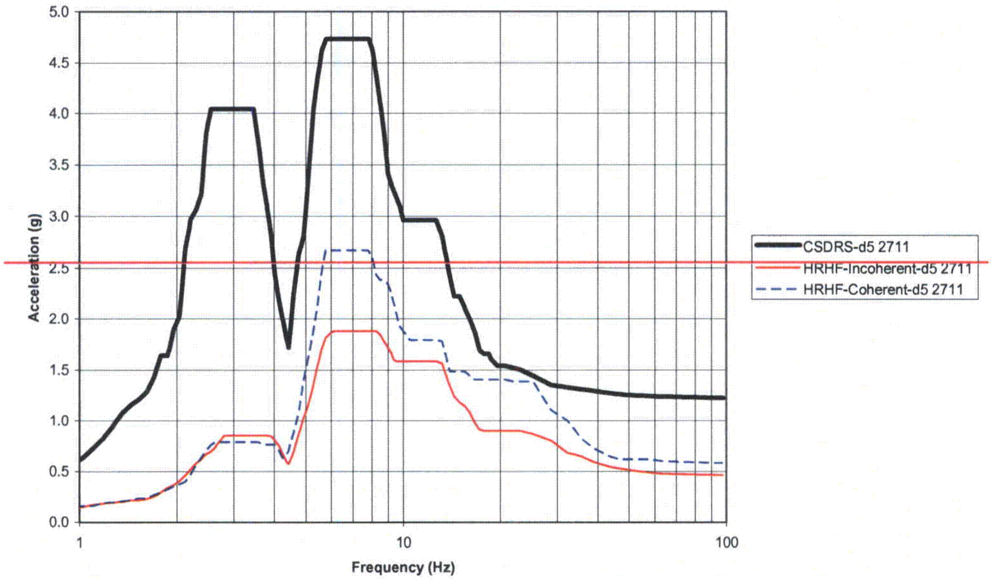

FRS Comparison Y Direction

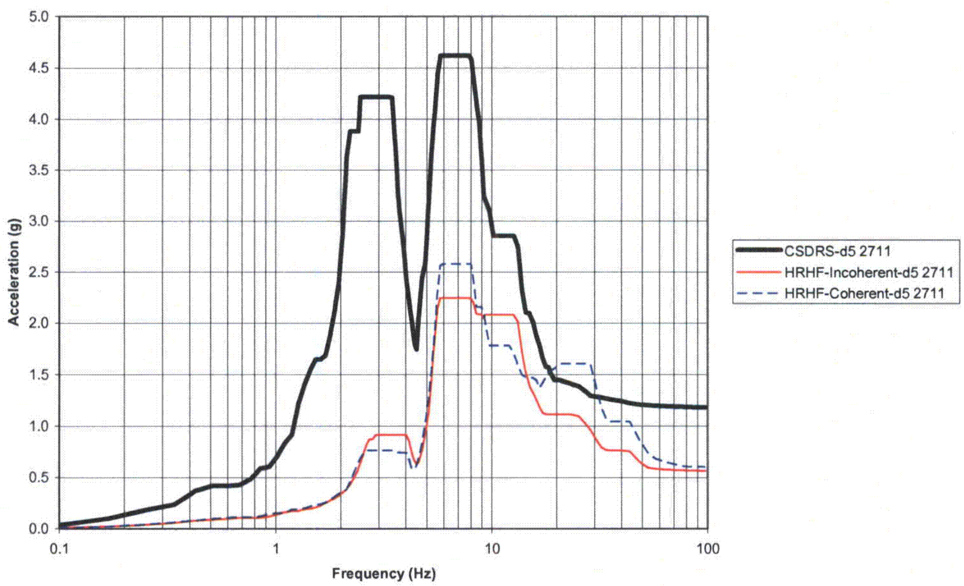

RAI-SRP3.7.1-SEB1-11-5: Seismic Response Spectra for West Side of Shield Building Y-Direction

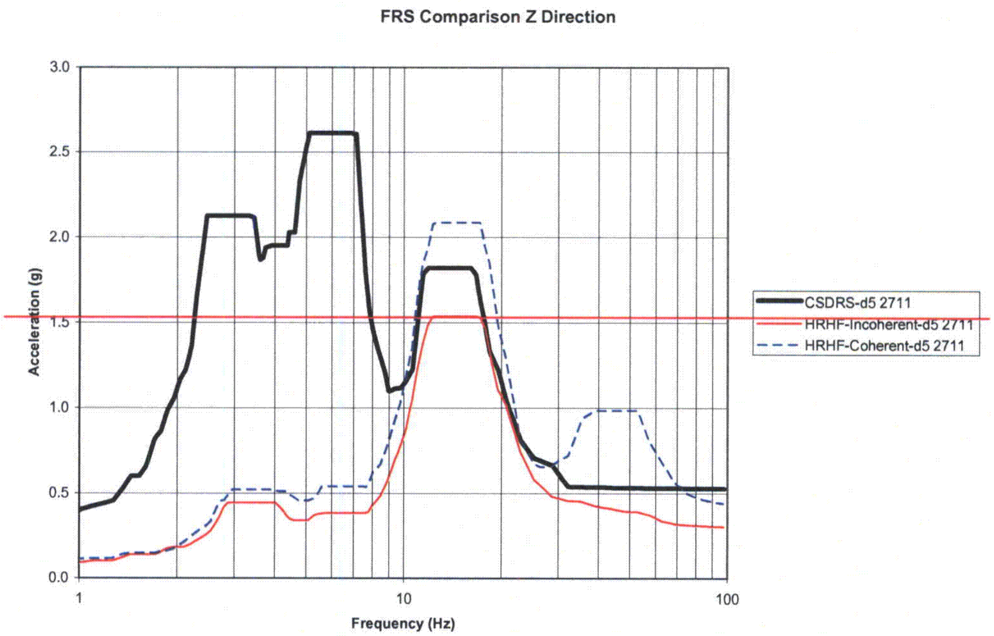

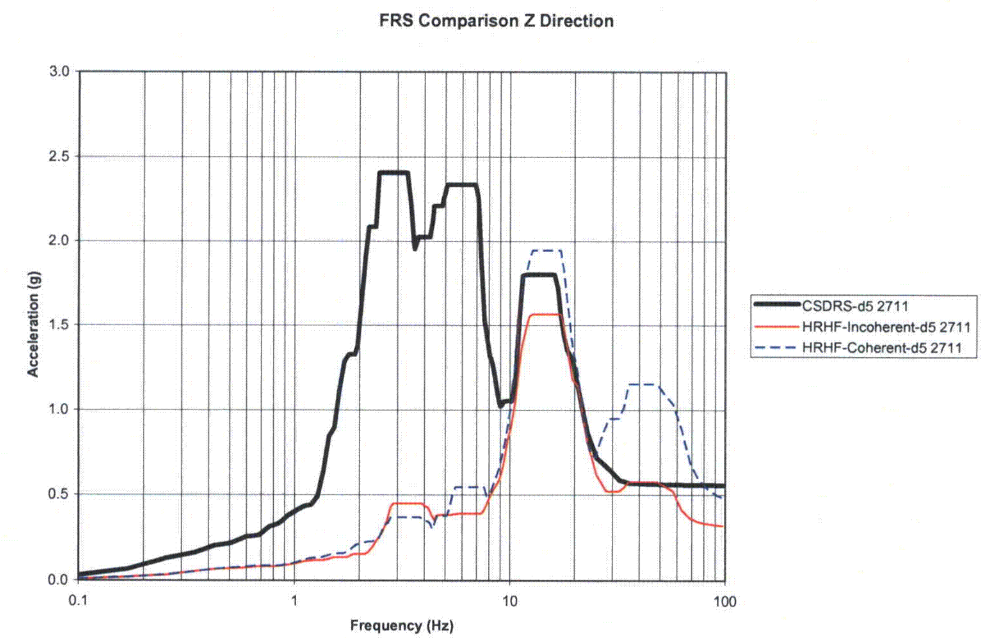

RAI-SRP3.7.1-SEB1-11-6: Seismic Response Spectra for West Side of Shield Building Z-Direction

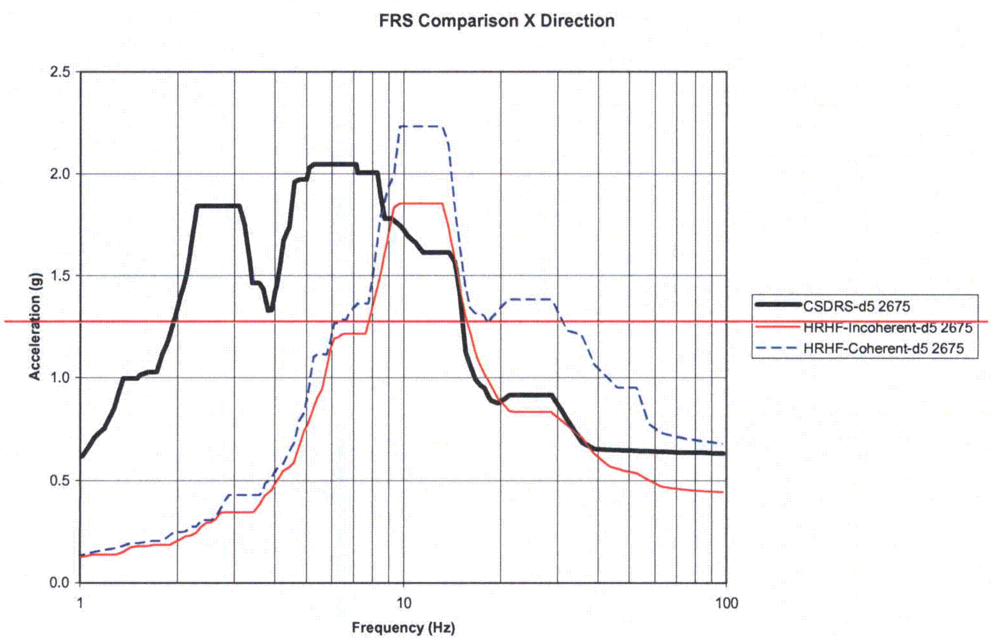

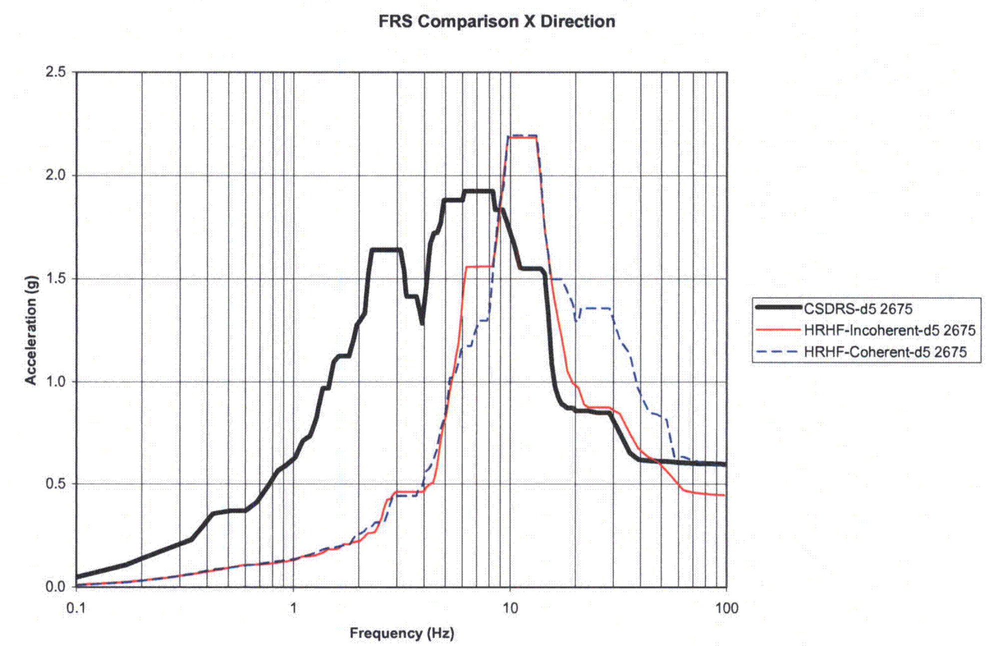

RAI-SRP3.7.1-SEB1-11-7: Seismic Response Spectra for South Side of Shield Building X-Direction

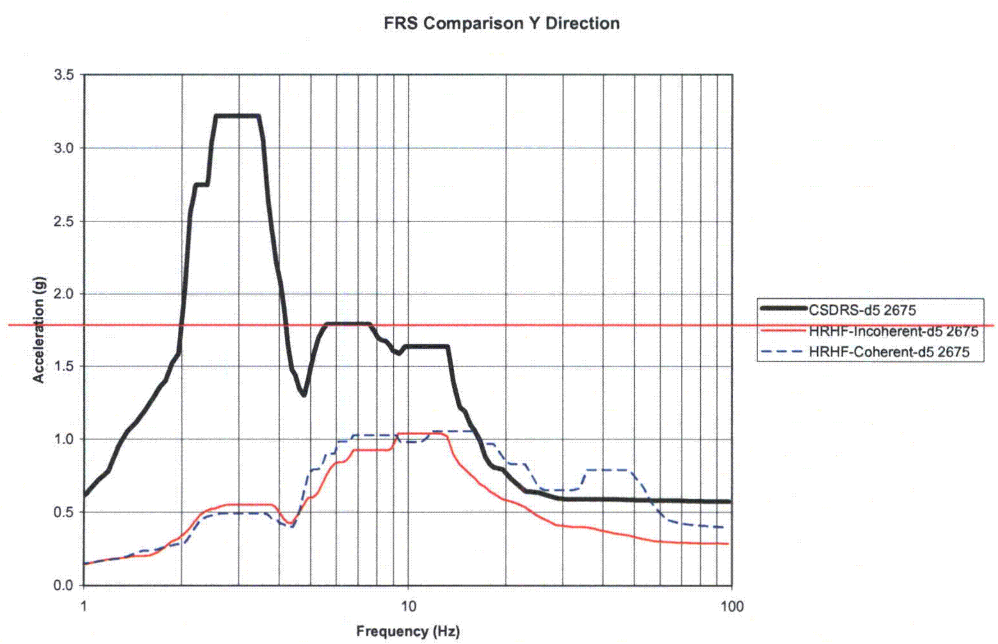

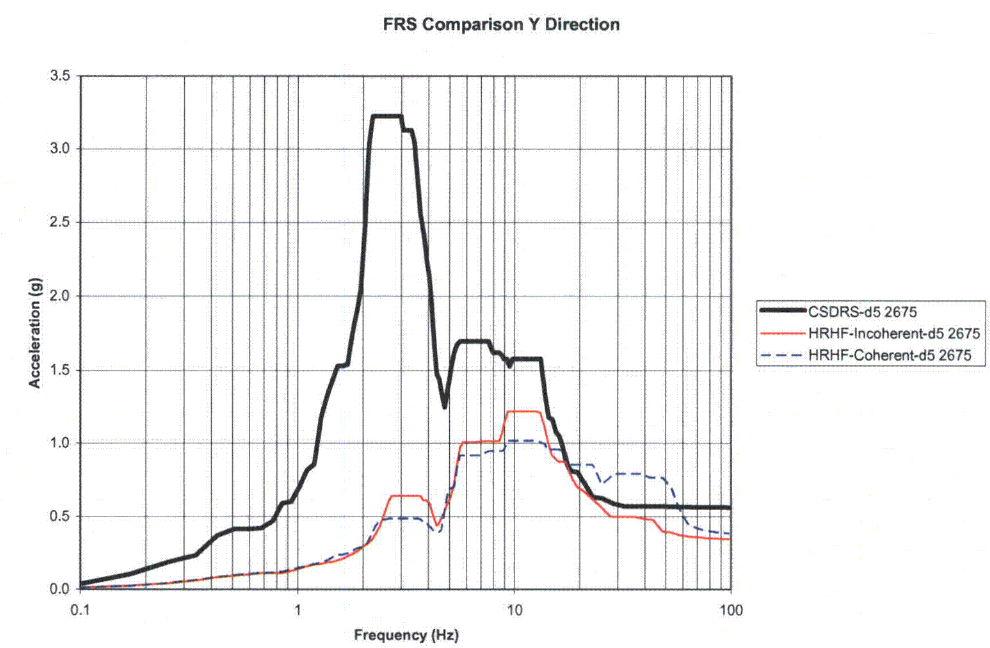

RAI-SRP3.7.1-SEB1-11-8: Seismic Response Spectra for South Side of Shield Building Y-Direction

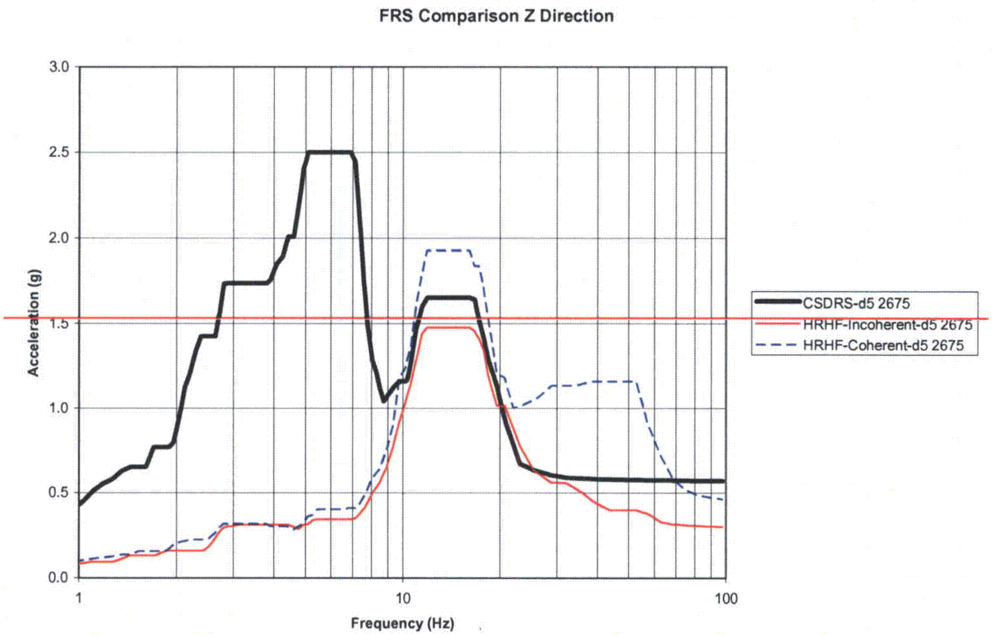

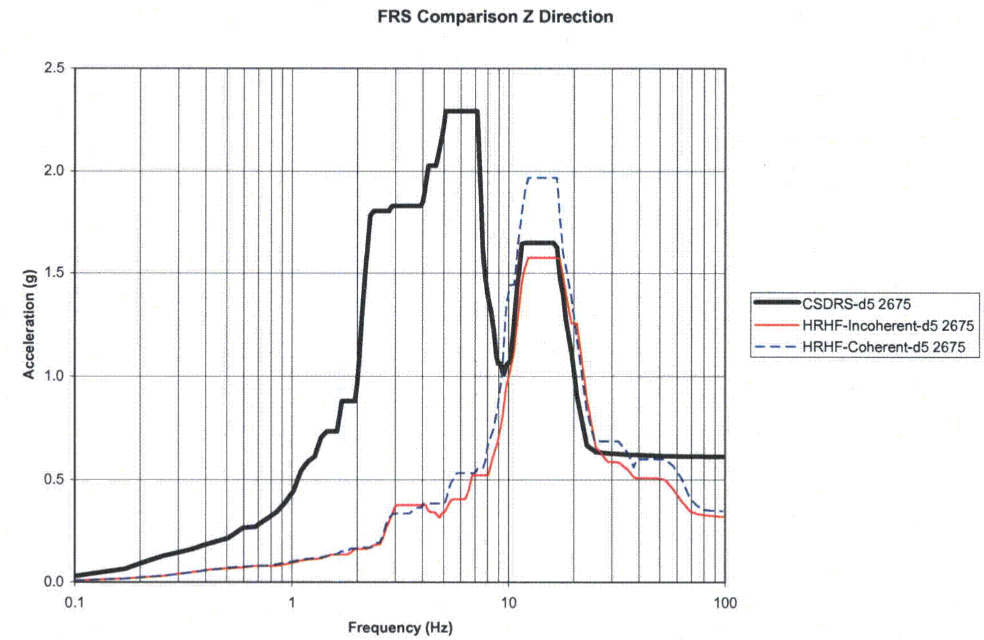

RAI-SRP3.7.1-SEB1-11-9: Seismic Response Spectra for South Side of Shield Building Z-Direction

Westinghouse Response (Revision 2):

Following the NRC Audit of AP1000 Seismic Design the week of April 13-17, 2009, the NRC has requested additional HRHF FRS at the four corners and center of the Nuclear Island basemat. The nodal locations of the response spectra comparisons have been provided in a plot shown in Figure RAI-SRP3.7.1-SEB1-11-10. A comparison of the SRSS combined X, Y and Z directions for incoherent simulations, average incoherent and coherent FRS are shown in Figures RAI-SRP3.7.1-SEB1-11-11 through RAI-SRP3.7.1-SEB1-11-25. The plots provided show a general reduction in the 25 incoherent simulations when compared to the coherent response in the higher frequencies. At lower elevations, the incoherent simulations exceed the coherent responses in the z-direction around the 10-20 Hz range; these exceedances do not exist at higher elevations as seen in Figures RAI-SRP3.7.1-SEB1-11-1 through RAI-SRP3.7.1-SEB1-11-9.

<u>Index for Figures RAI-SRP3.7.1-SEB1-11-11 through RAI-SRP3.7.1-SEB1-11-25:</u>

sim # - Incoherent Simulation (total of 25)
AVG – Average of the Incoherent Simulations
COH – Coherent Response

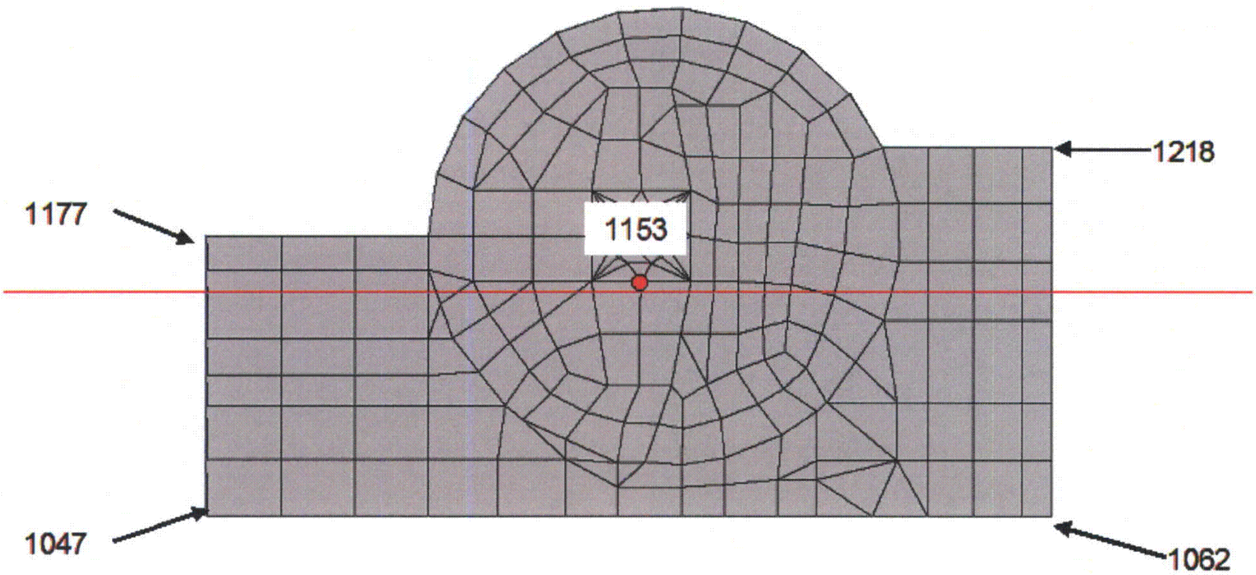

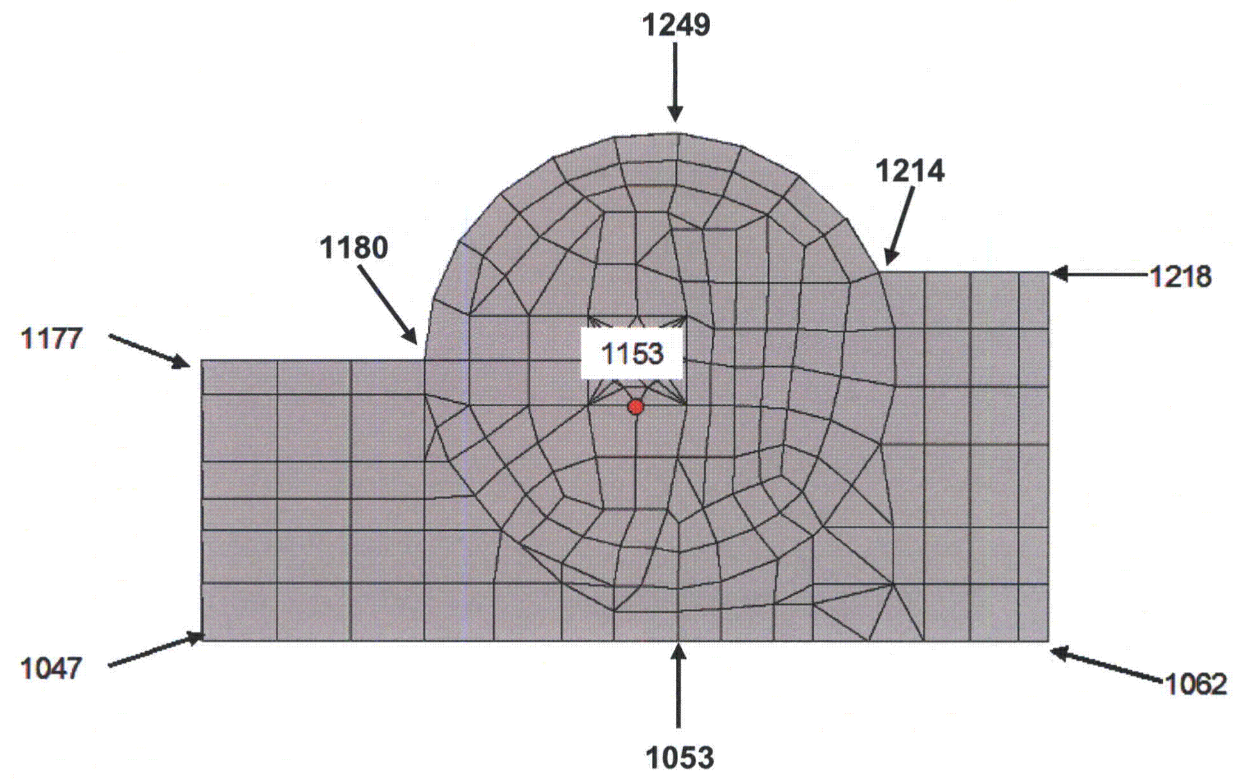

RAI-SRP3.7.1-SEB1-11-10: Basemat Nodal Locations, Elevation 60.5'

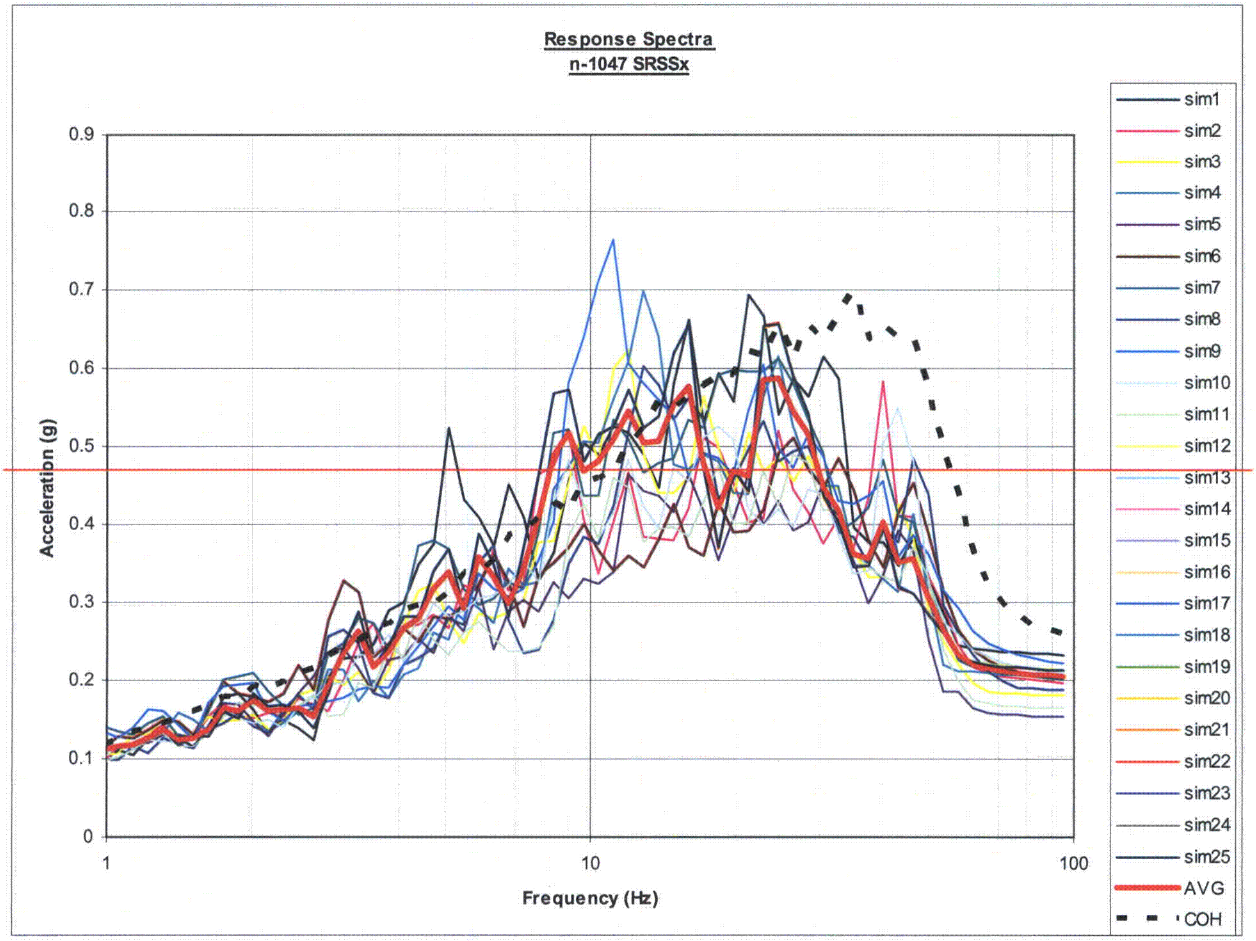

~~RAI-SRP3.7.1-SEB1-11-11: Node 1047 SRSS X-Direction, Southeast Corner through RAI-SRP3.7.1-SEB1-11- 25 have been updated and replaced by figures RAI-SRP3.7.1-SEB1-11-68 to RAI-SRP3.7.1-SEB1-11-82~~

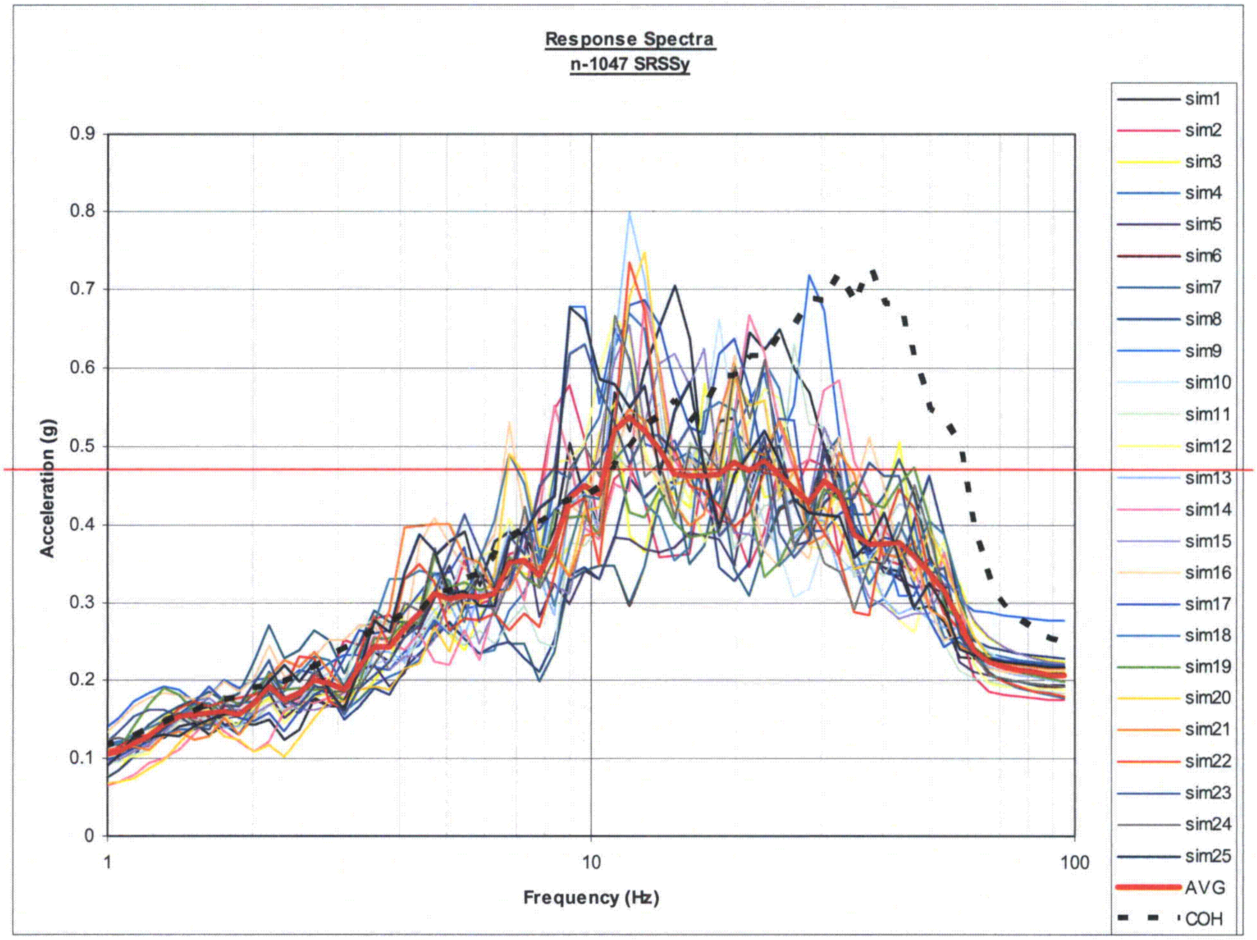

~~RAI-SRP3.7.1-SEB1-11-12: Node 1047 SRSS Y-Direction, Southeast Corner~~

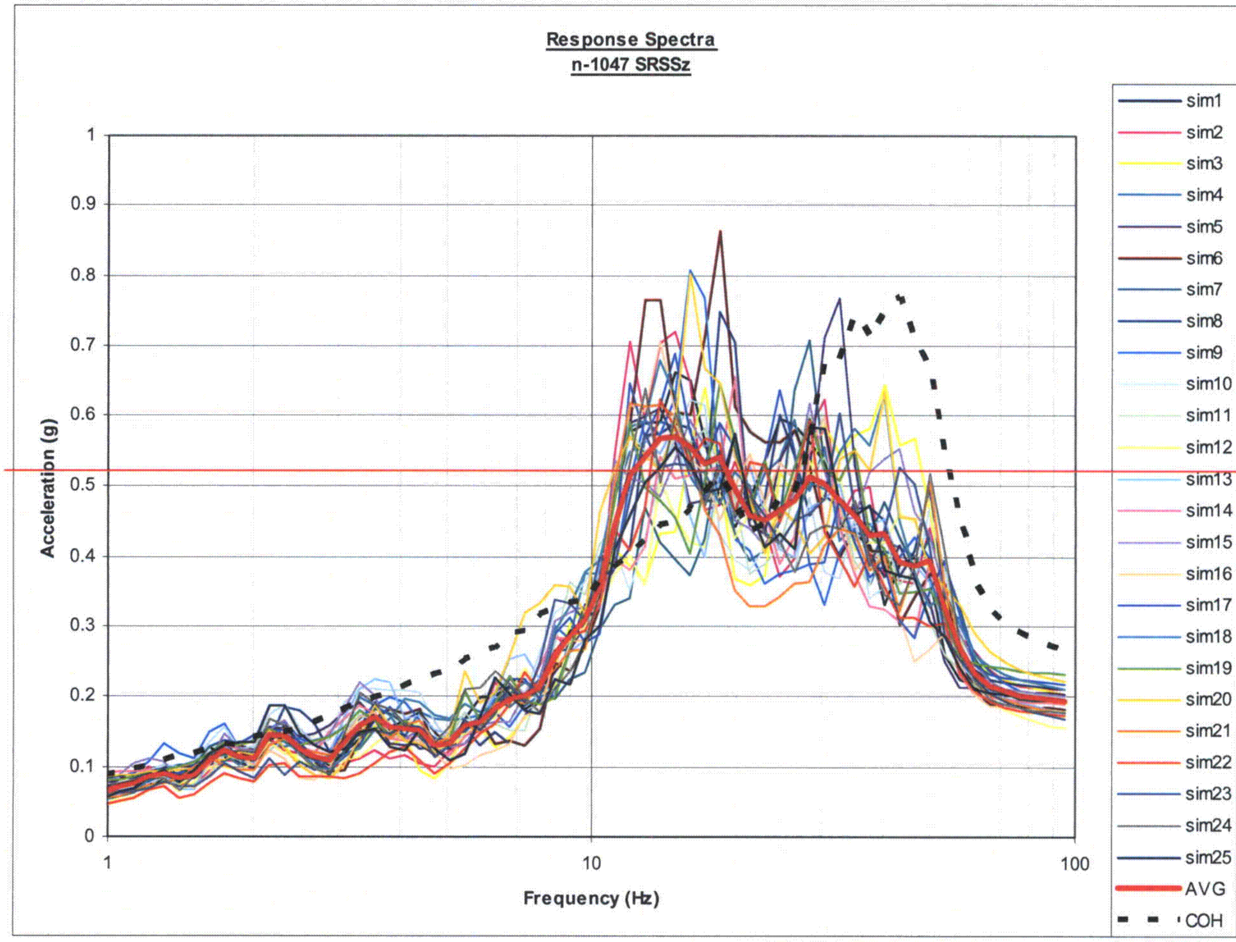

~~RAI-SRP3.7.1-SEB1-11-13: Node 1047 SRSS Z-Direction, Southeast Corner~~

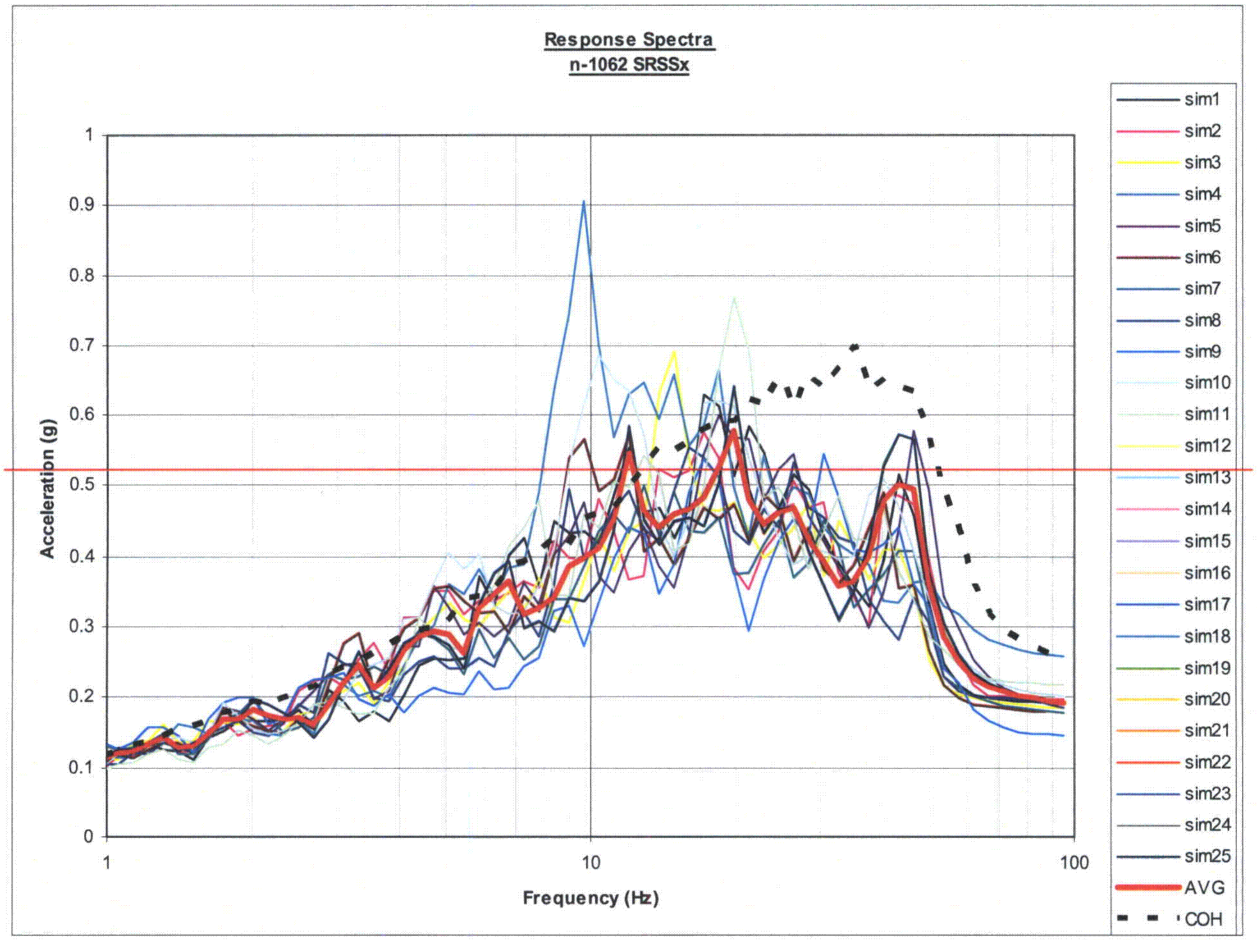

~~RAI-SRP3.7.1-SEB1-11-14: Node 1062-SRSS X-Direction, Northeast Corner~~

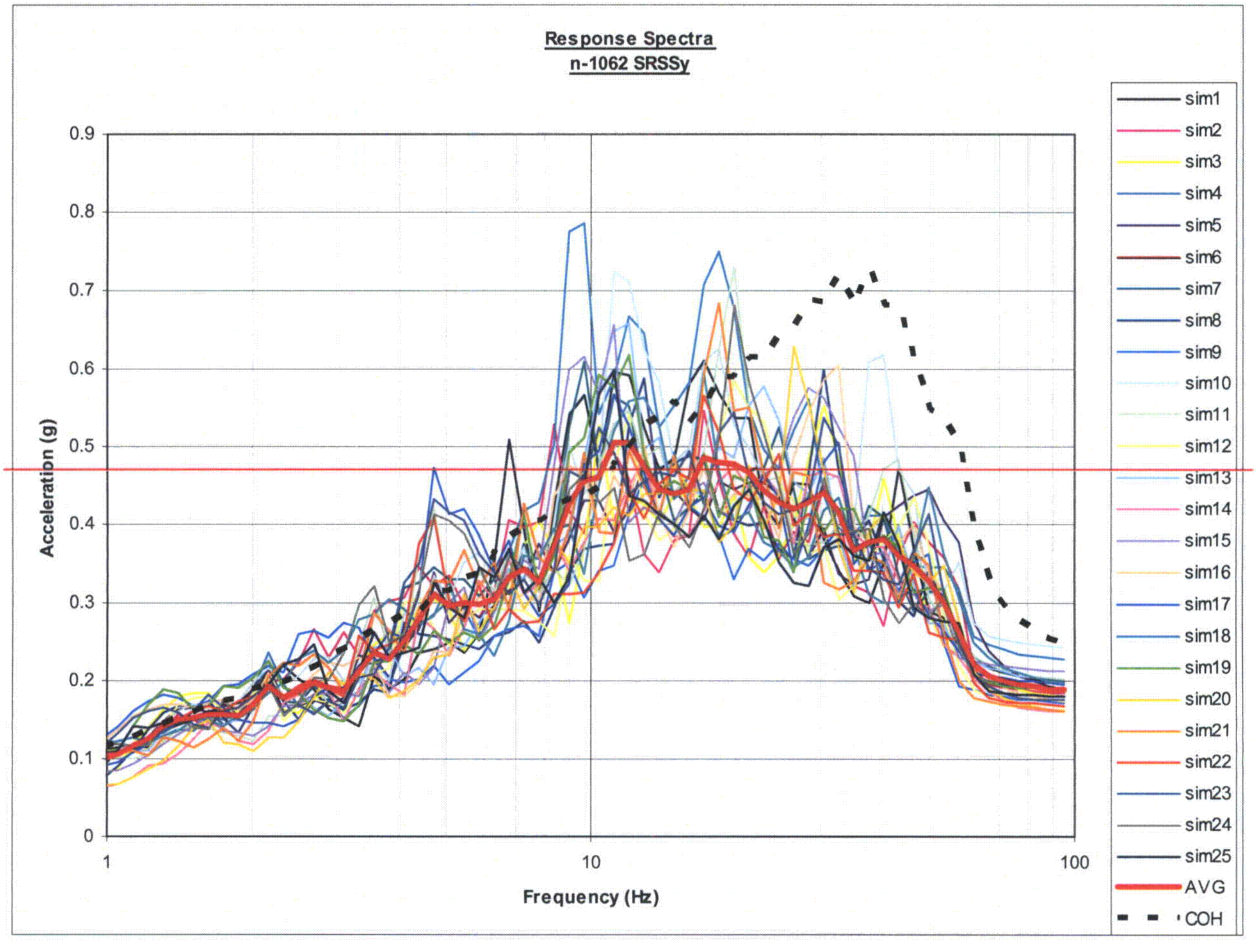

~~RAI-SRP3.7.1-SEB1-11-15: Node 1062 SRSS Y-Direction, Northeast Corner~~

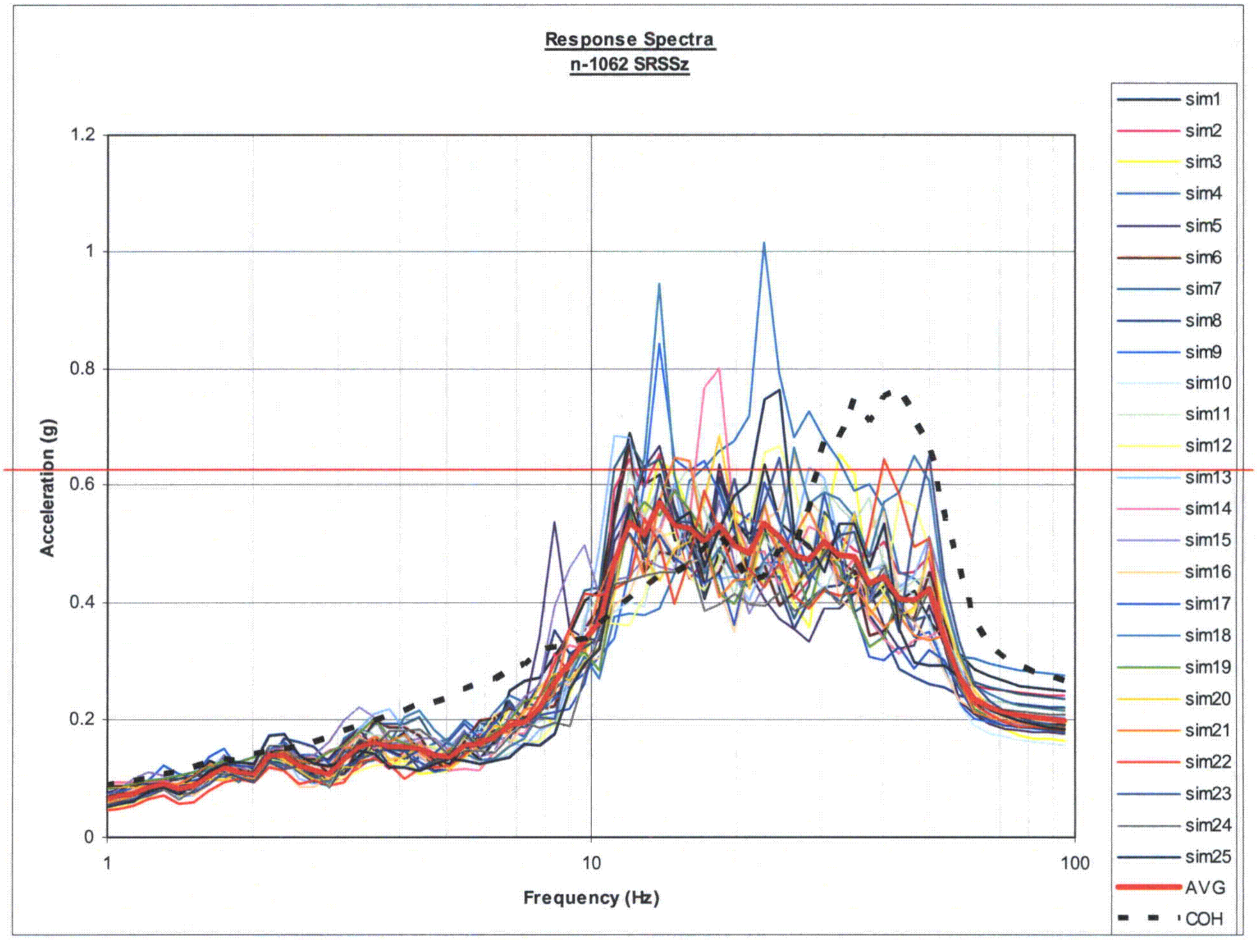

~~RAI-SRP3.7.1-SEB1-11-16: Node 1062 SRSS Z-Direction, Northeast Corner~~

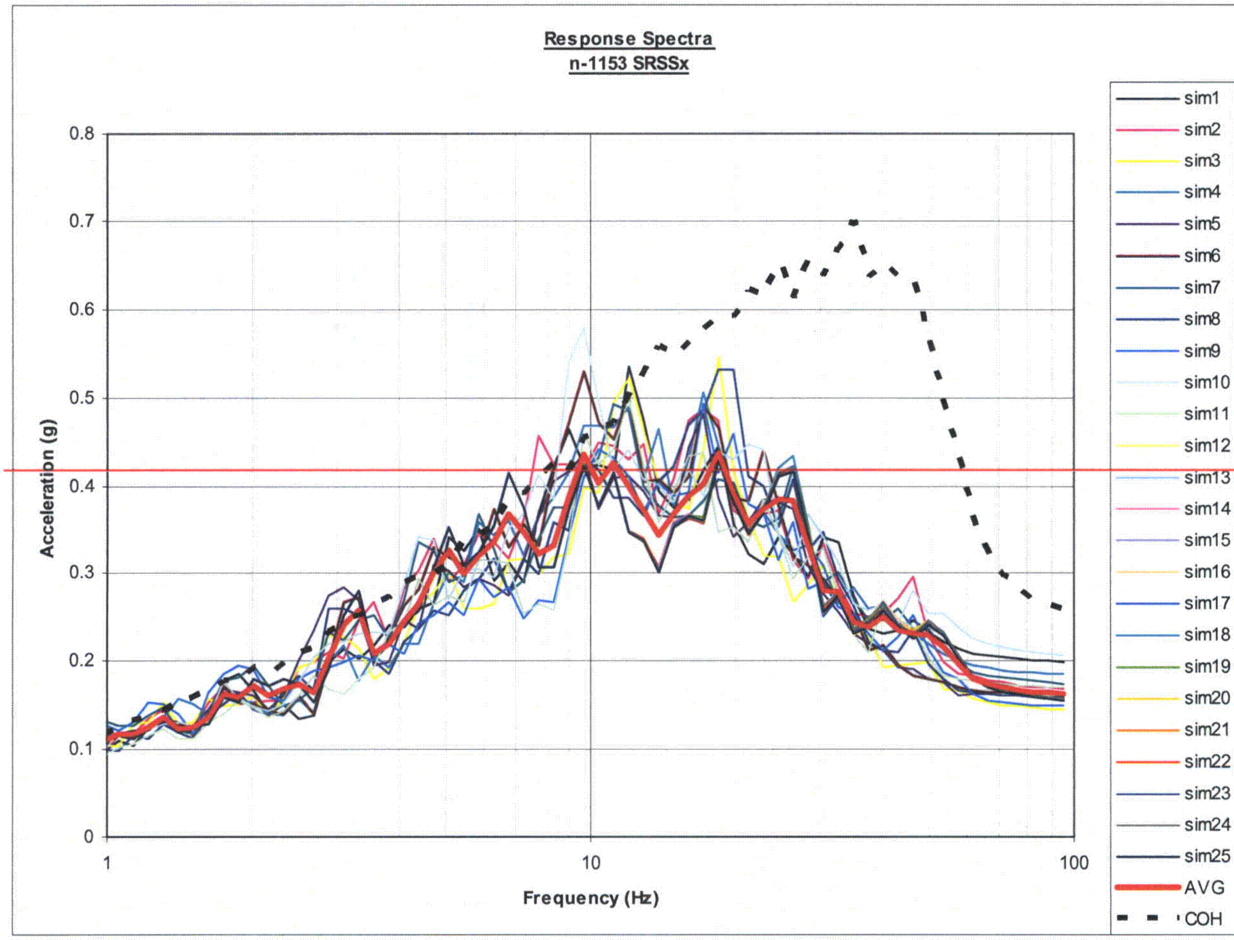

~~RAI-SRP3.7.1-SEB1-11-17: Node 1153-SRSS X-Direction, Center Basemat~~

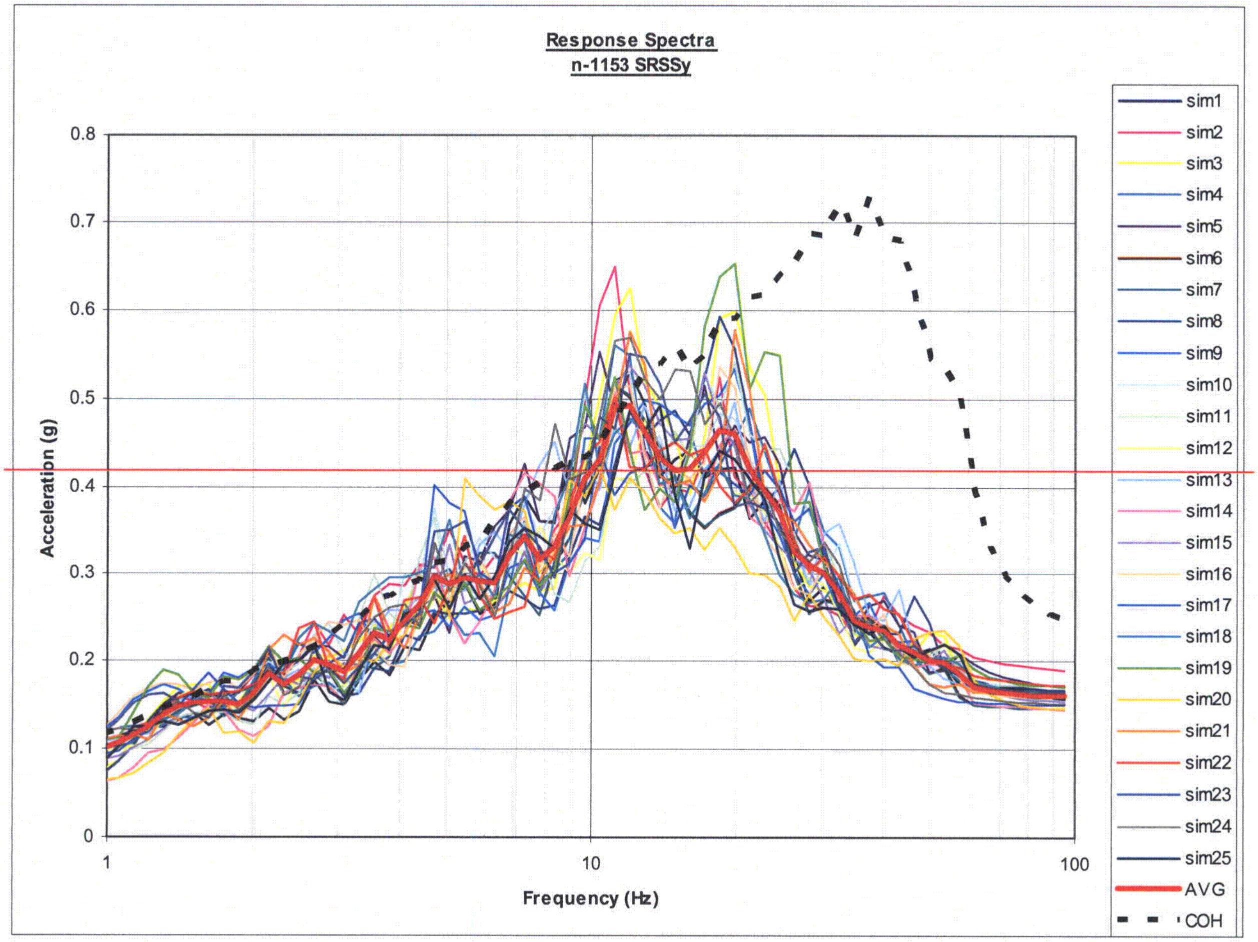

~~RAI-SRP3.7.1-SEB1-11-18: Node 1153-SRSS Y-Direction, Center Basemat~~

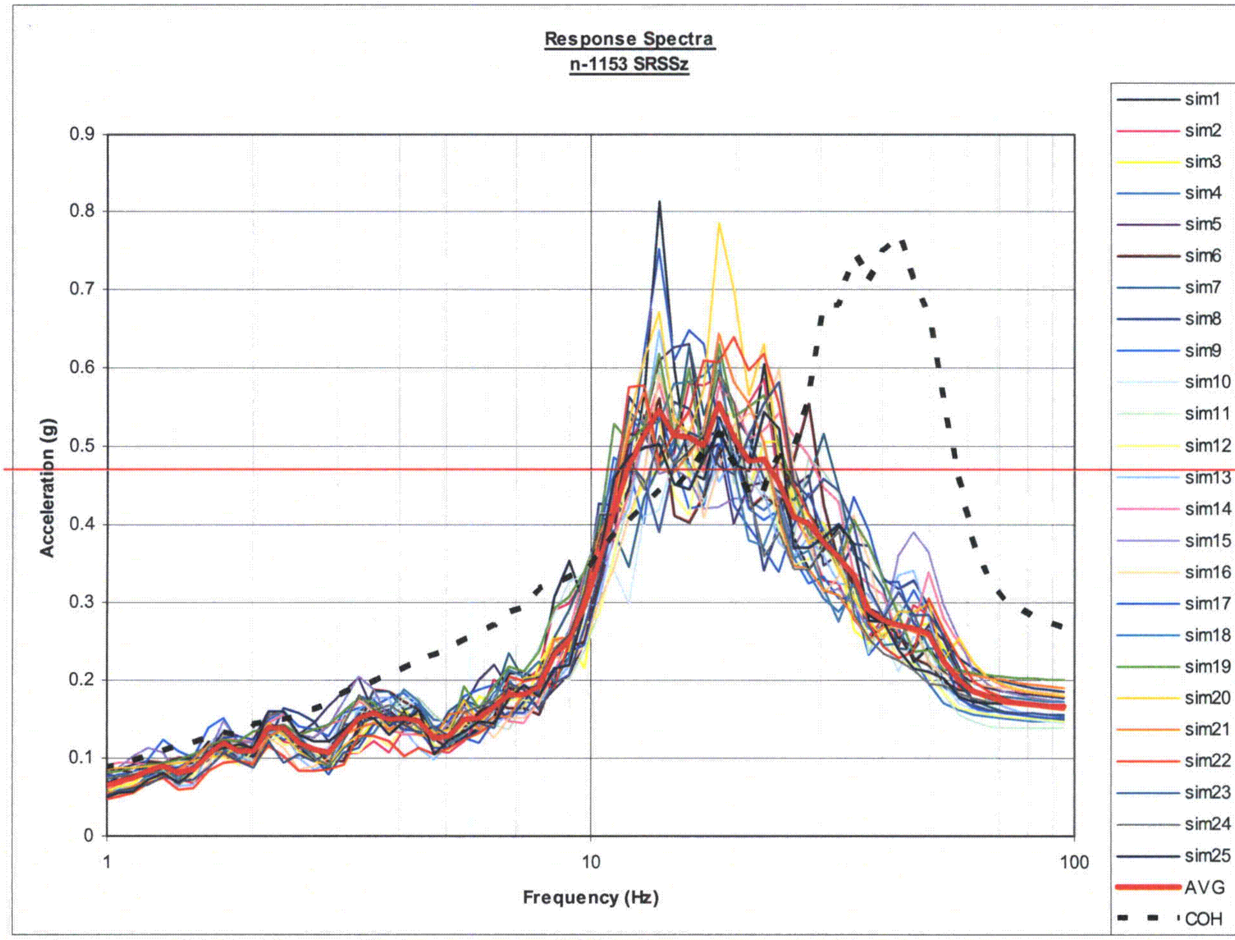

~~RAI-SRP3.7.1-SEB1-11-19: Node 1153-SRSS Z-Direction, Center Basemat~~

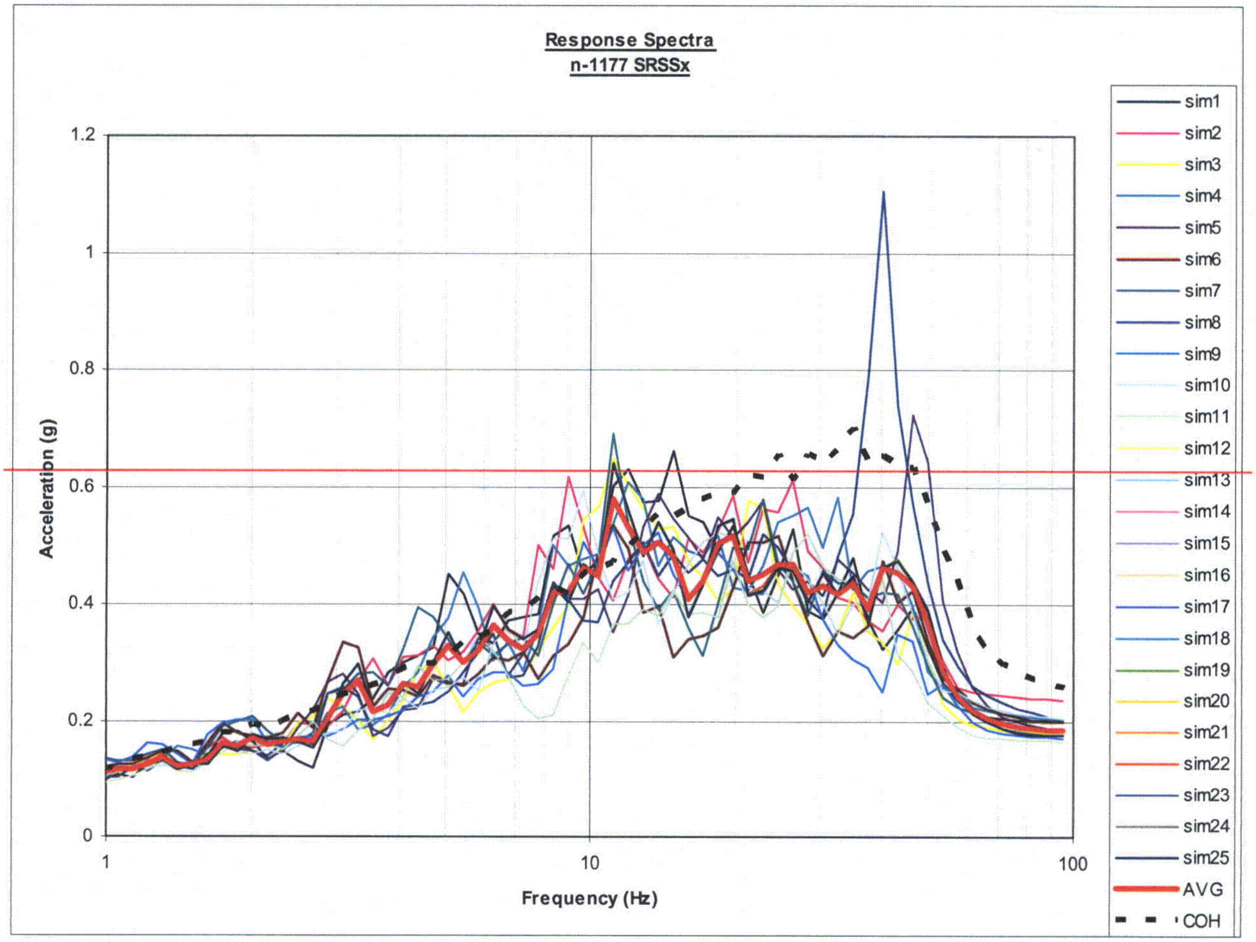

RAI-SRP3.7.1-SEB1-11-20: Node 1177 SRSS X-Direction, Southwest Corner

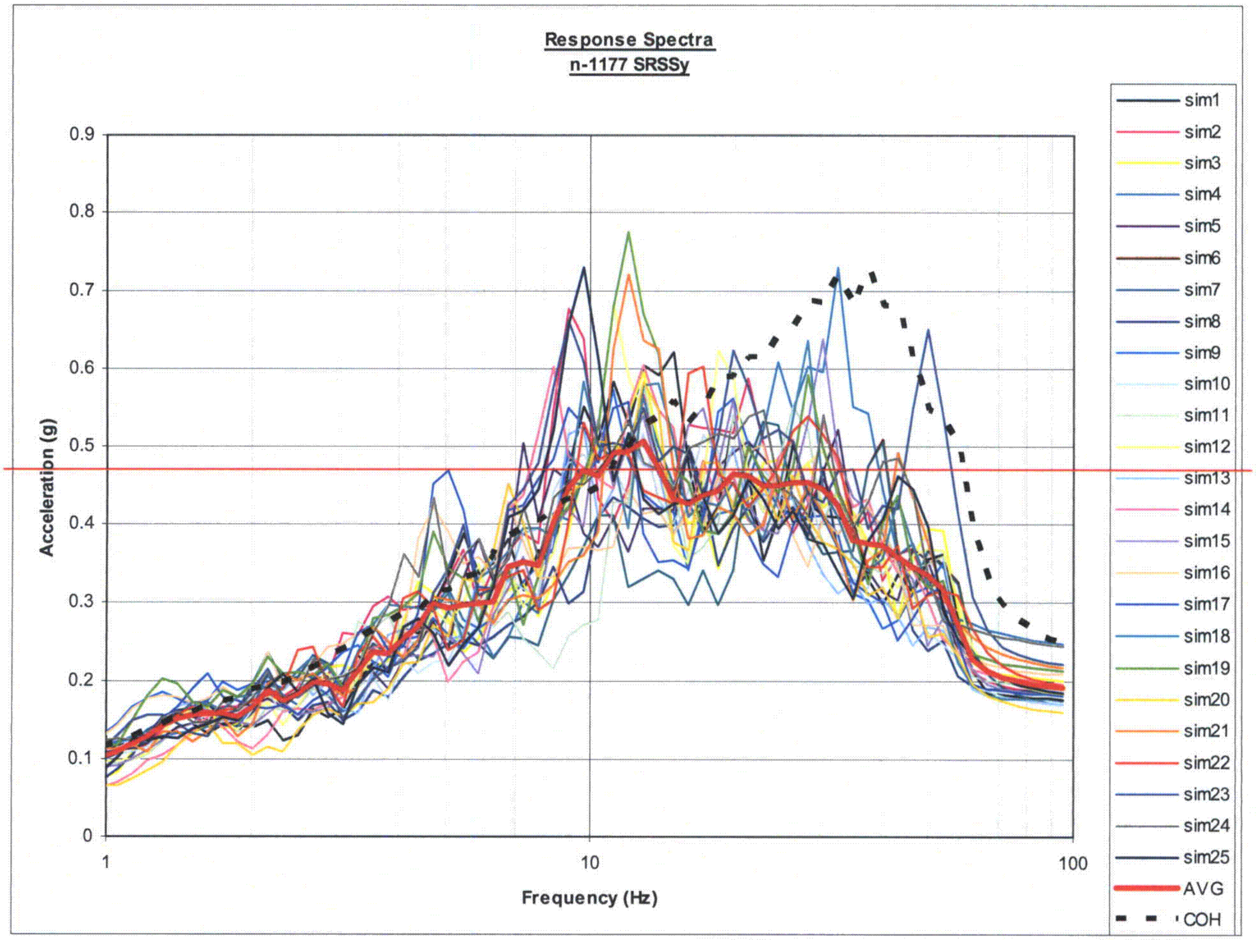

~~RAI-SRP3.7.1-SEB1-11-21: Node 1177 SRSS Y Direction, Southwest Corner~~

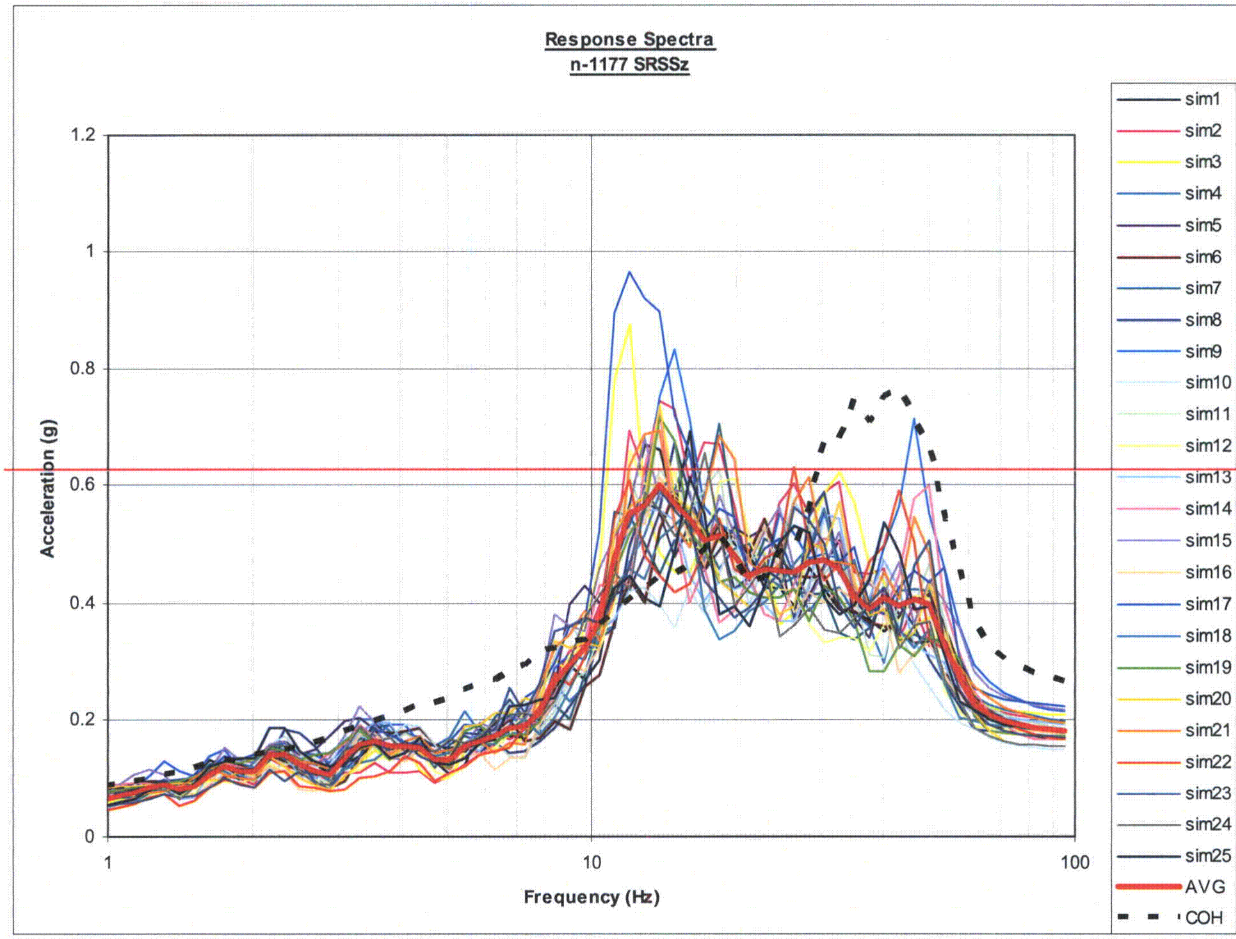

~~RAI-SRP3.7.1-SEB1-11-22: Node 1177 SRSS Z-Direction, Southwest Corner~~

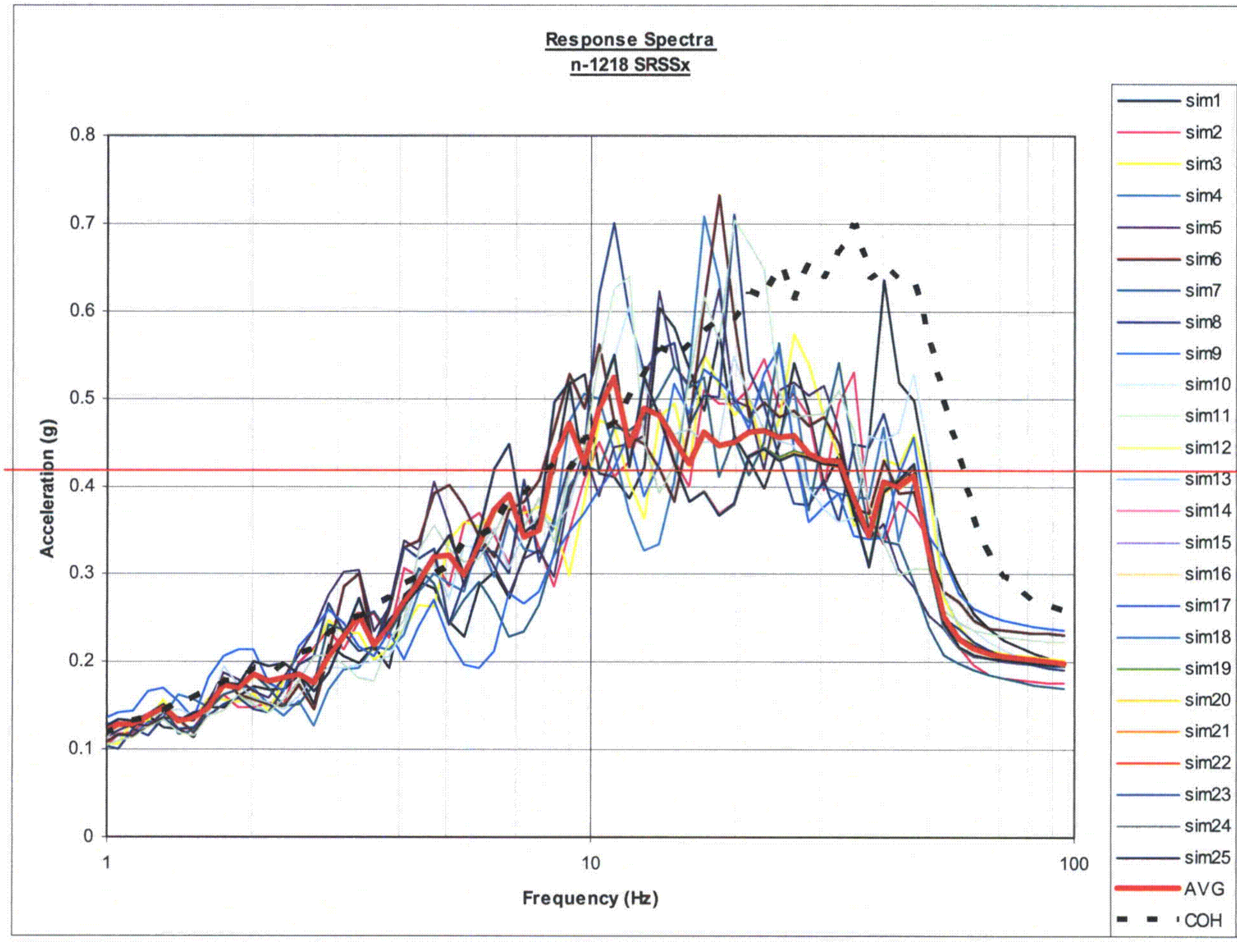

~~RAI-SRP3.7.1-SEB1-11-23: Node 1218 SRSS X-Direction, Northwest Corner~~

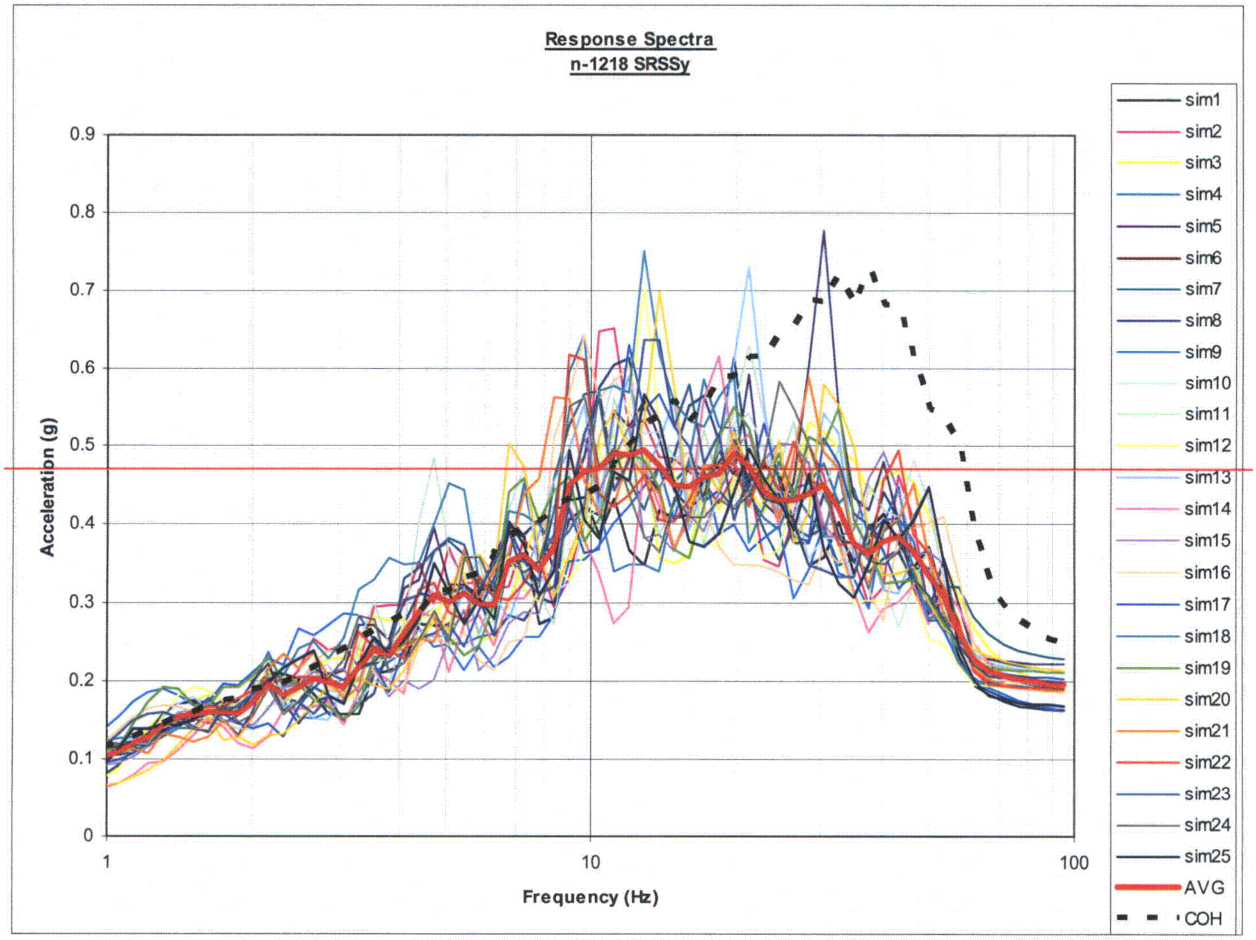

~~RAI-SRP3.7.1-SEB1-11-24: Node 1218 SRSS Y-Direction, Northwest Corner~~

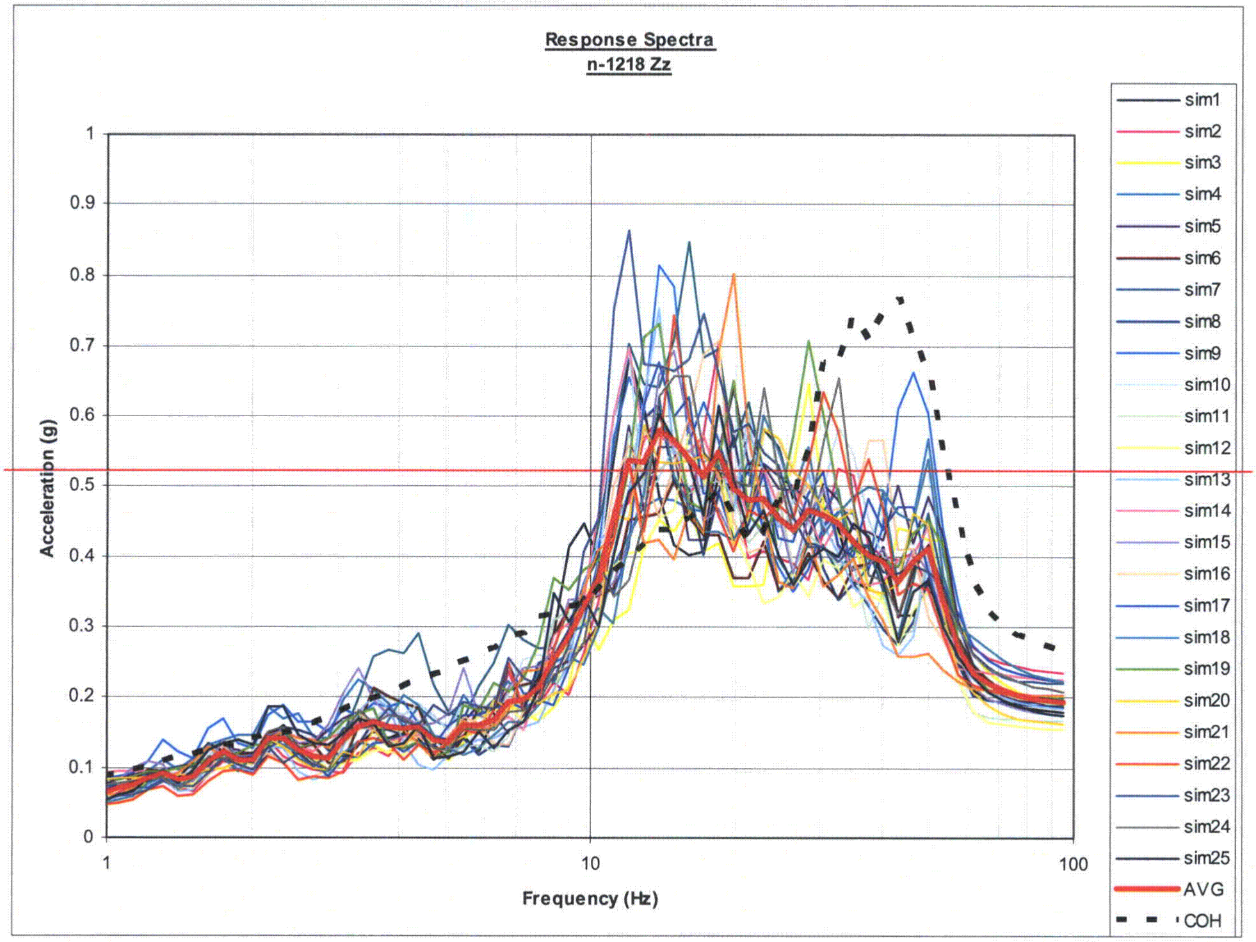

~~RAI-SRP3.7.1-SEB1-11-25: Node 1218 SRSS Z-Direction, Northwest Corner~~

Westinghouse Response (Revision 3):

A. Westinghouse has revised models and performed reanalysis to address modeling concerns, specifically beam element interactions and connections in the NI20 SASSI model. This was required in part due to a modeling limitation in the SASSI software, the connections were unable to transfer rotational moments between elements. The solid-beam element interactions require either a fixed connection or a shell element to transfer forces properly between the elements. In order to address the element interaction issue, modeling changes were made. The solid-beam element connections were selected in the ANSYS model and are shown in Figure RAI-SRP3.7.1-SEB1-11-26. Figure RAI-SRP3.7.1-SEB1-11-27 shows the solid elements attached to the beam elements.

The shell elements were added at the top of the solid elements at elevations 82.5 feet and 100 feet. These shell elements transfer the six degrees of freedom of the beam elements to the three degrees of freedom of the solid elements without adding mass. The shell elements ensure that stresses are passed through the solid elements uniformly as well as transfer moments through the beam elements. Figures RAI-SRP3.7.1-SEB1-11-28 and RAI-SRP3.7.1-SEB1-11-29 show the shell elements at elevations 100 feet and 82.5 feet, respectively.

In addition to the shell elements mentioned above, all beam elements that were connected only to solid elements were changed to fixed connections in the NI20 model. One specific area of concern addressed was in the connection between the steel containment vessel (SCV) stick model and the nuclear island. The connection consists of a series of beam elements in the form of a spoke, with the center piece attached to the SCV stick model. The other ends of the beam elements are now attached to both the solid and shell elements. Figure RAI-SRP3.7.1-SEB1-11-30 shows the interface between the SCV spoke ends and shell element at elevation 100 feet.

It is noted that additional work has been incorporated into the SASSI model, specifically modifications to the shield building design. The changes relevant to the Nuclear Island model used for dynamic analyses are the increased thickness of the steel liner along the shield building cylindrical wall and the shape of the air inlet openings.

B. Westinghouse also evaluated the transition shell to brick interface. Another change made was the addition of massless shell elements to the base of the containment internal structures (CIS) model. These elements distribute the stresses between the auxiliary building and the CIS structures as shown in Figure RAI-SRP3.7.1-SEB1-11-31.

C. Westinghouse manually checks the interpolation function for the NI20 model to ensure the correct starting point of one for the transfer functions. The interpolation function for the six key locations is shown in Figures RAI-SRP3.7.1-SEB1-11-32 through RAI-SRP3.7.1-SEB1-11-

49. Note that in these figures, XX-TFU and XX-TFI indicates the coherent transfer function TFU and coherent transfer function TFI, respectively

D. Analysis of the SASSI NI20 hard rock model was conducted using the ACS SASSI Incoherent 25 simulations which incorporates the model changes and phasing correction. The results for the six key locations are shown in Figures RAI-SRP3.7.1-SEB1-11-50 through RAI-SRP3.7.1-SEB1-11-67. A summary of the six key locations is provided in Table RAI-SRP3.7.1-SEB1-11-1. Overall, the changes made to the SASSI model did not result in significant changes in the analysis as shown in these figures by ni20rNOPH indicating the HRHF average of the incoherent simulations with no phase adjustment. However, the analysis also incorporates the phasing correction that resulted in changes in the analysis as shown in these figures by ni20rHRHF indicating the HRHF average of the incoherent simulations with phase adjustment. These changes are being addressed in Technical Report APP-GW-GLR-115, Revision 2 (TR115). Provided below is the legend for Figures RAI-SRP3.7.1-SEB1-11-50 through RAI-SRP3.7.1-SEB1-11-67.

Legend for Figures RAI-SRP3.7.1-SEB1-11-50 through RAI-SRP3.7.1-SEB1-11-67

____ ssienv: CSDRS response spectra (ni20k model)

____ ni20rHRHF: HRHF average of the incoherent simulations with phase adjustment

----- avg25: HRHF average of the incoherent simulations (ni20k model)

----- ni20rNOPH: HRHF average of the incoherent simulations with no phase adjustment

Additional information is provided based on the 02-16-10 conference call with the NRC in which updated Figures RAI-SRP3.7.1-SEB1-11-11 through RAI-SRP3.7.1-SEB1-11-25 were requested. The HRHF FRS at the four corners and center of the Nuclear Island basemat for comparison of the X, Y and Z directions for incoherent simulations, average incoherent and coherent FRS are shown in Figures RAI-SRP3.7.1-SEB1-11-68 through RAI-SRP3.7.1-SEB1-11-82. Note that in these figures, ni20rHRHF indicates the HRHF average of the incoherent simulations with phase adjustment and ni20rCOH indicates the ni20r coherent response spectra.

Westinghouse Response (Revision 4)

In response to an NRC request, Figures RAI-SRP3.7.1-SEB1-11-11 through RAI-SRP3.7.1-SEB1-11-25 have been updated and replaced by Figures RAI-SRP3.7.1-SEB1-11-68 through RAI-SRP3.7.1-SEB1-11-82.

Reference(s):

None

Design Control Document (DCD) Revision: None

PRA Revision: None

Technical Report (TR) Revision:

The figures presented in Revision 1 of this response request will be added to Section 5.2 of the TR-115 to supplement the existing data as Figures 5.2-7 and 5.2-8. Note that Figure 5.2-5 will be replaced by Figures RAI-SRP3.7.1-SEB1-11-4 to RAI-SRP-SEB1-11-6. Each figure will have the floor response spectra associated with the X, Y, and Z response. See also RAI-SRP-3.7.1-10 for additional changes to Section 5.2.

5.2 Comparison of CSDRS and HRHF Response Spectra

To show the significance of the HRHF response spectra, the CSDRS and HRHF seismic responses are compared. Figures 5.2-1 through 5.2-8 (5% damping) compare the response spectra with coherent and incoherent considerations at a number of locations in the nuclear island. There are some exceedances, mostly above the 15 Hz region. These curves are typical of the plant comparative responses found throughout the plant.

Table RAI-SRP3.7.1-SEB1-11-1: Six Key Nuclear Island Locations

Six Key Nuclear Island Locations		
Location		**Node**
Containment Internal Structure (CIS) at Elevation of Reactor Pressure Vessel (RPV) Support	~~99'~~	1761
Auxiliary Building NE Corner (Main Control Room)	~~116.5'~~	2078
Containment Operating Floor	~~134.25'~~	2199
Shield Building at Fuel Building Roof	~~179'~~	2675
Steel Containment Vessel (SCV) at Polar Crane Support	~~224'~~	2788
Shield Building Roof	~~327.4'~~	3329

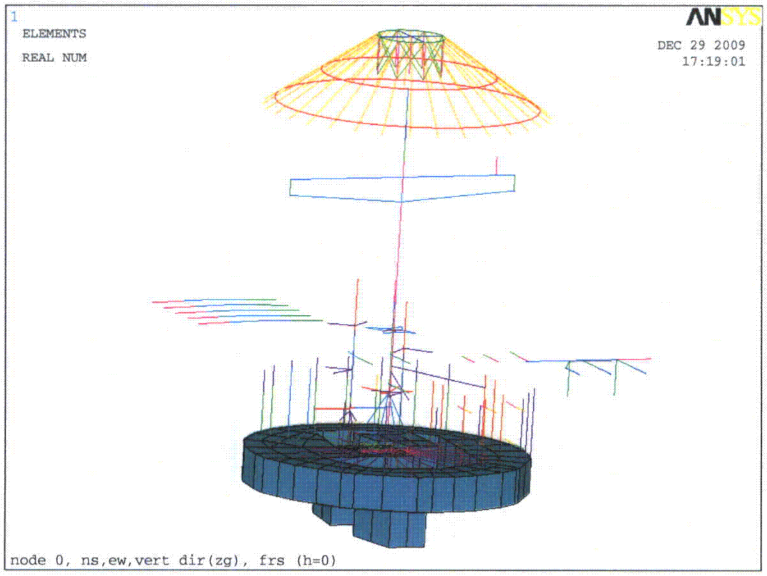

Figure RAI-SRP3.7.1-SEB1-11-26: Solid-Beam Element Connections

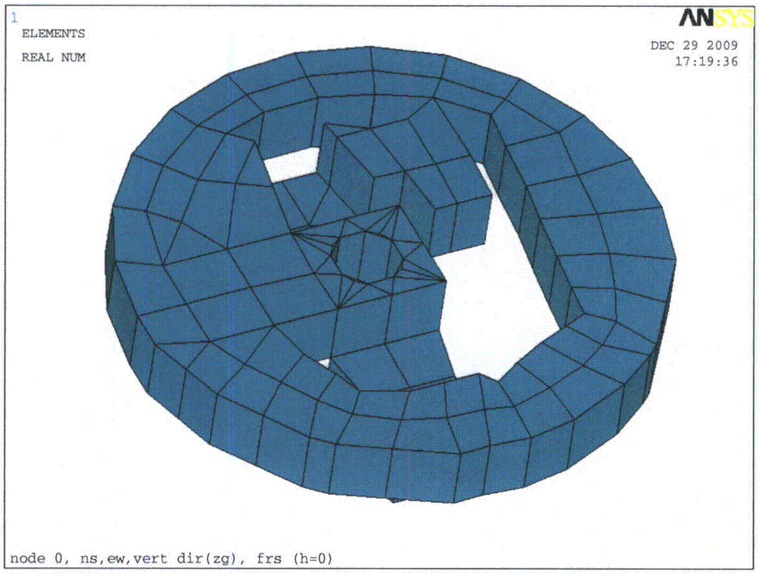

Figure RAI-SRP3.7.1-SEB1-11-27: Solid Elements Attached to the Beam Elements

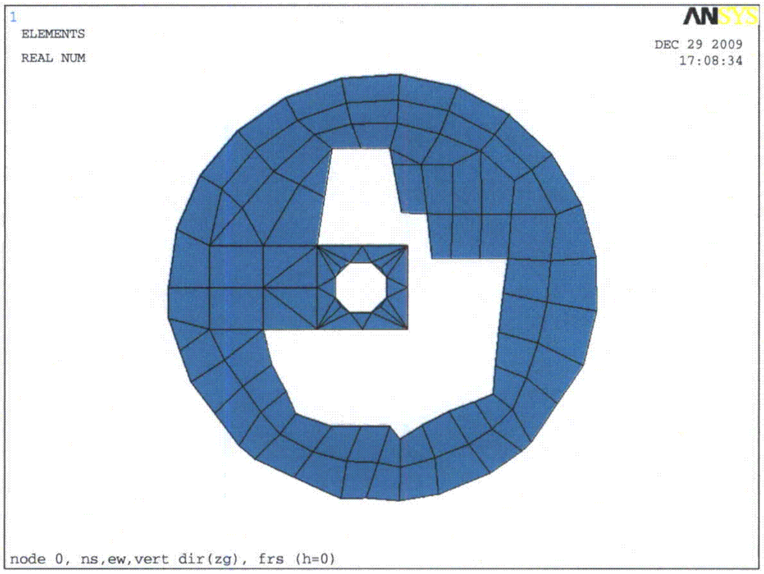

Figure RAI-SRP3.7.1-SEB1-11-28: Shell Elements at Elev. 100'

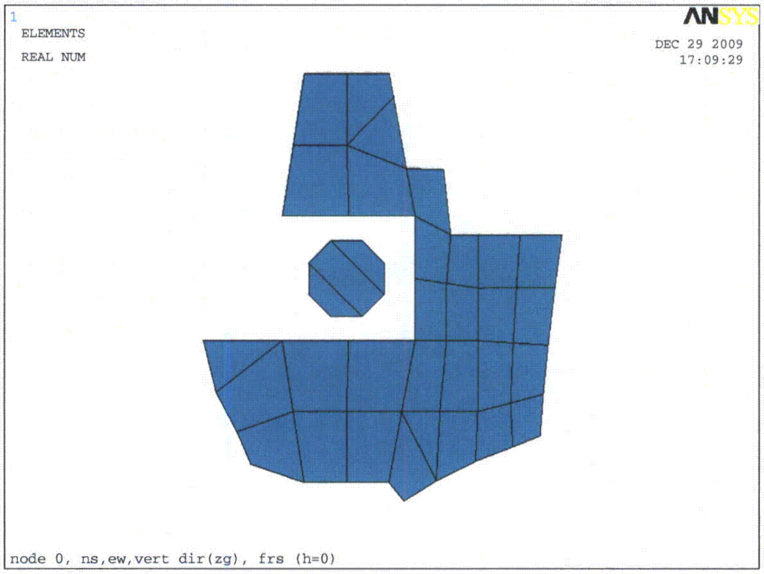

Figure RAI-SRP3.7.1-SEB1-11-29: Shell Elements at Elev. 82.5'

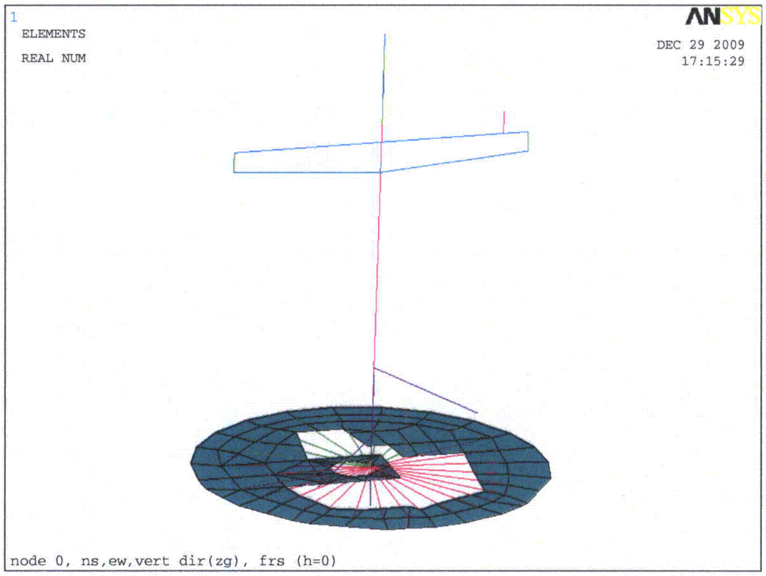

Figure SRP3.7.1-SEB1-11-30: Interface Between SCV Spoke Ends and Shell Elements at Elev. 100'

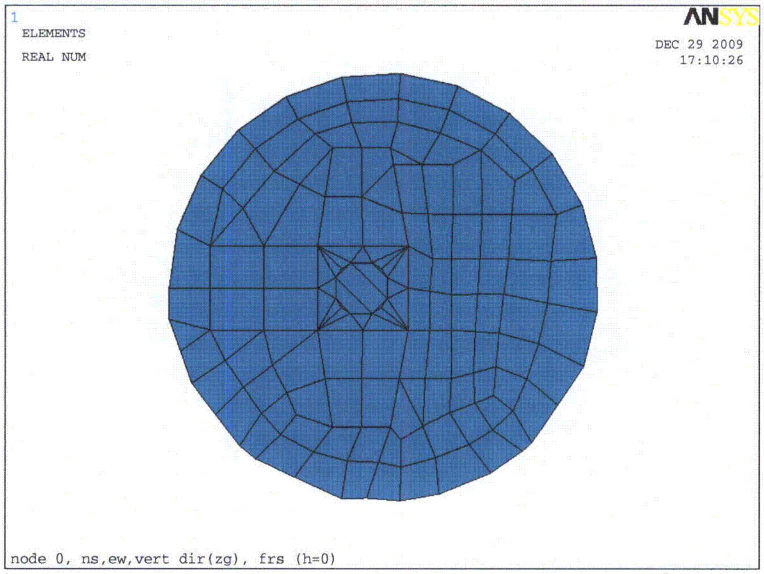

Figure RAI-SRP3.7.1-SEB1-11-31: Shell Elements at Elev. 60.5'

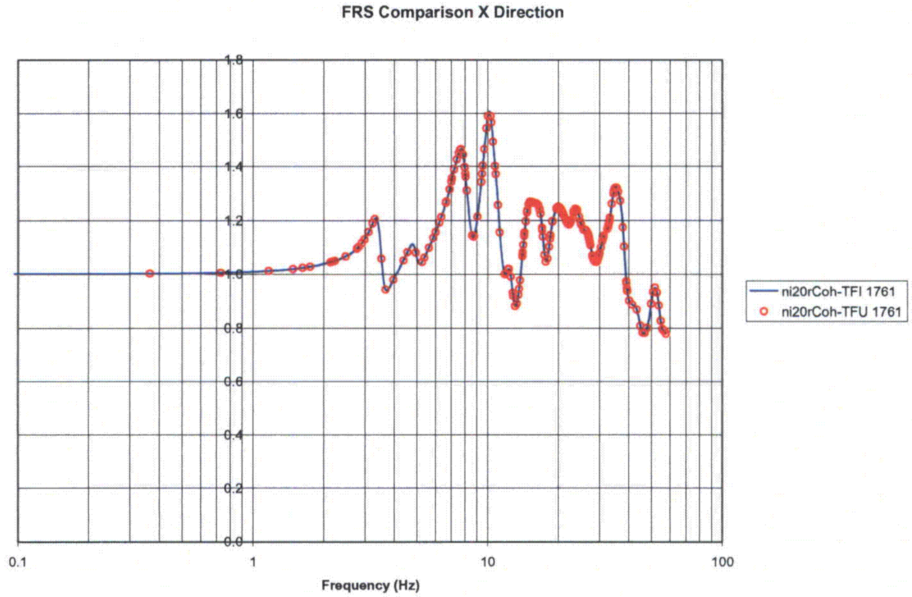

Figure RAI-SRP3.7.1-SEB1-11-32: Transfer Function Node 1761 X-Dir

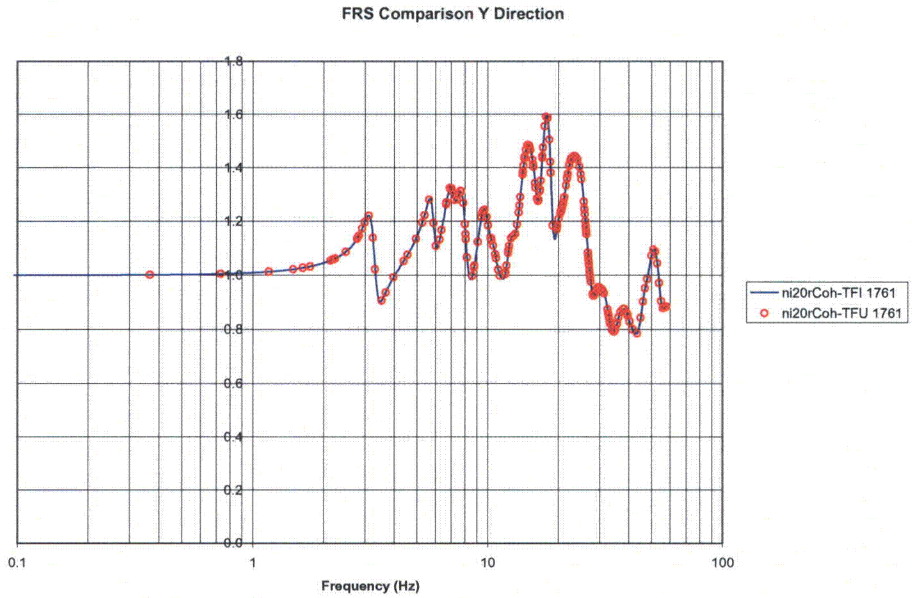

Figure RAI-SRP3.7.1-SEB1-11-33: Transfer Function Node 1761 Y-Dir

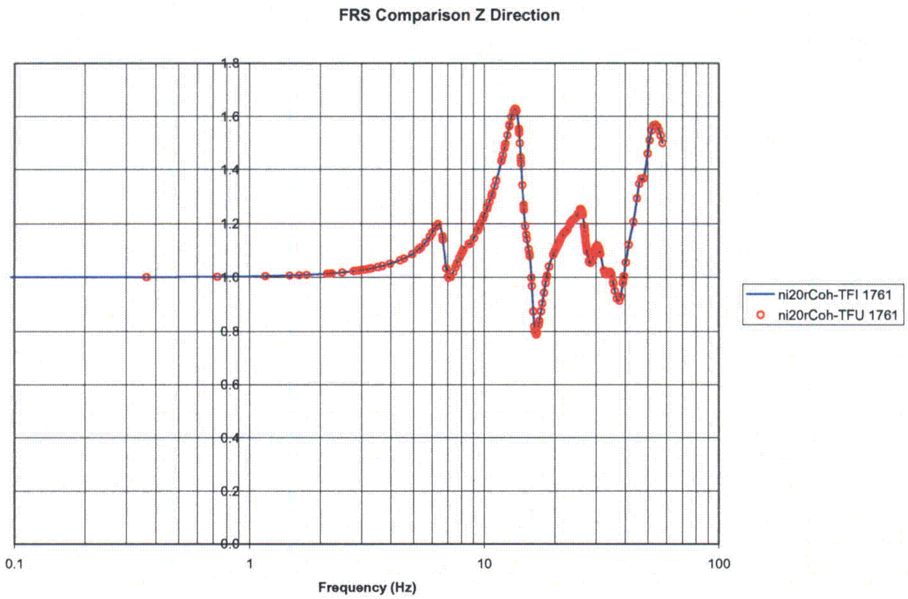

Figure RAI-SRP3.7.1-SEB1-11-34: Transfer Function Node 1761 Z-Dir

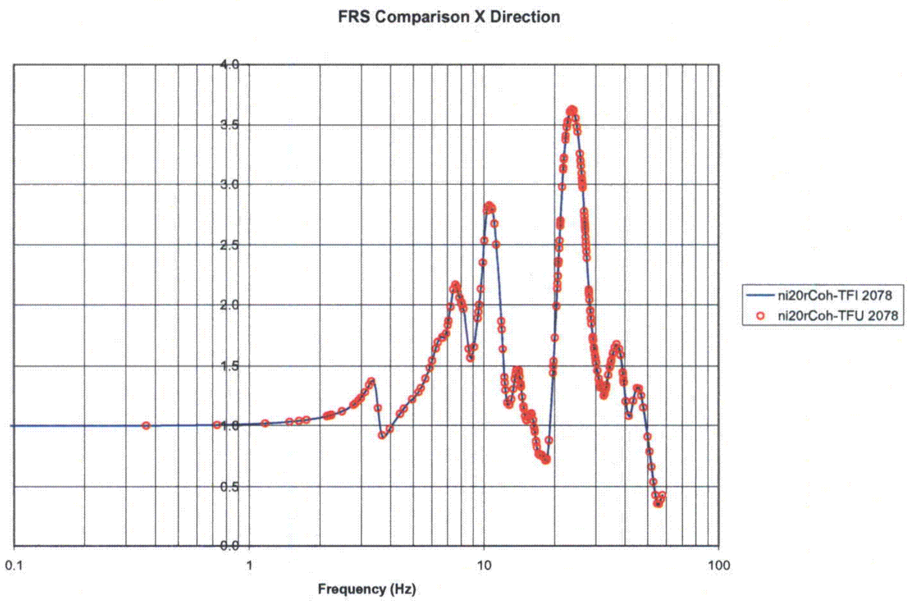

Figure RAI-SRP3.7.1-SEB1-11-35: Transfer Function Node 2078 X-Dir

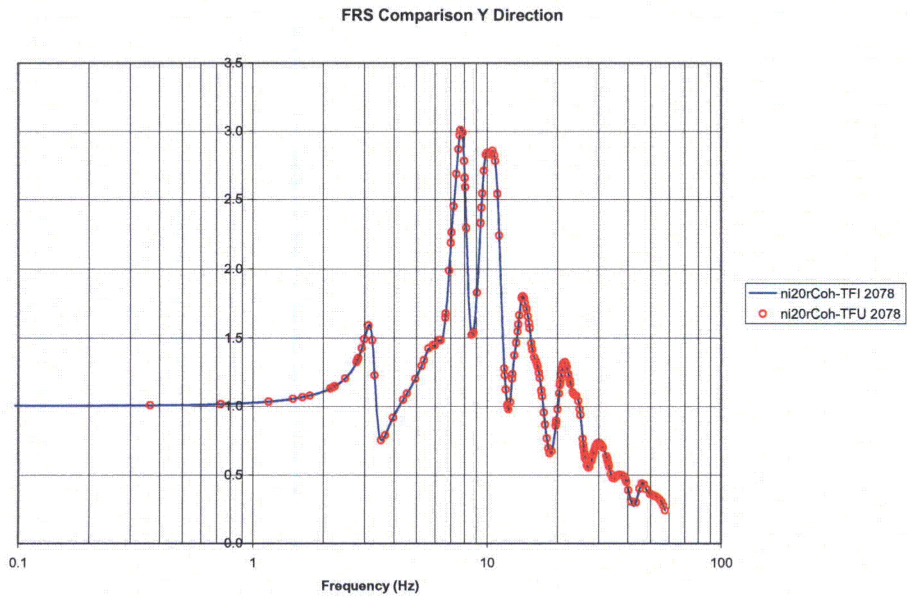

Figure RAI-SRP3.7.1-SEB1-11-36: Transfer Function Node 2078 Y-Dir

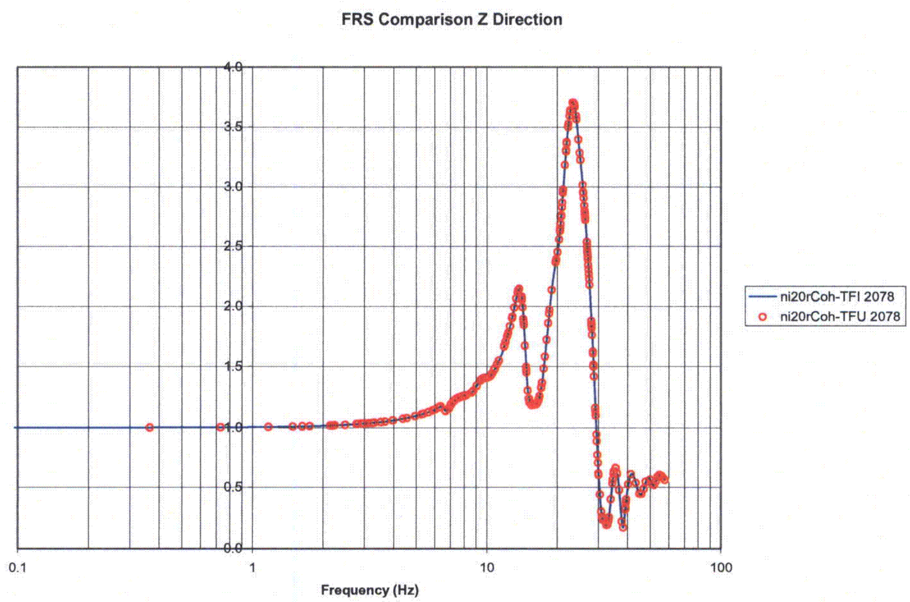

Figure RAI-SRP3.7.1-SEB1-11-37: Transfer Function Node 2078 Z-Dir

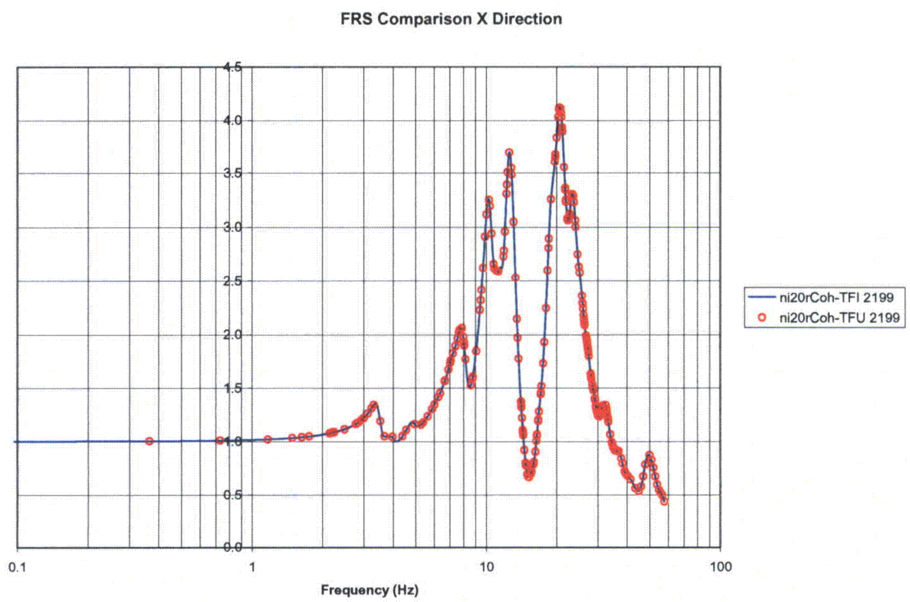

Figure RAI-SRP3.7.1-SEB1-11-38: Transfer Function Node 2199 X-Dir

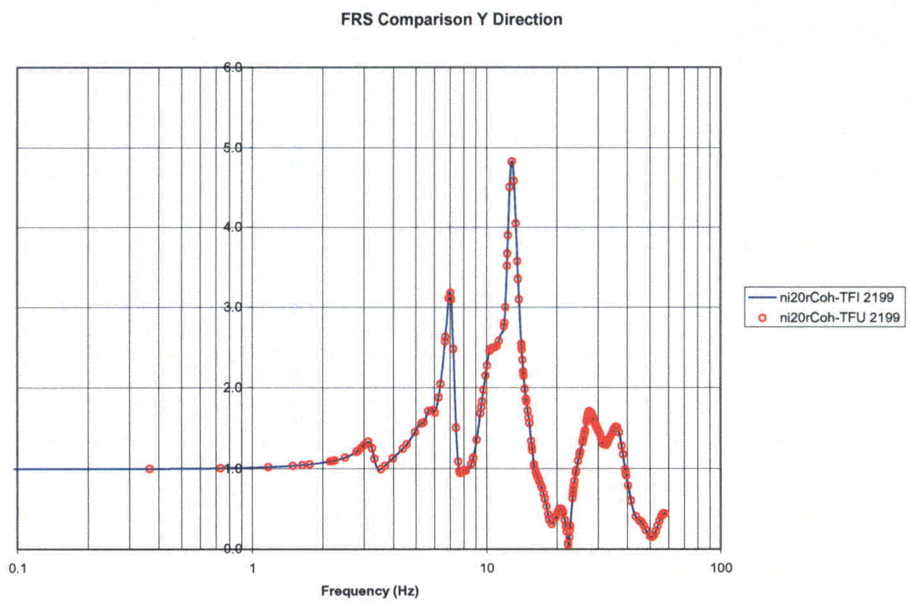

Figure RAI-SRP3.7.1-SEB1-11-39: Transfer Function Node 2199 Y-Dir

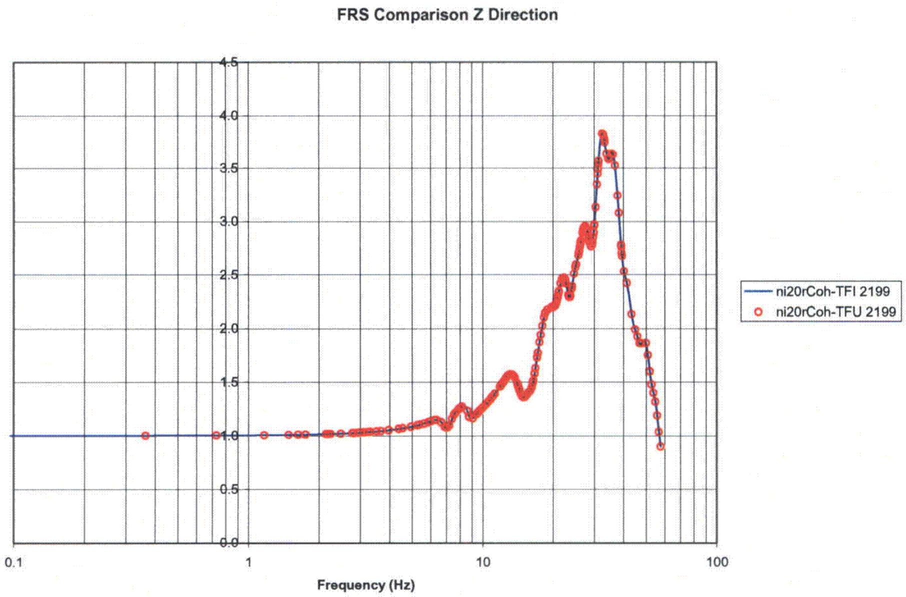

Figure RAI-SRP3.7.1-SEB1-11-40: Transfer Function Node 2199 Z-Dir

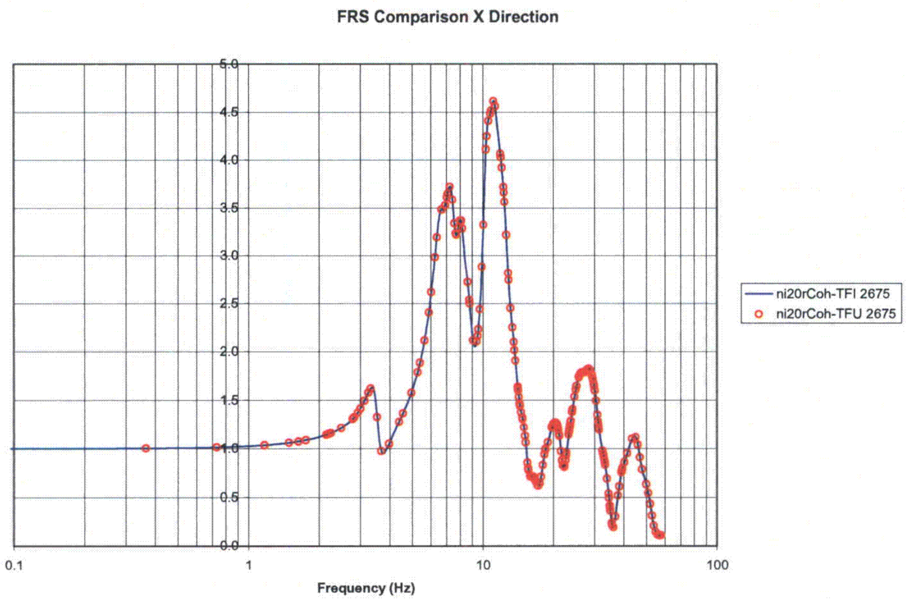

Figure RAI-SRP3.7.1-SEB1-11-41: Transfer Function Node 2675 X-Dir

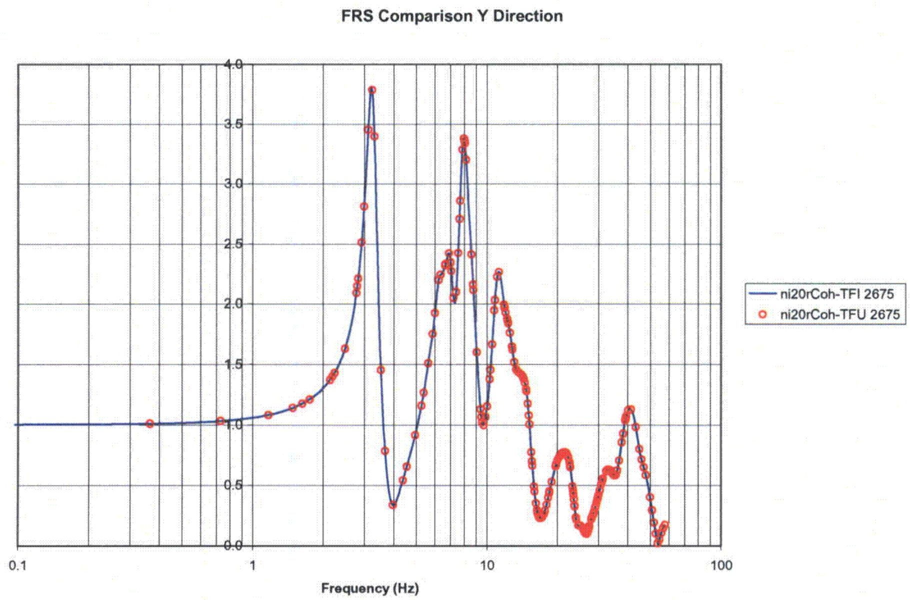

Figure RAI-SRP3.7.1-SEB1-11-42: Transfer Function Node 2675 Y-Dir

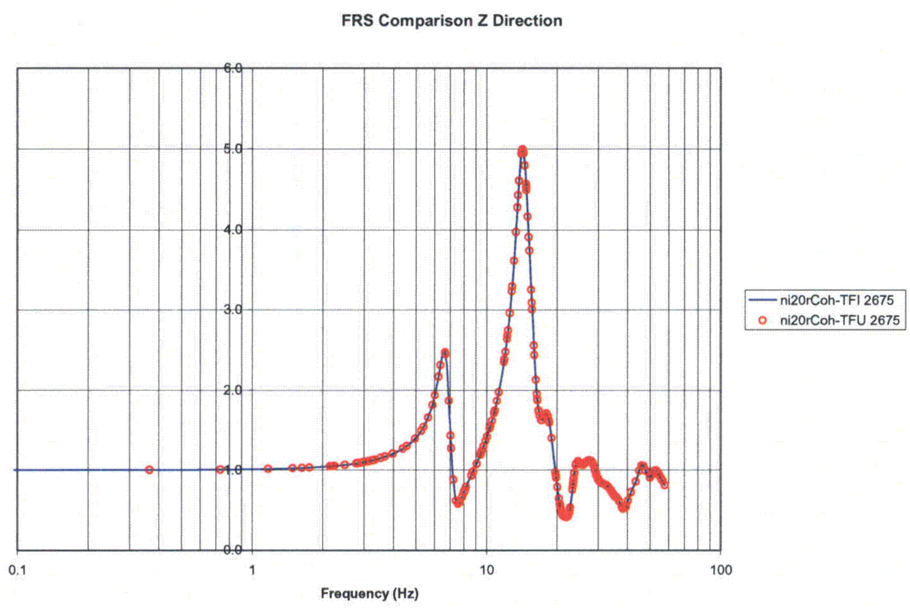

Figure RAI-SRP3.7.1-SEB1-11-43: Transfer Function Node 2675 Z-Dir

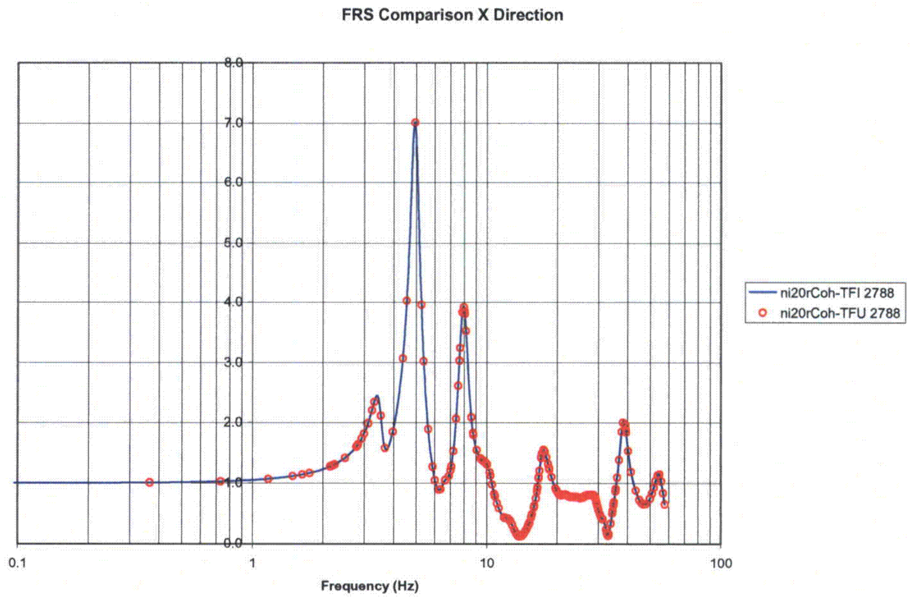

Figure RAI-SRP3.7.1-SEB1-11-44: Transfer Function Node 2788 X-Dir

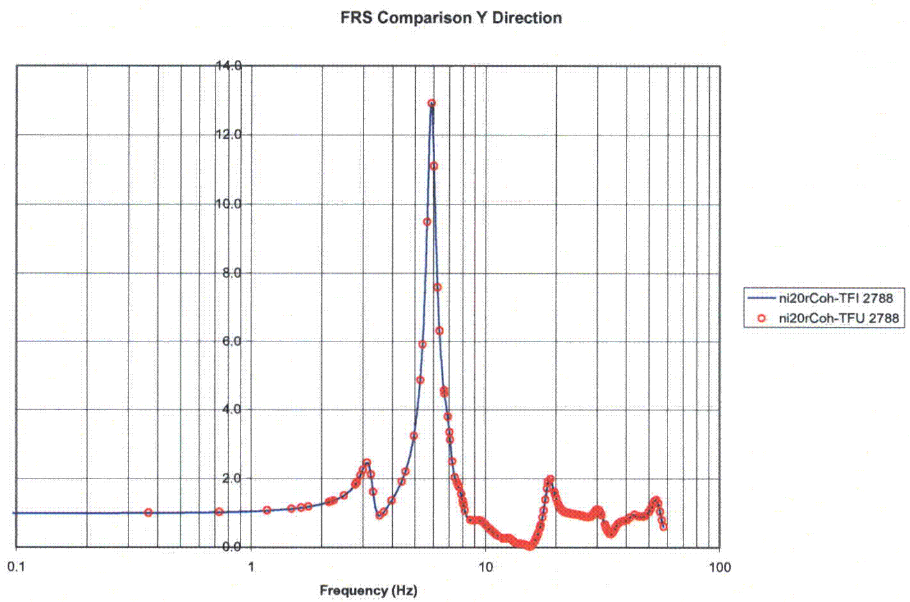

Figure RAI-SRP3.7.1-SEB1-11-45: Transfer Function Node 2788 Y-Dir

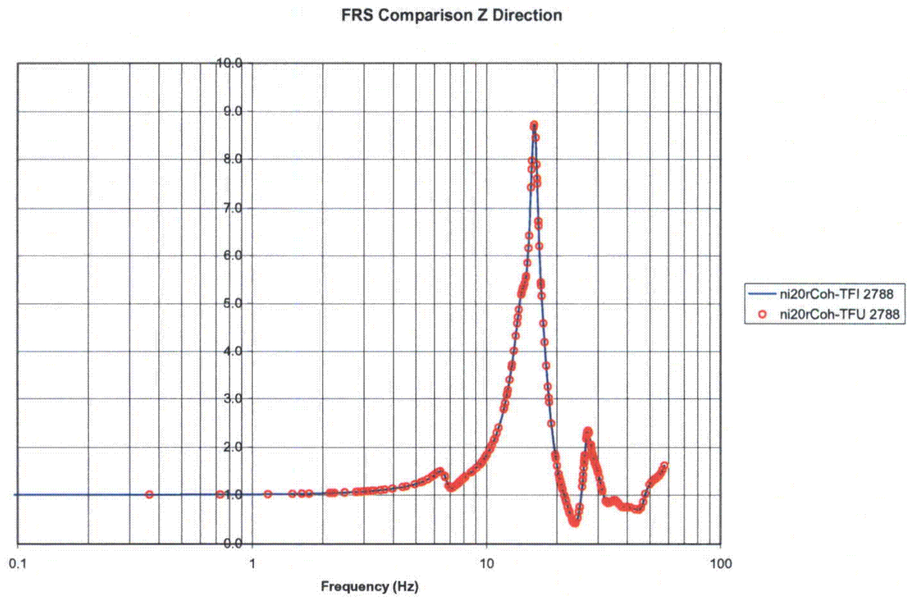

Figure RAI-SRP3.7.1-SEB1-11-46: Transfer Function Node 2788 Z-Dir

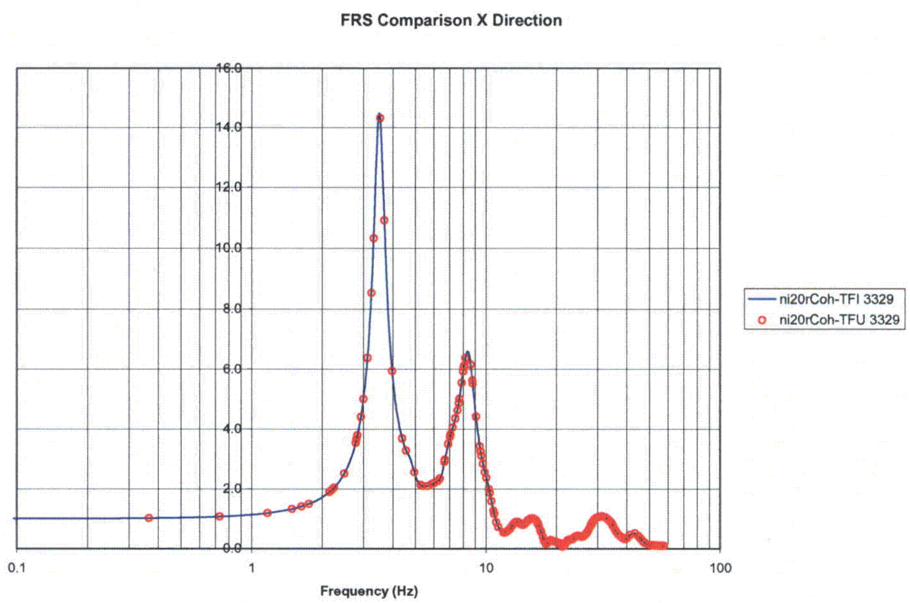

Figure RAI-SRP3.7.1-SEB1-11-47: Transfer Function Node 3329 X-Dir

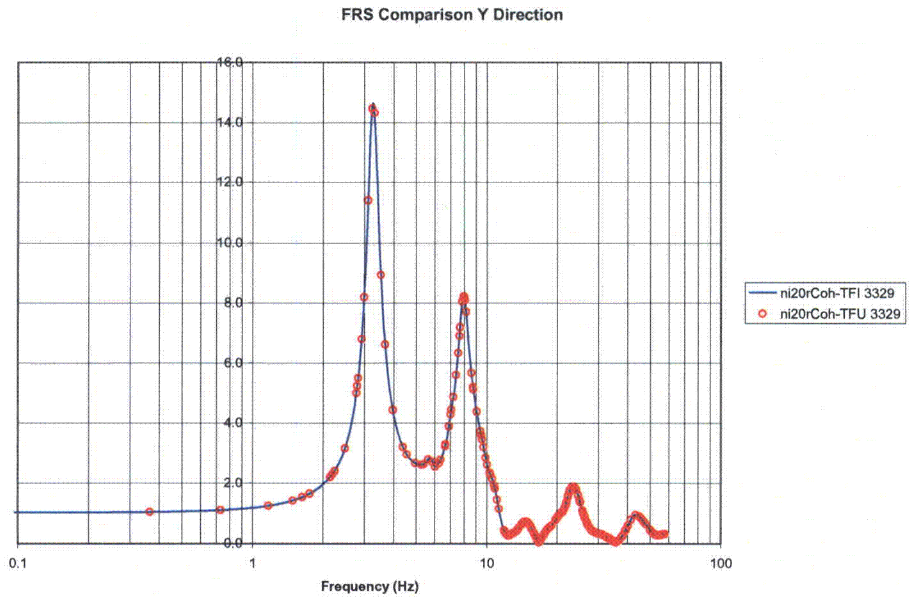

Figure RAI-SRP3.7.1-SEB1-11-48: Transfer Function Node 3329 Y-Dir

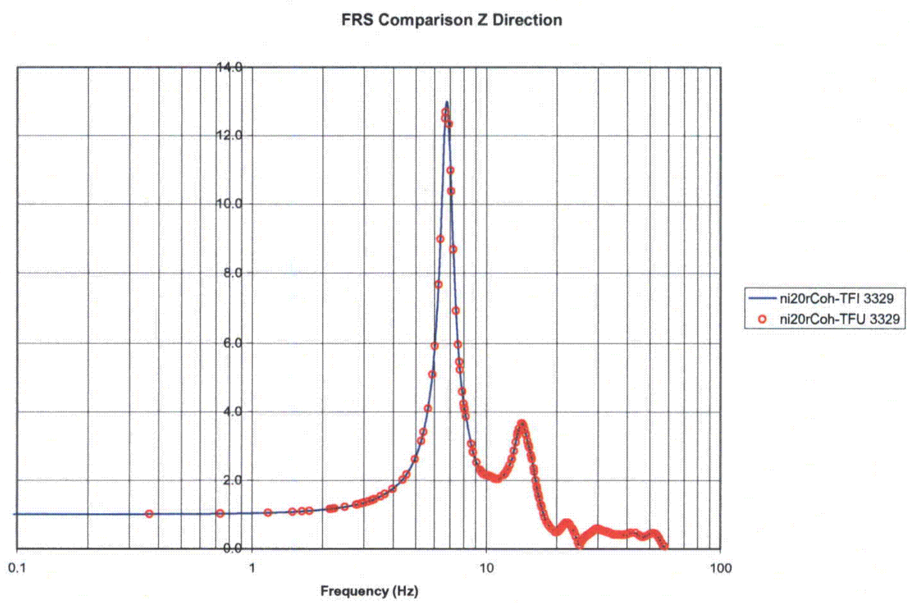

Figure RAI-SRP3.7.1-SEB1-11-49: Transfer Function Node 3329 Z-Dir

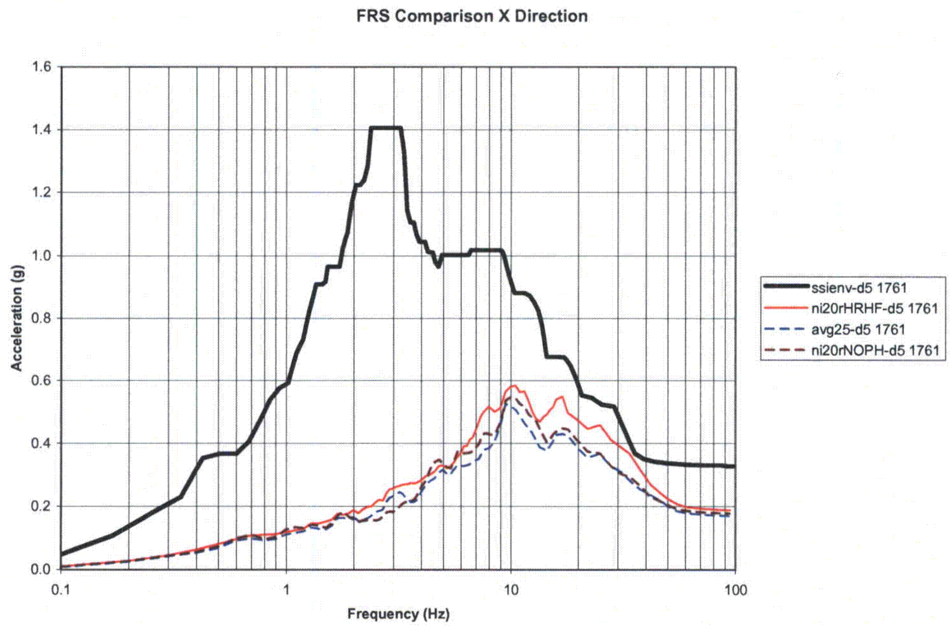

Figure RAI-SRP3.7.1-SEB1-11-50: CIS at Reactor Vessel Support Elevation X-Dir

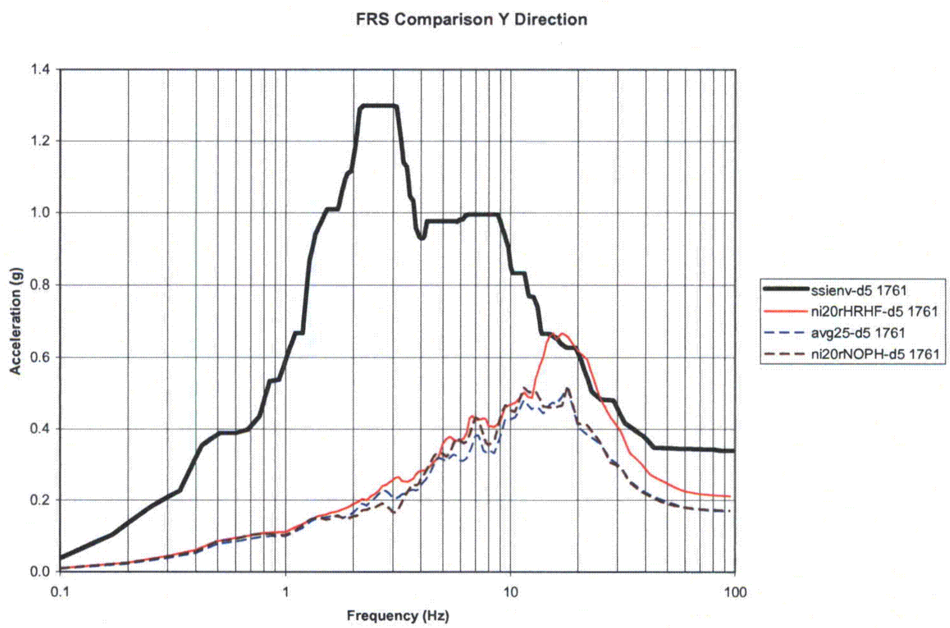

Figure RAI-SRP3.7.1-SEB1-11-51: CIS at Reactor Vessel Support Elevation Y-Dir

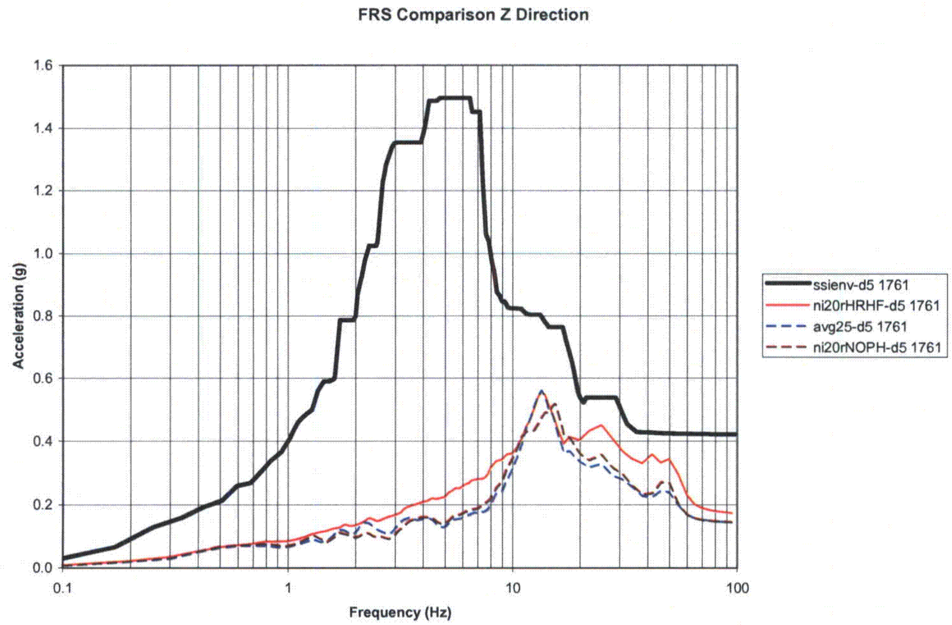

Figure RAI-SRP3.7.1-SEB1-11-52: CIS at Reactor Vessel Support Elevation Z-Dir

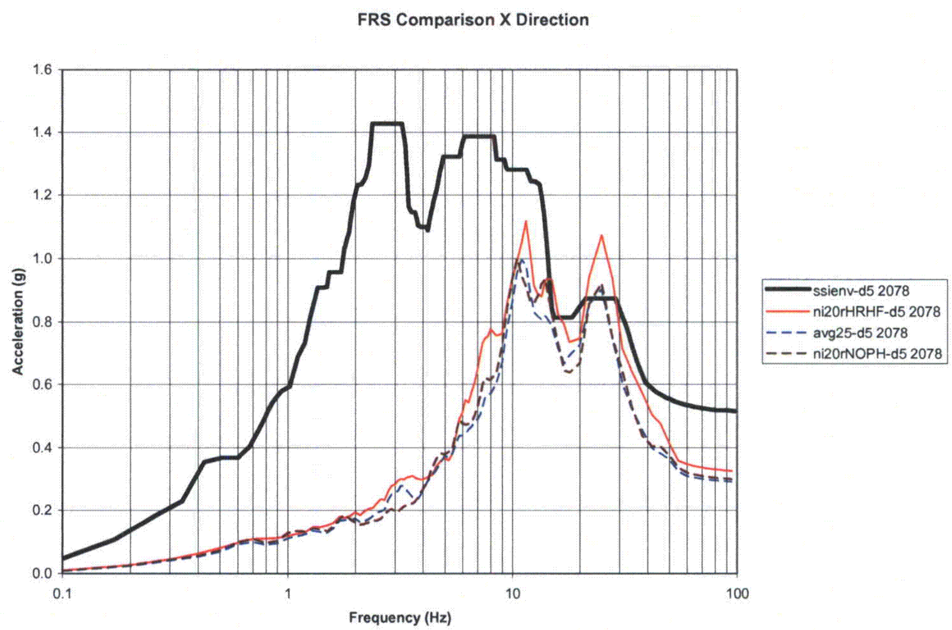

Figure RAI-SRP3.7.1-SEB1-11-53: ASB NE Corner at Control Room Floor X-Dir

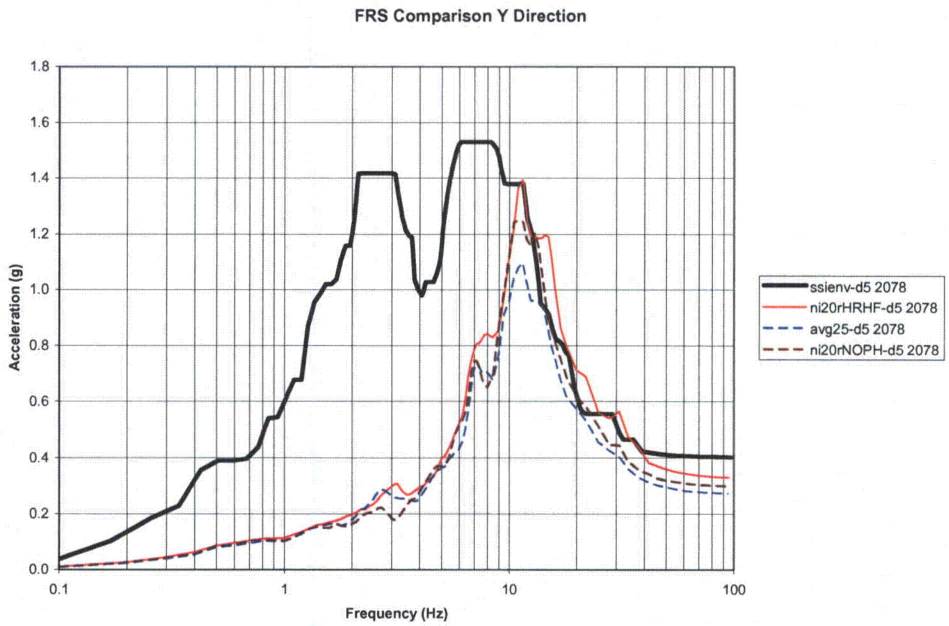

Figure RAI-SRP3.7.1-SEB1-11-54: ASB NE Corner at Control Room Floor Y-Dir

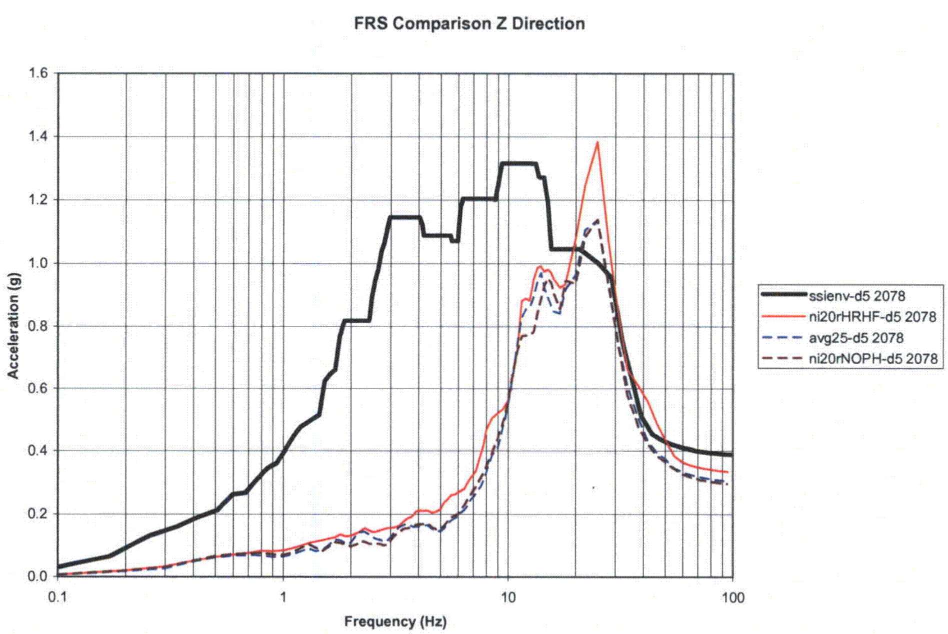

Figure RAI-SRP3.7.1-SEB1-11-55: ASB NE Corner at Control Room Floor Z-Dir

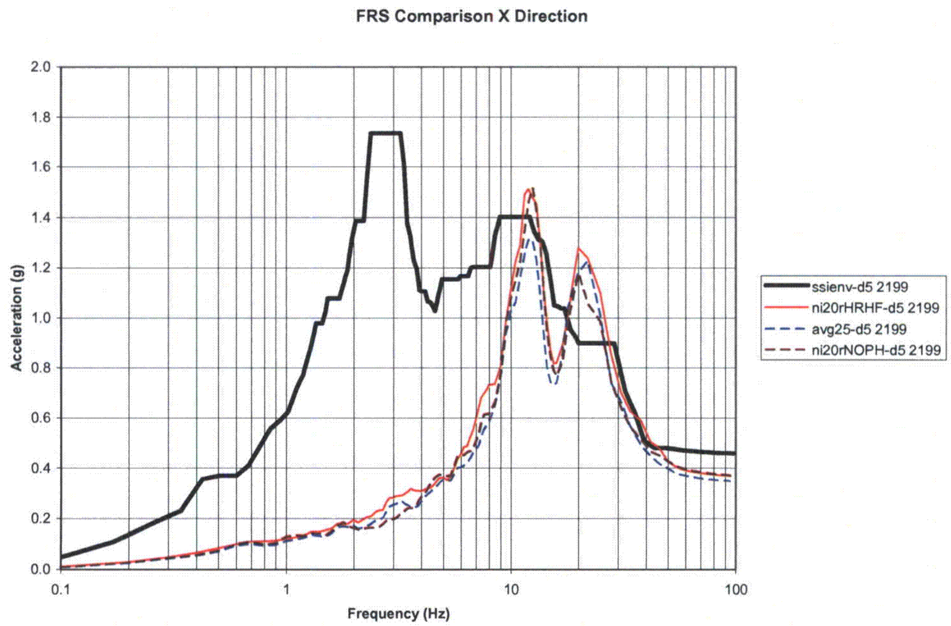

Figure RAI-SRP3.7.1-SEB1-11-56: CIS at Operating Deck X-Dir

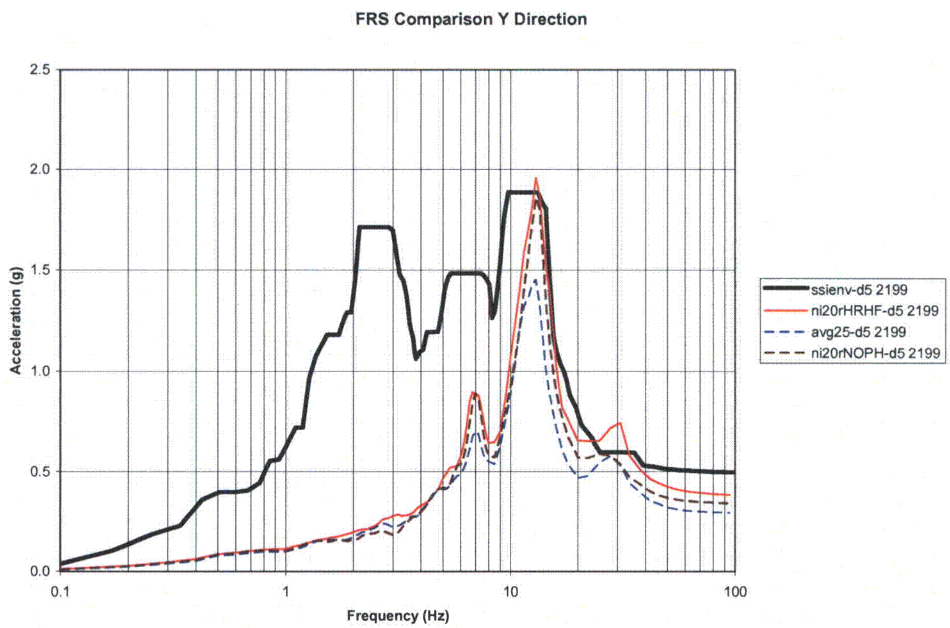

Figure RAI-SRP3.7.1-SEB1-11-57: CIS at Operating Deck Y-Dir

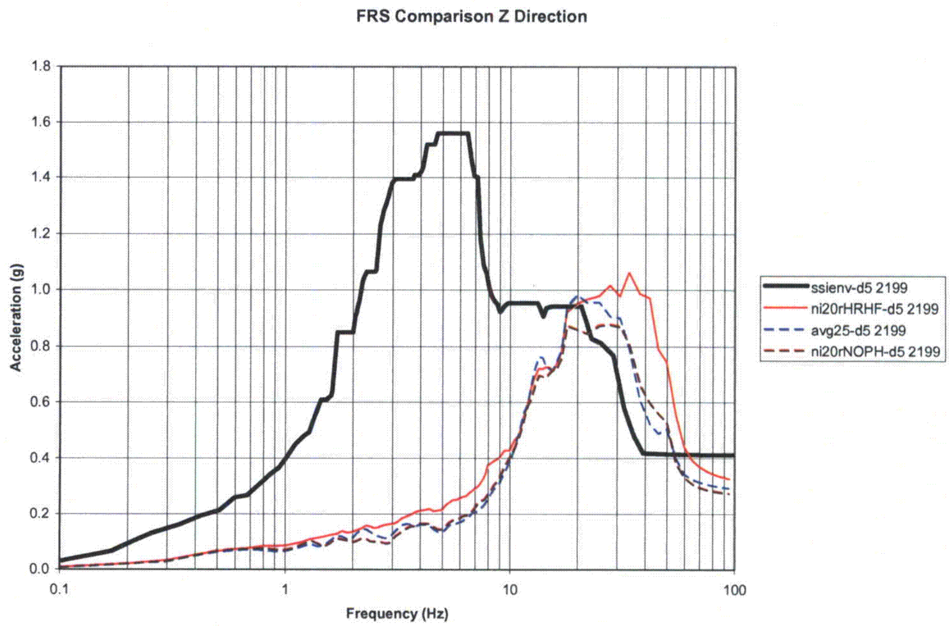

Figure RAI-SRP3.7.1-SEB1-11-58: CIS at Operating Deck Z-Dir

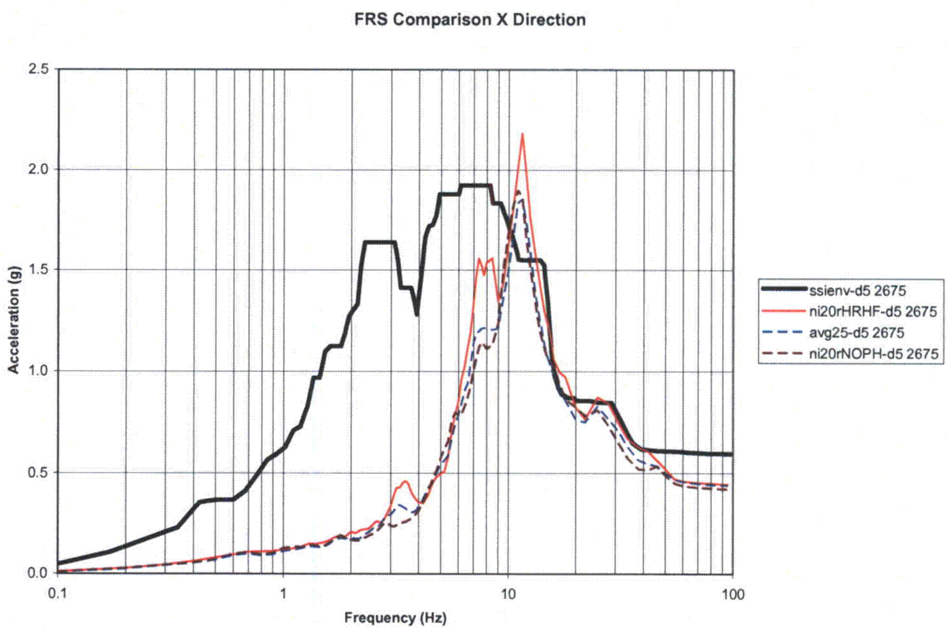

Figure RAI-SRP3.7.1-SEB1-11-59: ASB Corner of Fuel Building Roof X-Dir

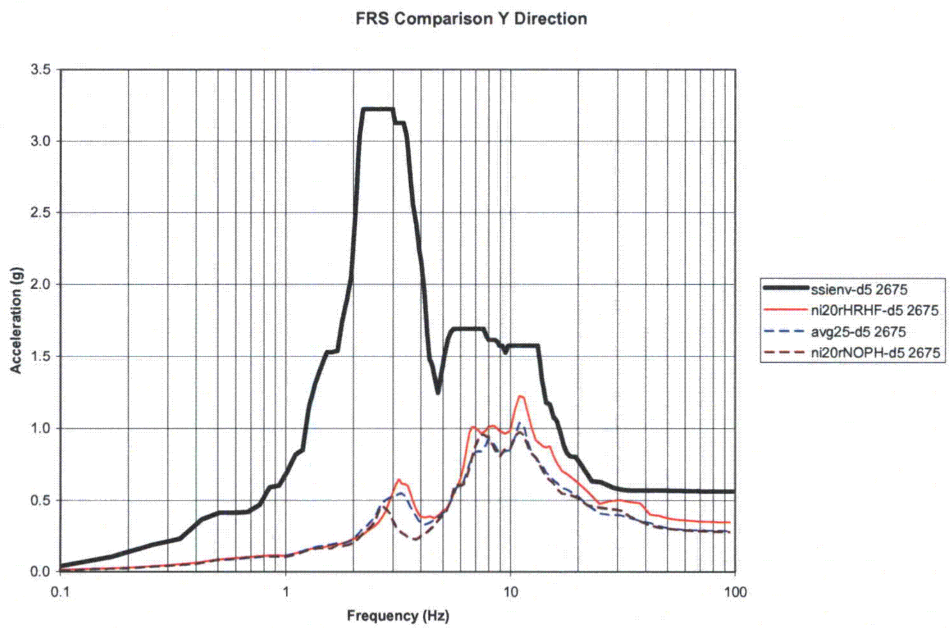

Figure RAI-SRP3.7.1-SEB1-11-60: ASB Corner of Fuel Building Roof Y-Dir

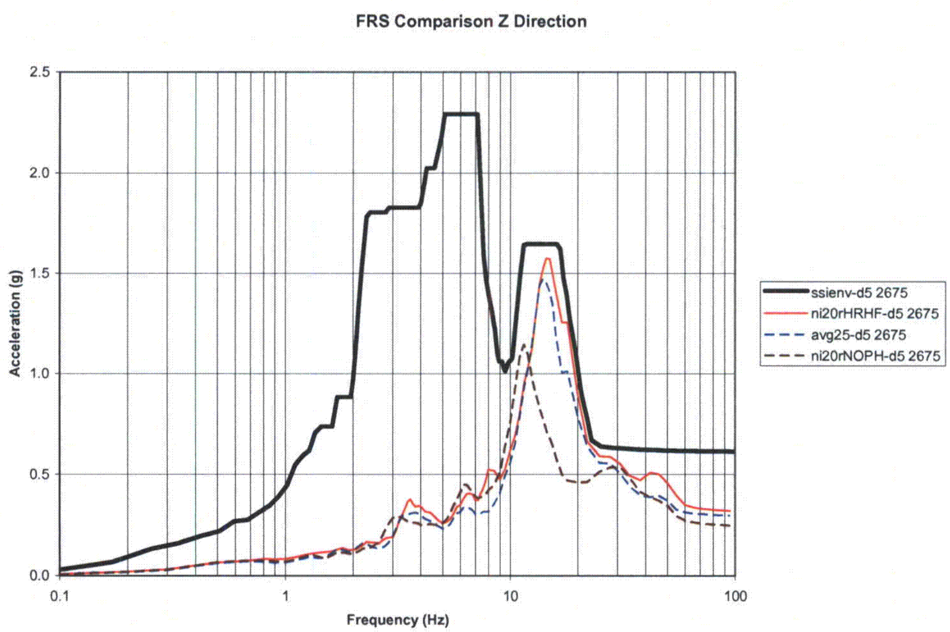

Figure RAI-SRP3.7.1-SEB1-11-61: ASB Corner of Fuel Building Roof Z-Dir

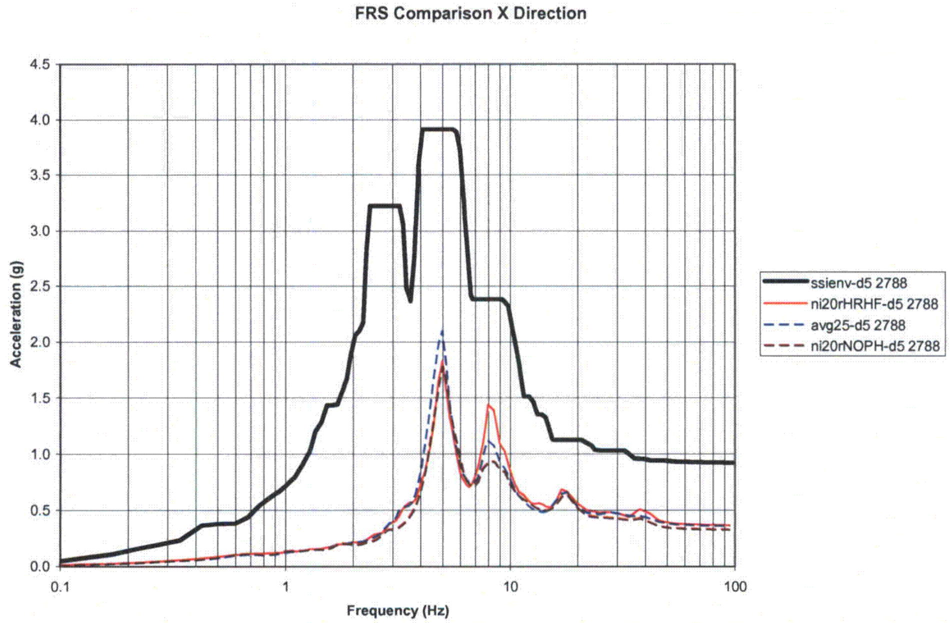

Figure RAI-SRP3.7.1-SEB1-11-62: SCV at Polar Crane Support X-Dir

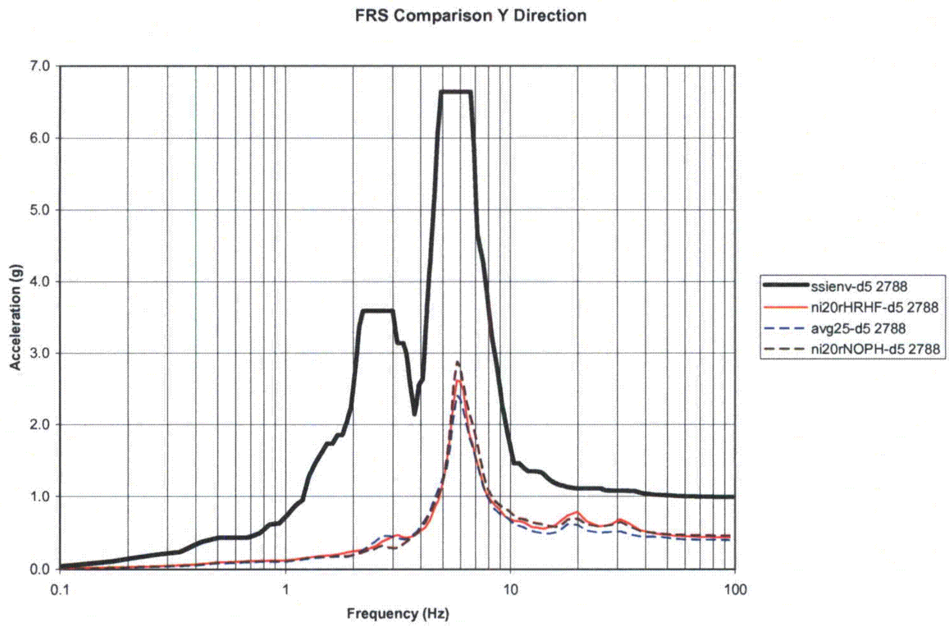

Figure RAI-SRP3.7.1-SEB1-11-63: SCV at Polar Crane Support Y-Dir

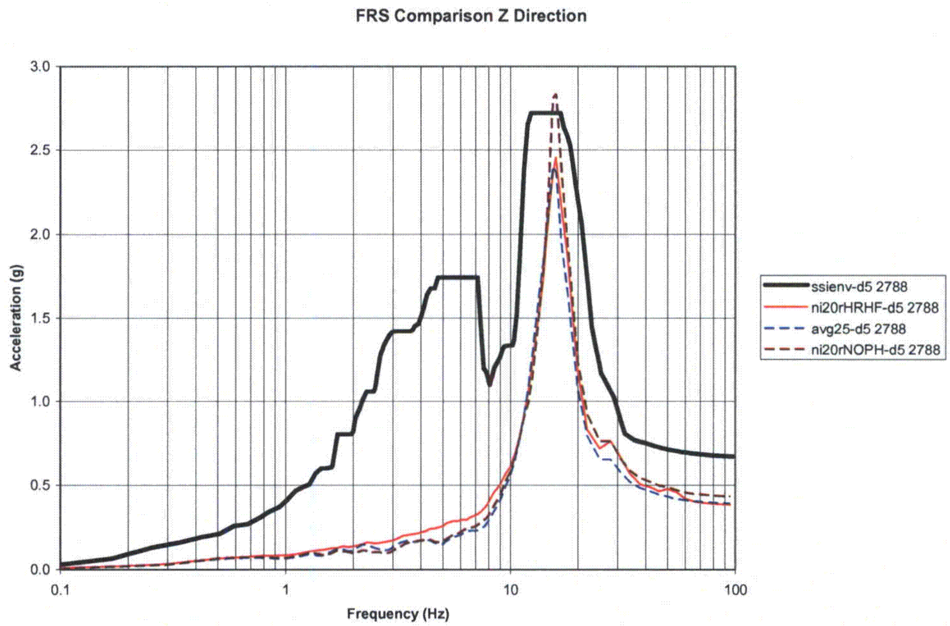

Figure RAI-SRP3.7.1-SEB1-11-64: SCV at Polar Crane Support Z-Dir

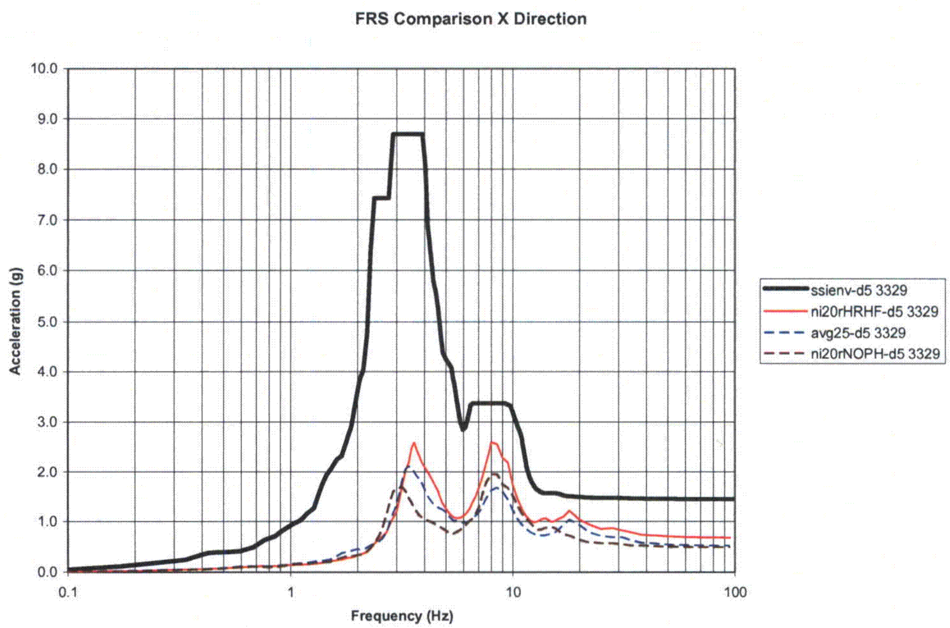

Figure RAI-SRP3.7.1-SEB1-11-65: Shield Building Roof X-Dir

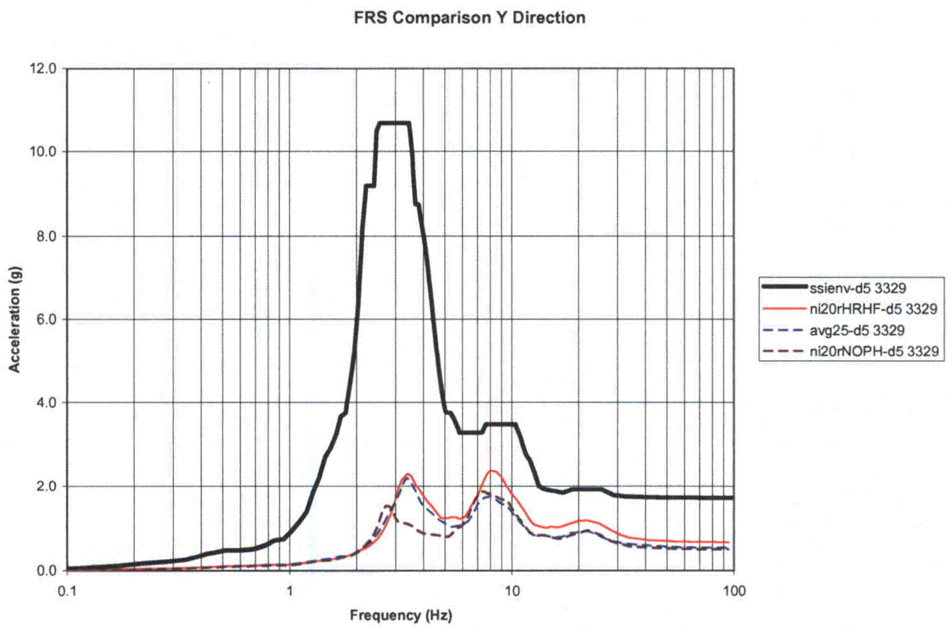

Figure RAI-SRP3.7.1-SEB1-11-66: Shield Building Roof Y-Dir

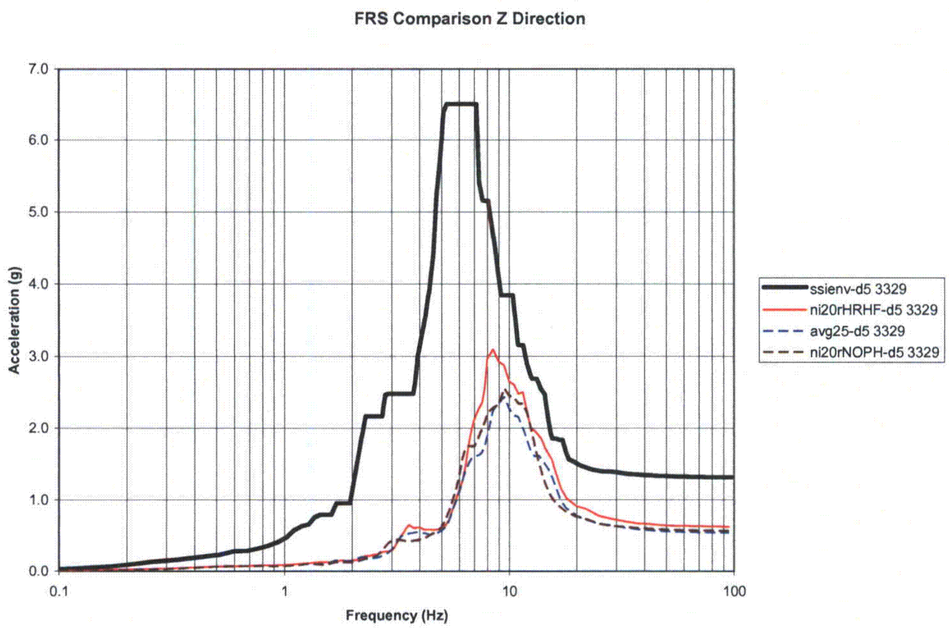

Figure RAI-SRP3.7.1-SEB1-11-67: Shield Building Roof Z-Dir

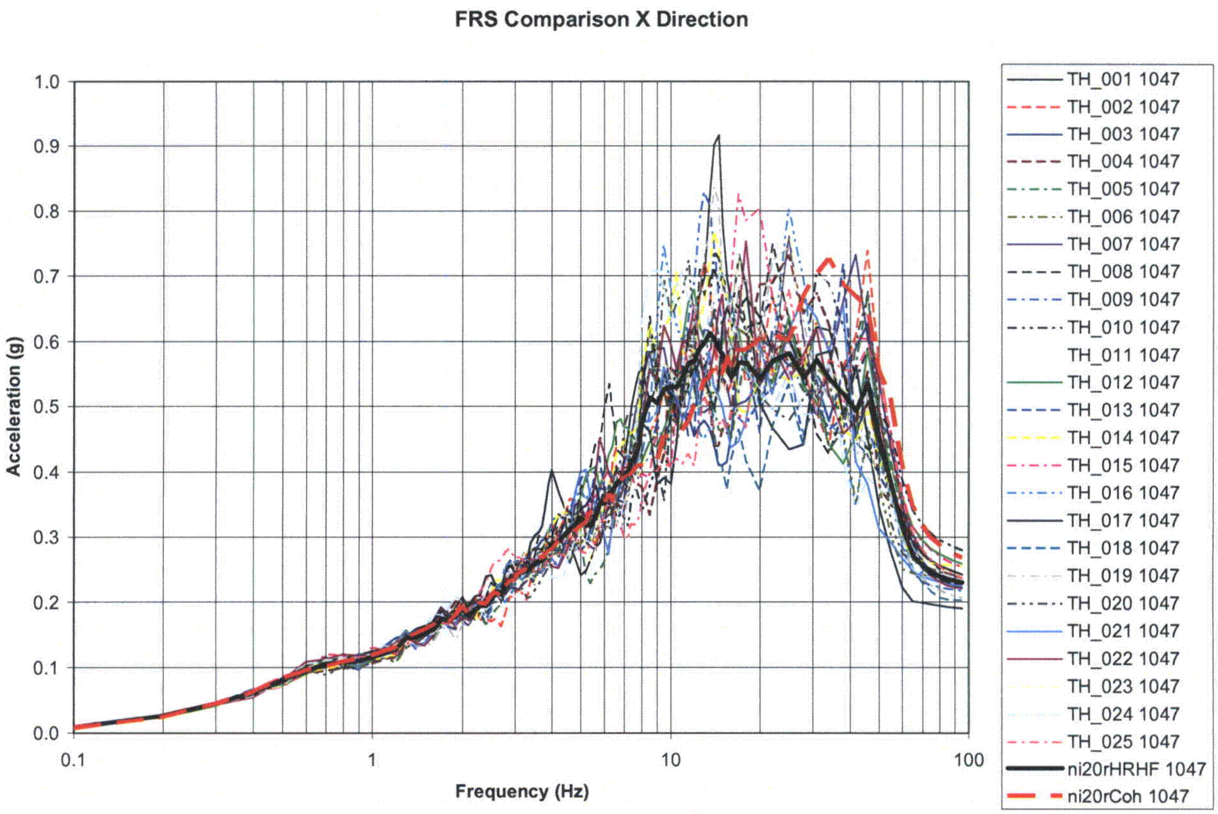

RAI-SRP3.7.1-SEB1-11-68: Node 1047 X-Direction, Southeast Corner

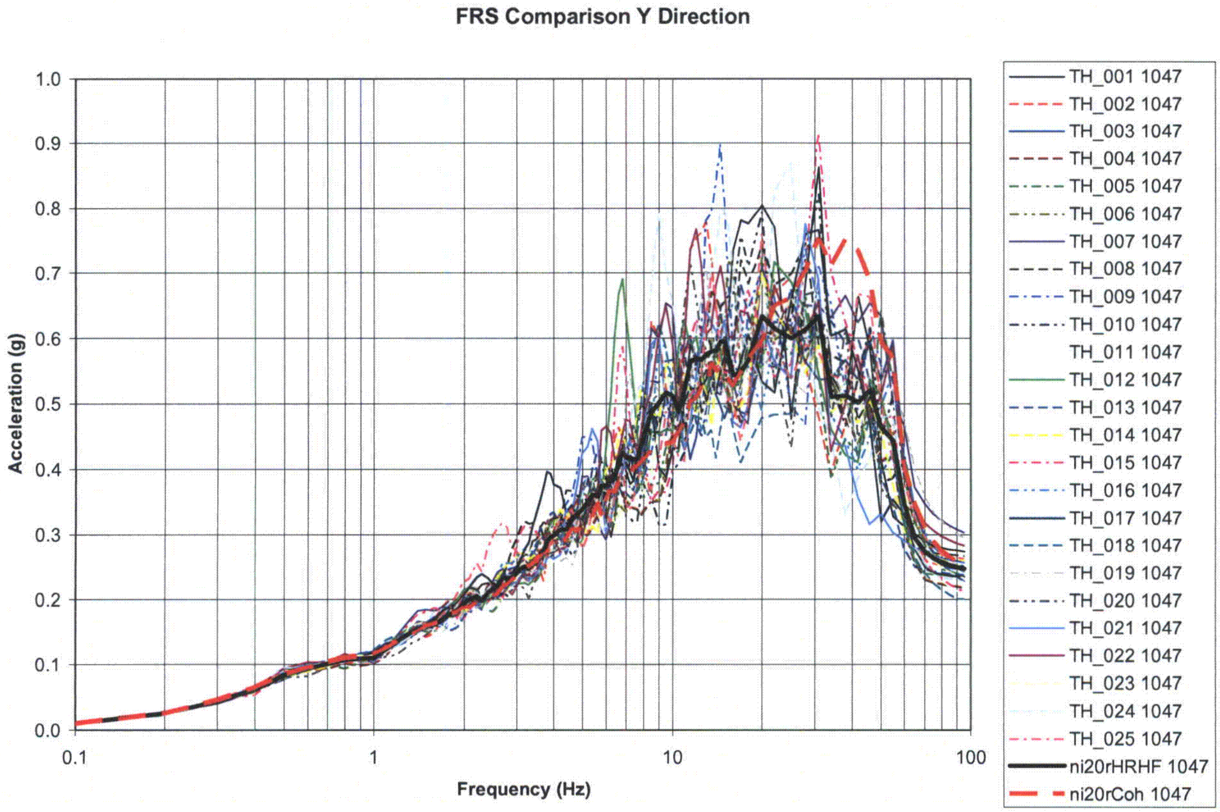

RAI-SRP3.7.1-SEB1-11-69: Node 1047 Y-Direction, Southeast Corner

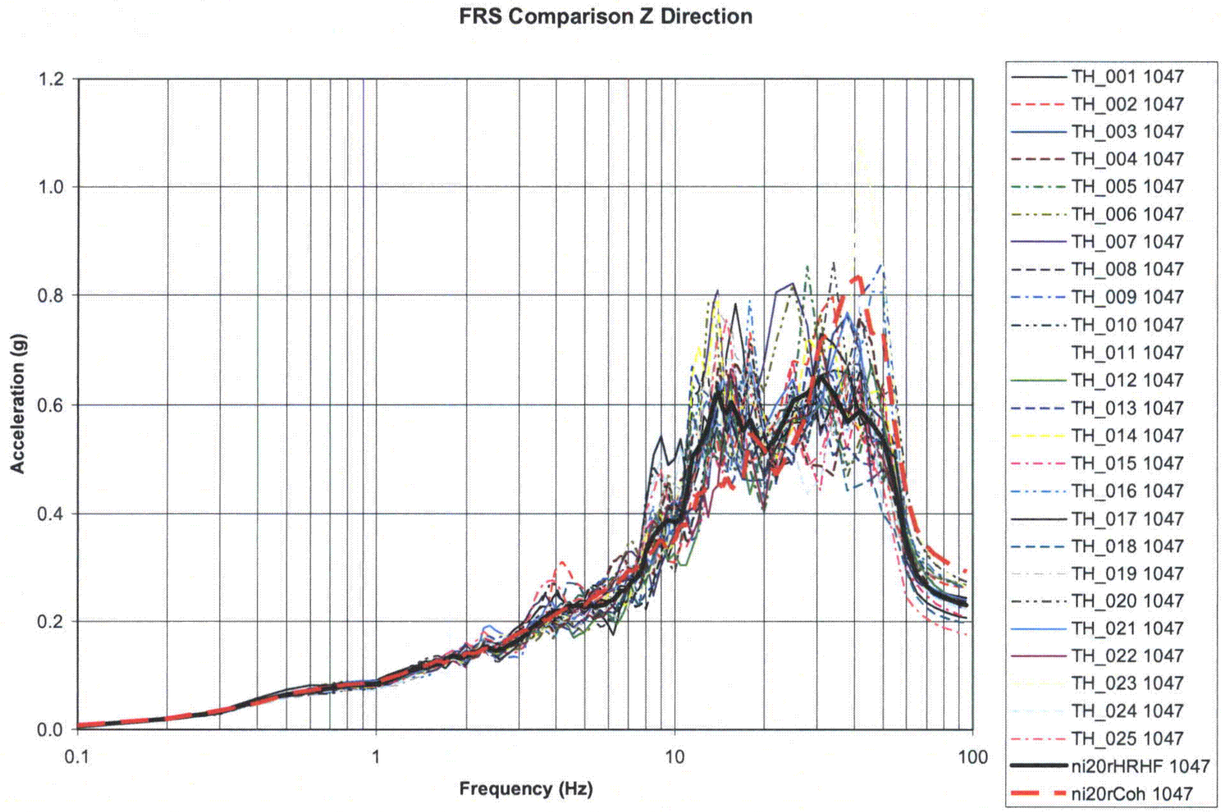

RAI-SRP3.7.1-SEB1-11-70: Node 1047 Z-Direction, Southeast Corner

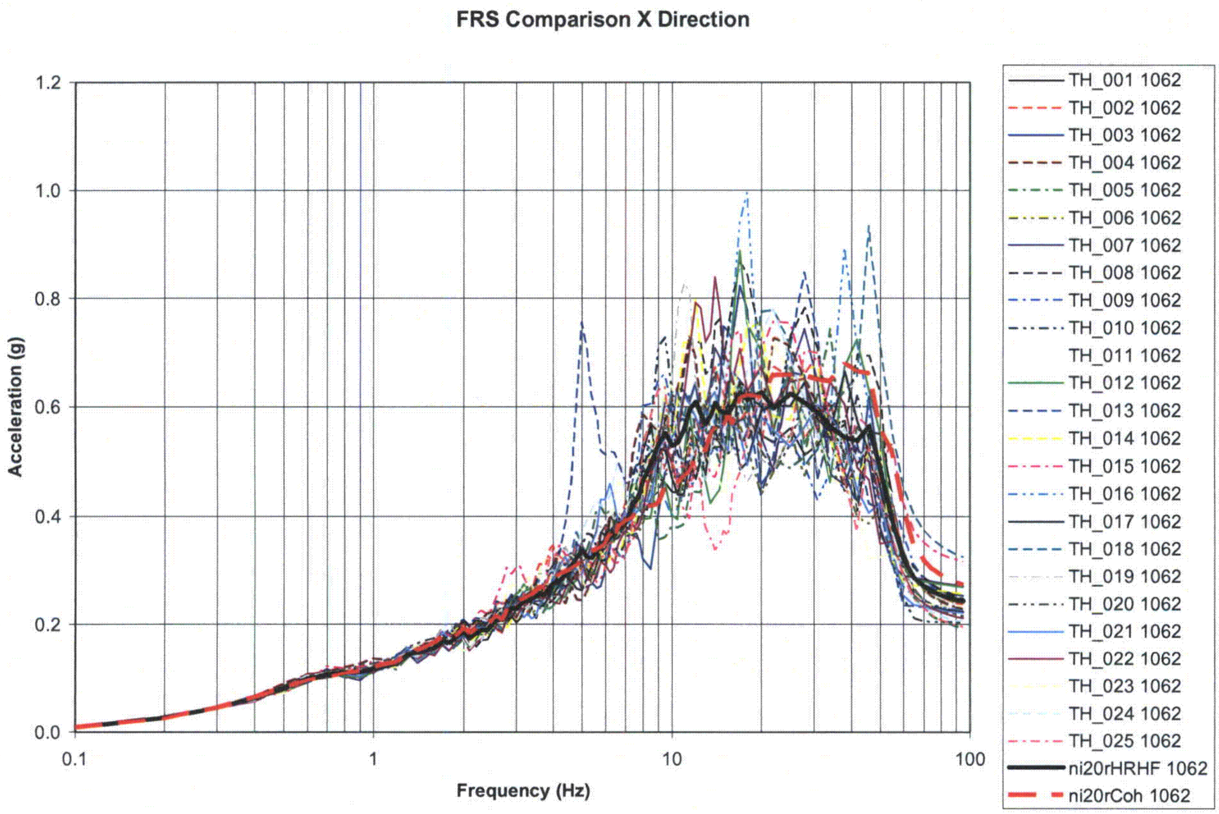

RAI-SRP3.7.1-SEB1-11-71: Node 1062 X-Direction, Northeast Corner

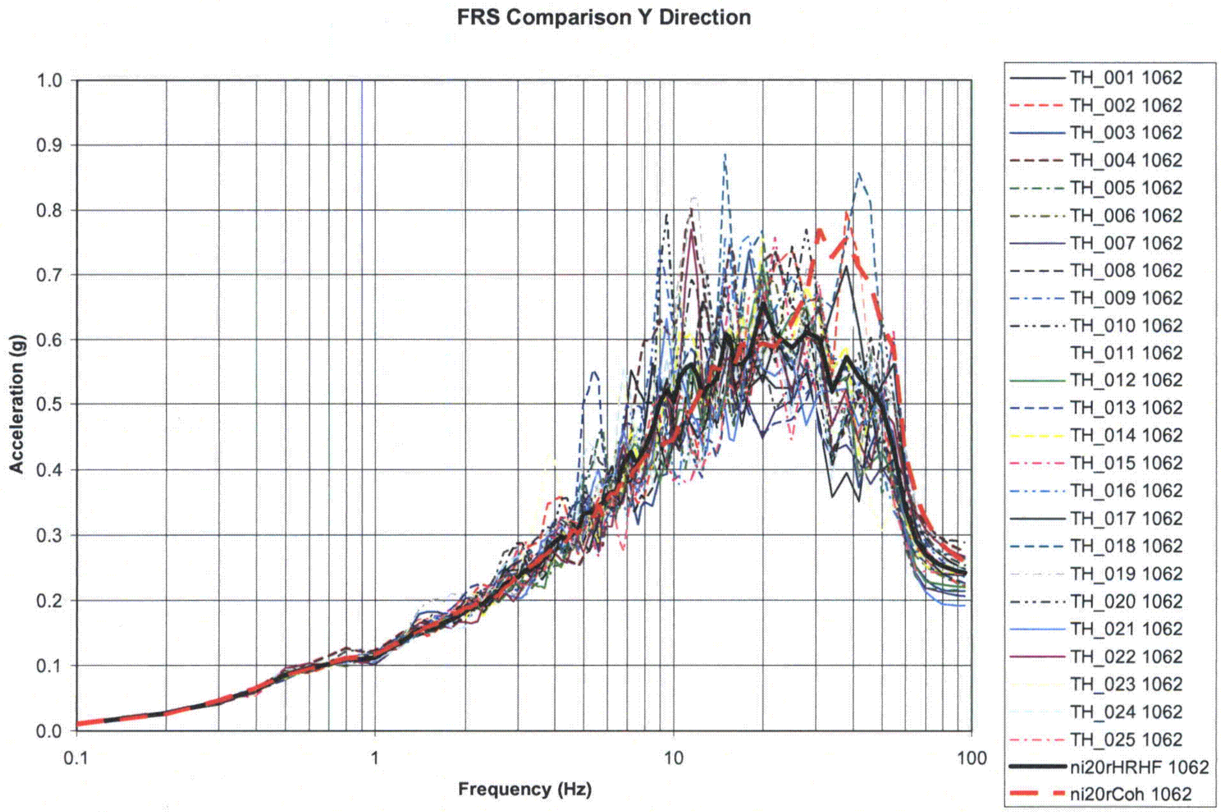

RAI-SRP3.7.1-SEB1-11-72: Node 1062 Y-Direction, Northeast Corner

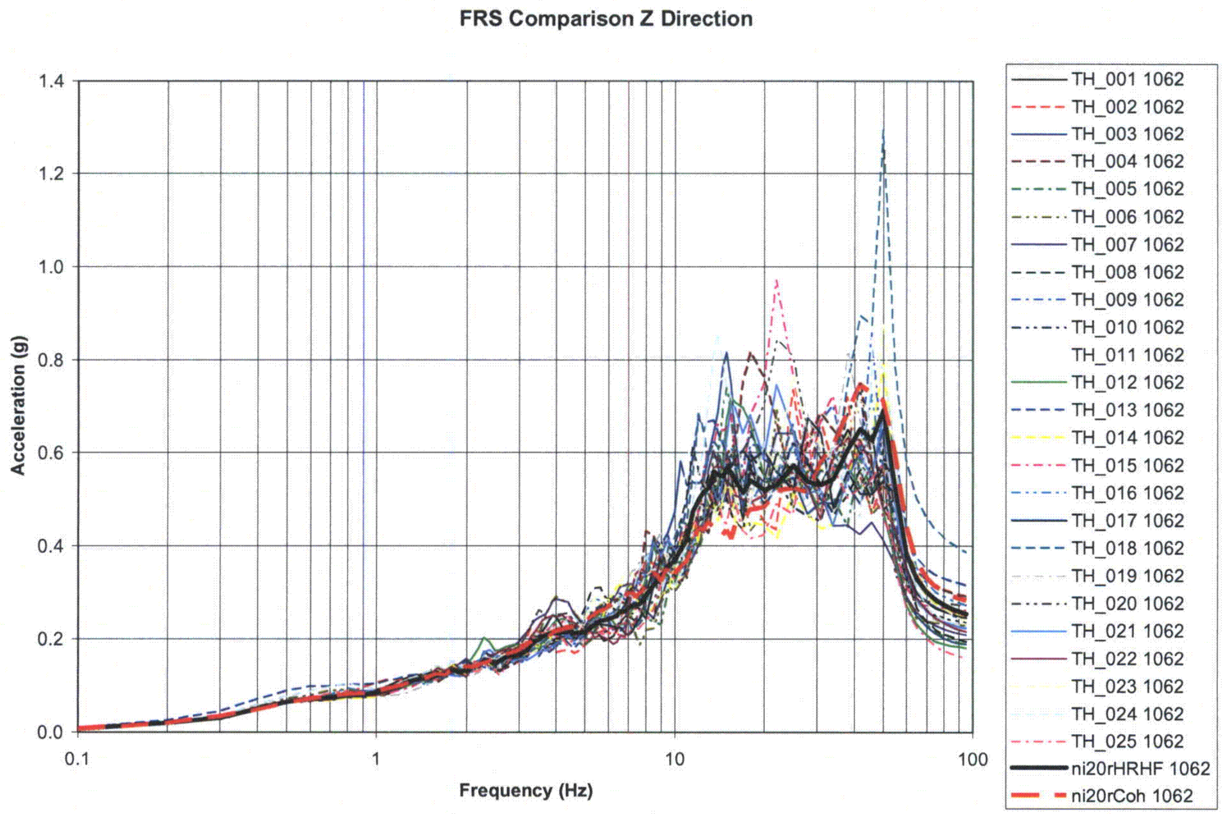

RAI-SRP3.7.1-SEB1-11-73: Node 1062 Z-Direction, Northeast Corner

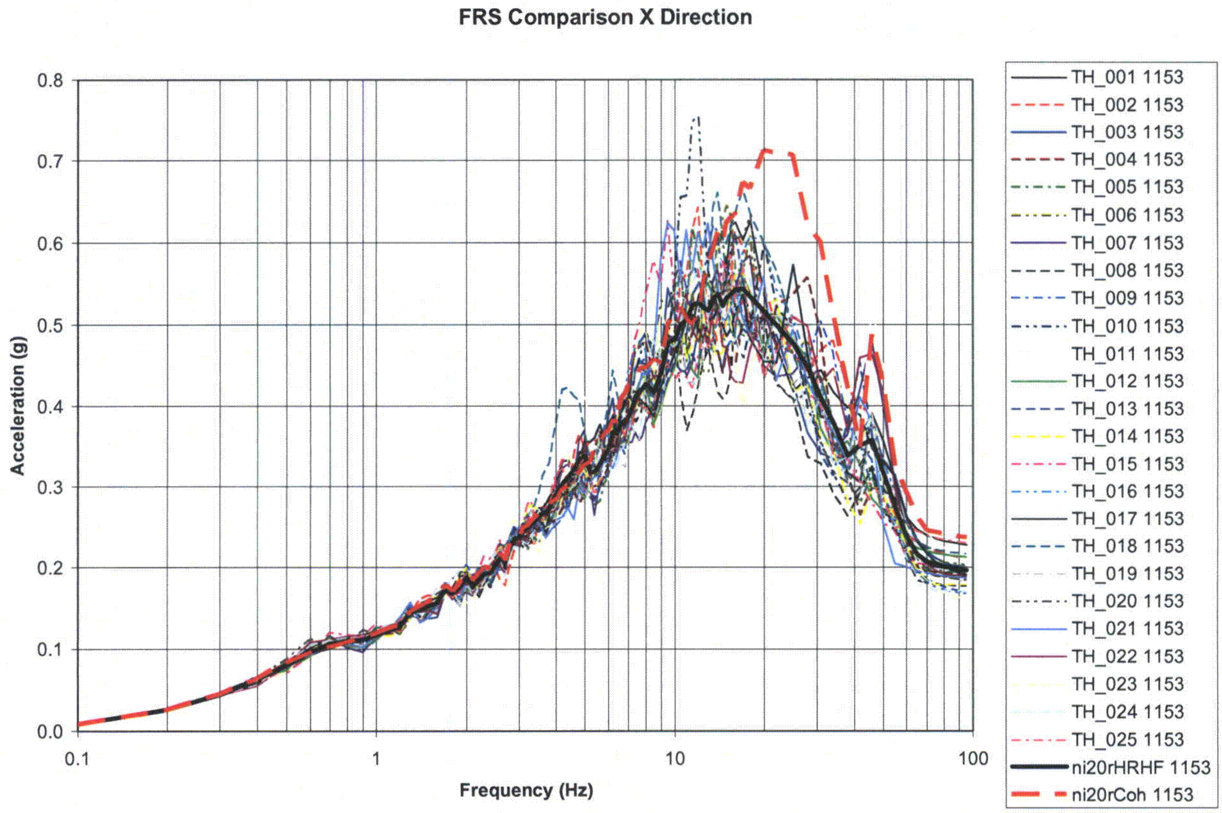

RAI-SRP3.7.1-SEB1-11-74: Node 1153 X-Direction, Center Basemat

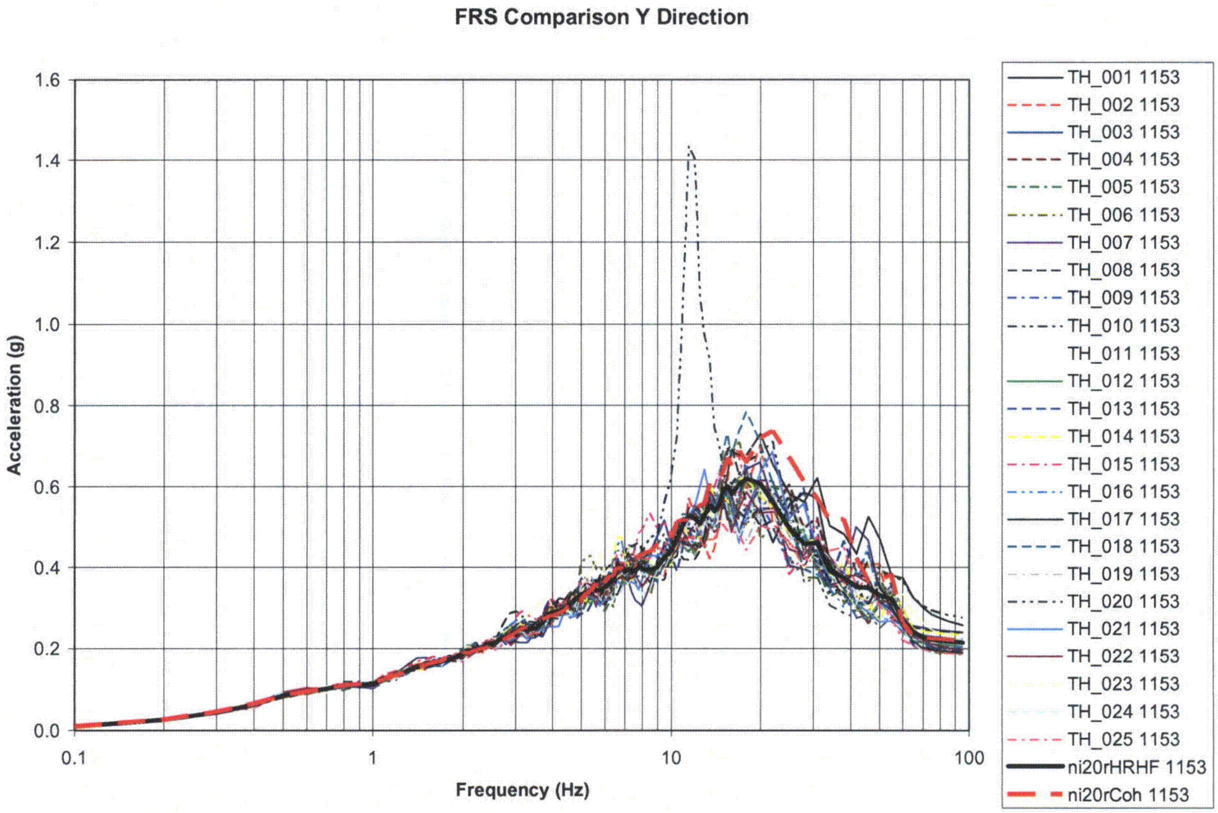

RAI-SRP3.7.1-SEB1-11-75: Node 1153 Y-Direction, Center Basemat

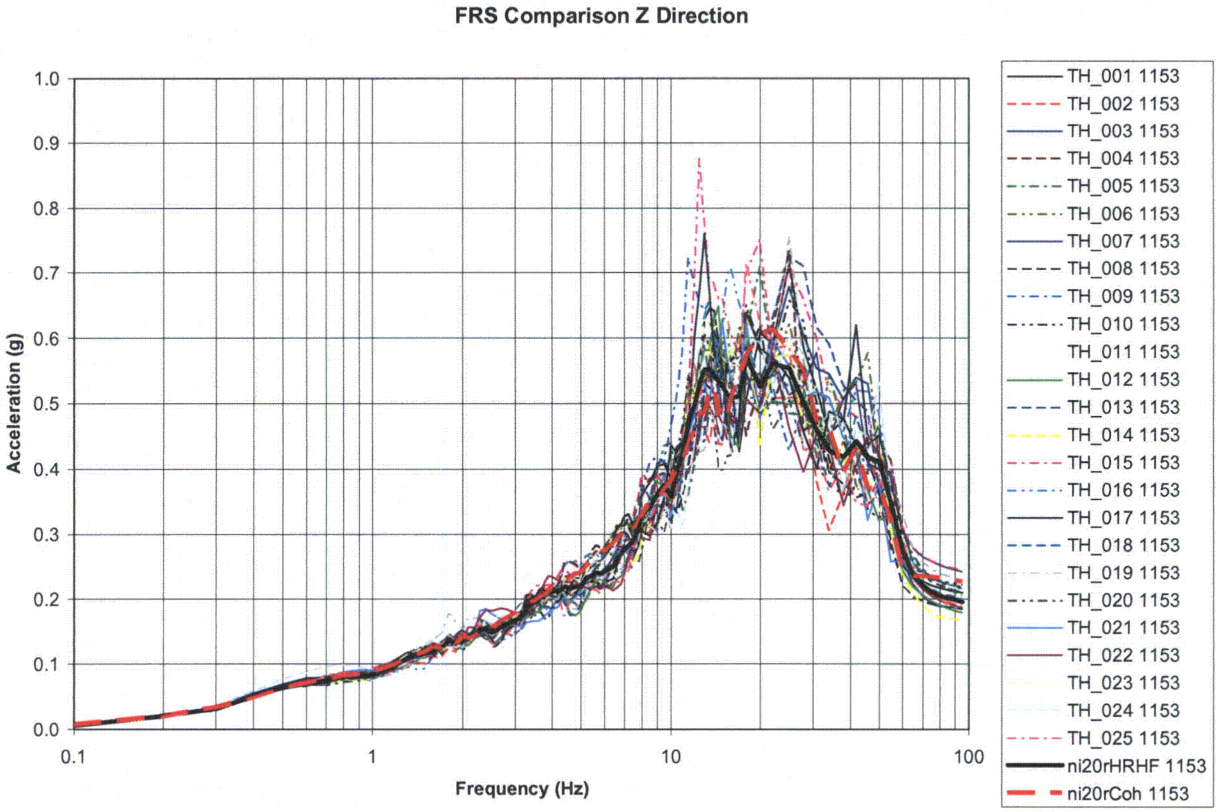

RAI-SRP3.7.1-SEB1-11-76: Node 1153 Z-Direction, Center Basemat

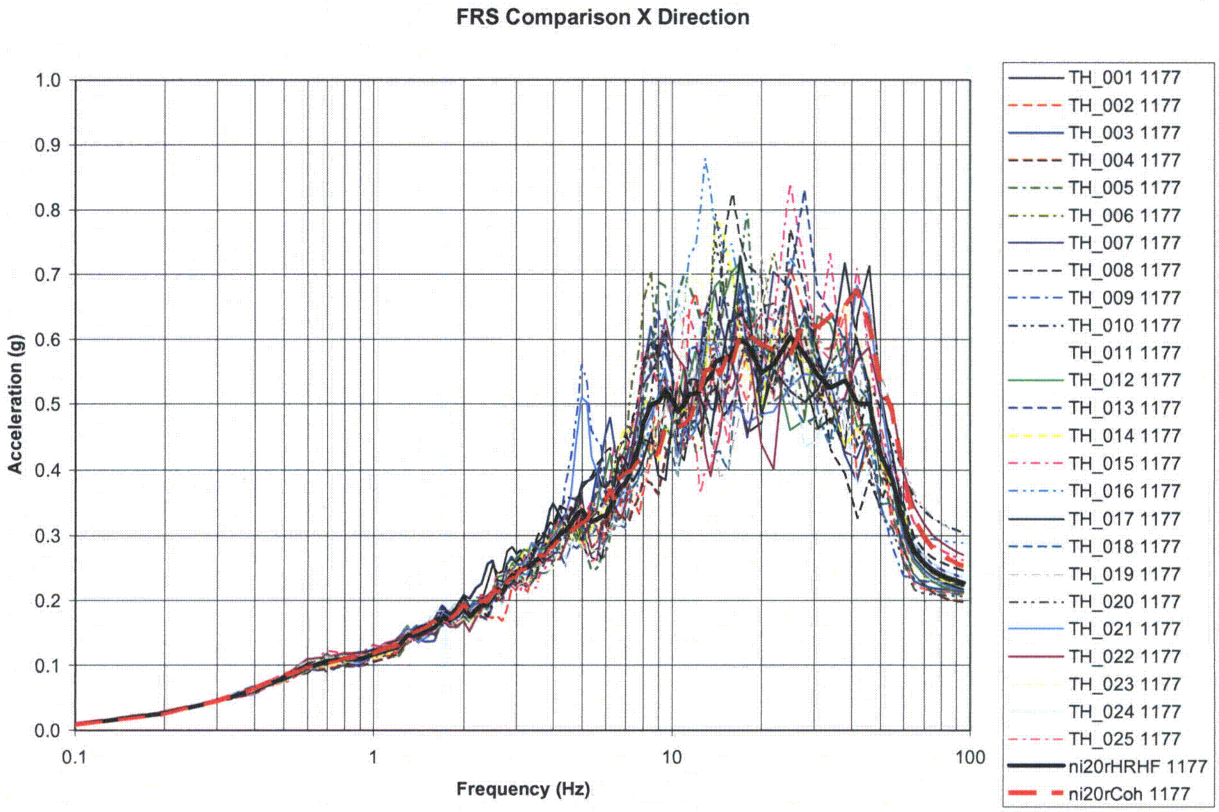

RAI-SRP3.7.1-SEB1-11-77: Node 1177 X-Direction, Southwest Corner

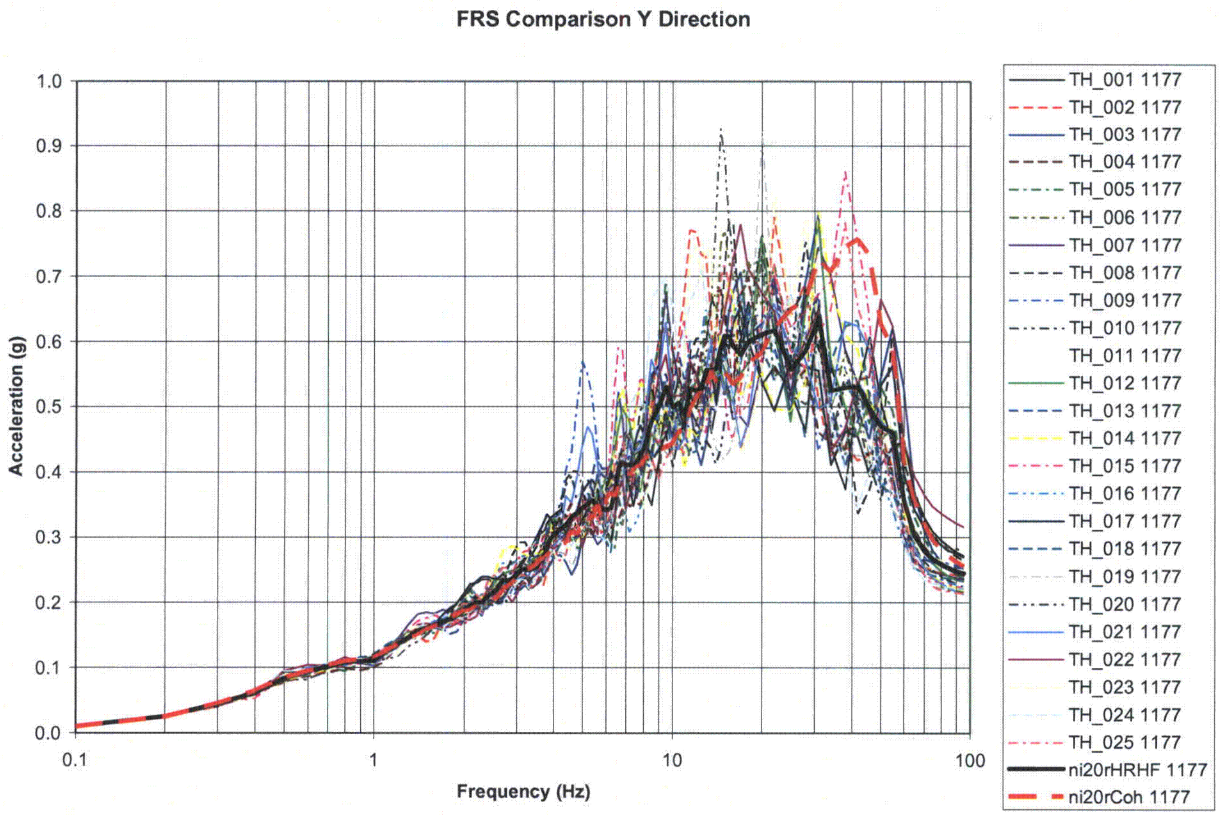

RAI-SRP3.7.1-SEB1-11-78: Node 1177 Y-Direction, Southwest Corner

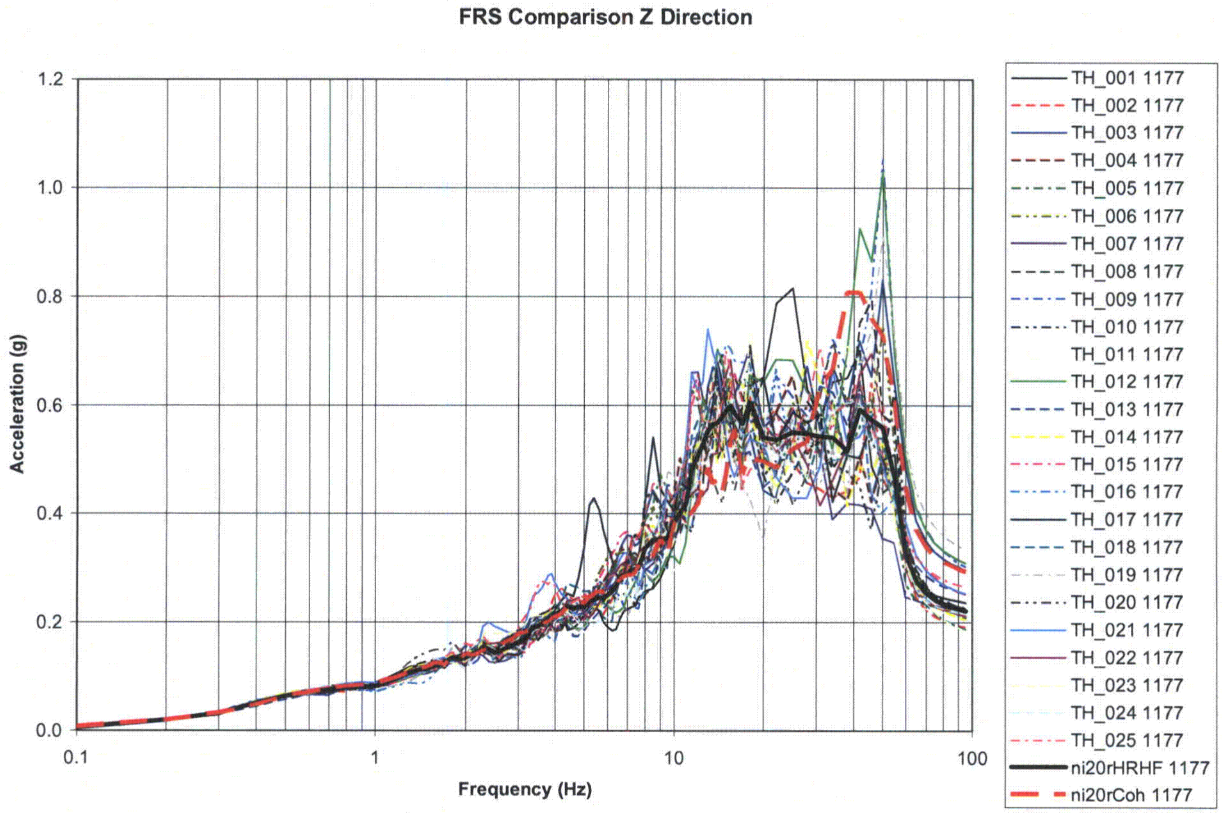

RAI-SRP3.7.1-SEB1-11-79: Node 1177 Z-Direction, Southwest Corner

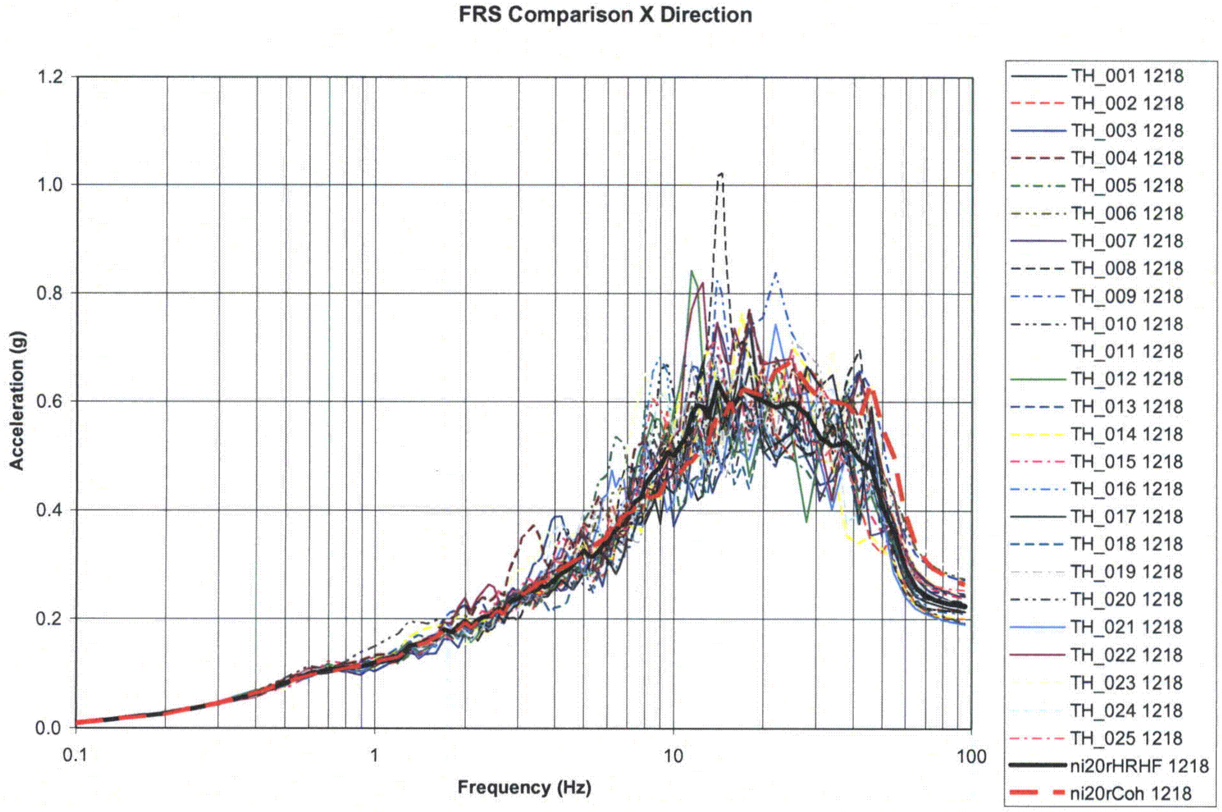

RAI-SRP3.7.1-SEB1-11-80: Node 1218 X-Direction, Northwest Corner

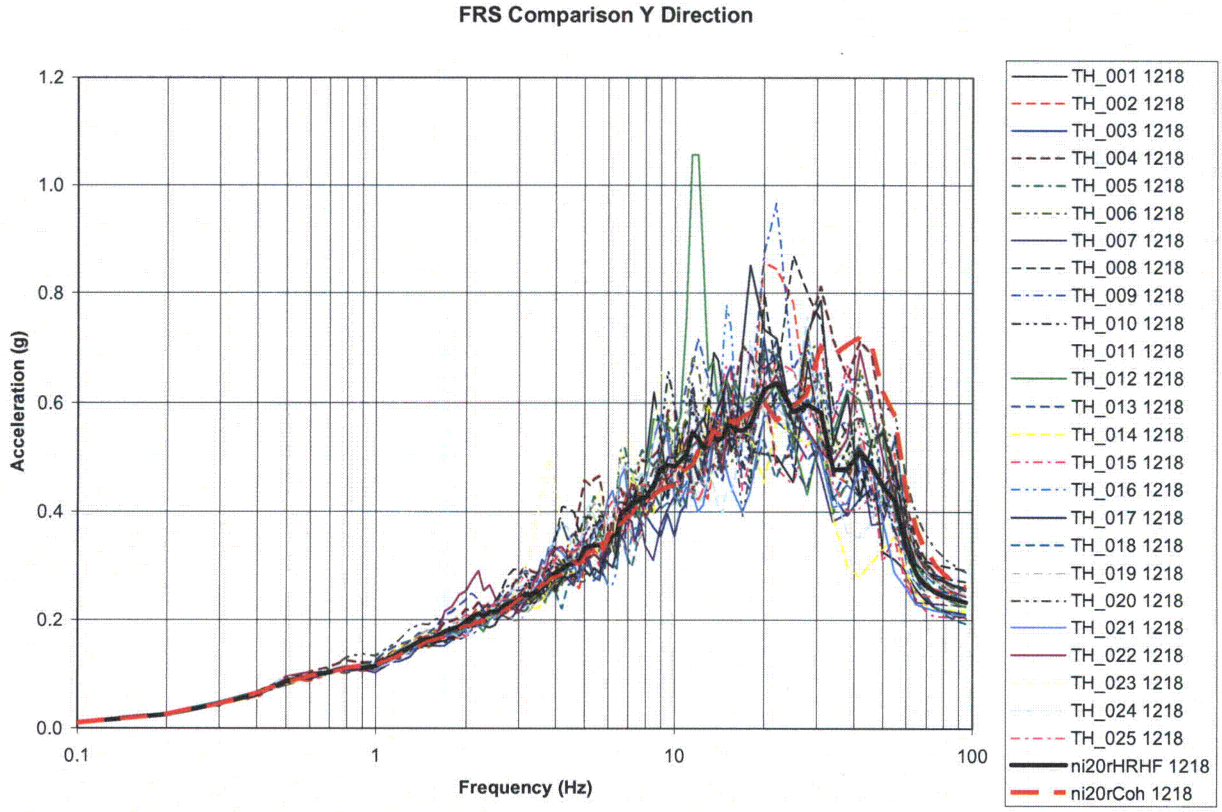

RAI-SRP3.7.1-SEB1-11-81: Node 1218 Y-Direction, Northwest Corner

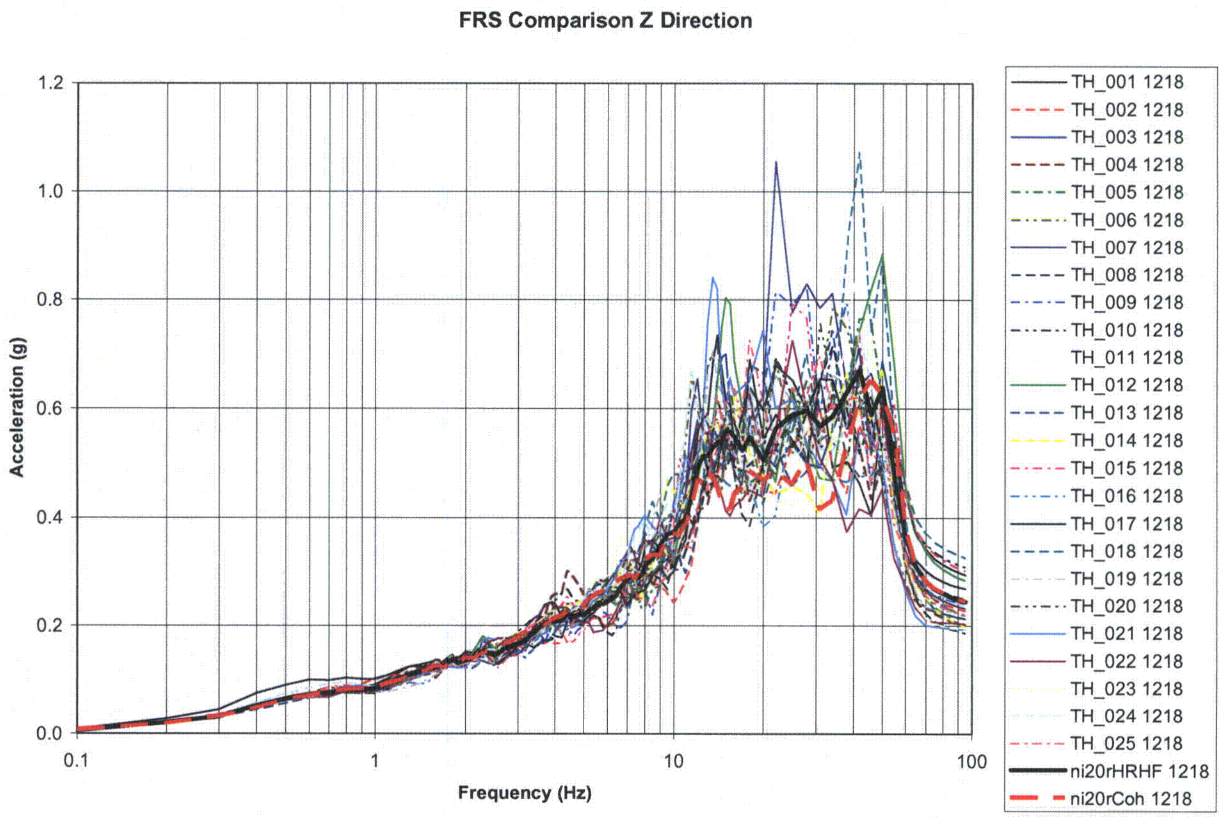

RAI-SRP3.7.1-SEB1-11-82: Node 1218 Z-Direction, Northwest Corner

AP1000 TECHNICAL REPORT REVIEW

Response to Request For Additional Information (RAI)

RAI Response Number: RAI-SRP3.8.2-CIB1-01
Revision: 5

Question:

Tier 2, Section 3.8.2.6 of the AP1000 DCD, describes the materials used to fabricate the containment vessel. The material selected satisfies the lowest service metal temperature requirement, established by analysis for the portion of the vessel exposed to the environment when the ambient air temperature is -40 °F. Westinghouse Technical Report APP-GW-GLN-113 (TR-113), "AP1000 Containment Vessel Shell Material Specification," Revision 0, submitted by Westinghouse letter dated May 11, 2007, revised this section by replacing the material specification Supplementary Requirement S17 with Supplementary Requirement S1 concerning the material fabrication process. However, Revision 16 to AP1000, Section 3.8.2.6 was changed to specify the lowest service temperature of -18.5 degrees F instead of -15 °F which was previously stated in Revision 15 of the AP1000 DCD. TR-113 did not specify the change to the service temperature nor provided any justification for this change in service temperature as required by 10 CFR 52.63(a)(1). In NUREG-1793, Section 3.8.2.6, the NRC staff approved -15 °F as the lowest service temperature based on the staff review of Westinghouse calculation APP-PCS-M3C-002, Revision 1, "AP1000 Containment Shell Minimum Service Temperature." Therefore, provide the reason and justification for the change in minimum service temperature of the containment vessel in accordance with 10 CFR 52.63(a)(1), and the analysis that supports the new service temperature proposed in Revision 16 of the AP1000 DCD.

Additional Question (Revision 1)

In a letter dated July 22, 2008, Westinghouse stated that an additional scenario was postulated for the containment vessel shell analysis, which determined that the containment vessel will be subjected to a service metal temperature of -18.5 °F. This evaluation postulated that an SSE event occurred in conjunction with -40 °F outside temperature and inadvertent actuation of active containment cooling. Westinghouse Technical Report APP-GW-GLR-005 (TR-9) only describes the analysis, and inadvertently did not include the corresponding service metal temperature.

Since TR-9 does not include the analysis or the service metal temperature, the NRC staff cannot confirm that -18.5 °F is the lowest service metal temperature of the containment vessel shell, which is fabricated from SA-738 Grade B material. This material must meet the requirements of NE-2000 for fracture toughness (Charpy V-notch test) in the as-welded condition for thicknesses up to and including 1.75 inches, and in the post-weld heat treated condition for thicknesses greater than 1.75 inches. The minimum service temperature is used to determine the testing temperature for the Charpy V-notch tests required by ASME Code, Section III, Subsections NE-2300 and NE-4300. Previously, Westinghouse stated in its letter dated April 22, 2003, that the SA-738, Grade B plate material will be procured using the service metal temperature of -15 °F (i.e., -55 °F Charpy V-notch test temperature as required by ASME

Code, Section III, Subsections NE-4335.2(b)(2) and Tables NE-4622.7(b)-1, note (2)(b)(1) in order to account for degradation during welding of the heat affected zone in the base material). In addition, Westinghouse stated in a letter dated March 13, 2003, that the previous analysis added an 8 °F conservative factor to obtain a minimum service metal temperature of -15 °F.

Therefore, the NRC staff requires additional information to verify the minimum service metal temperature. This information includes the details of the analysis (e.g., calculation methodology, assumptions made, similarities/differences from previous analysis, etc.) to confirm that -18.5 °F is the lowest service metal temperature to ensure that the material will be tested to have adequate toughness for the design and environment the containment shell will experience. Also, clarification is needed of whether the conservative factors described in the Westinghouse letter dated March 13, 2003, were also used in this analysis. Otherwise, justification for not including these conservative factors should be included

***Additional Question (*Revision 2)**

The response to RAI-SRP 3.8.2-CIB1-01 Rev. 1 was inadequate because it did not provide the information specifically requested in the last paragraph of the Rev. 1 Additional Question. This includes details of the analysis (e.g., calculation methodology, assumptions made, similarities/differences from previous analysis, etc.) and a discussion of the conservatisms.

Additional Question (Revision 3)

1) Please provide a plot of the containment shell temperature response in cold conditions discussed in the RAI response, similar to Figure E-1 provided in response to RAI-SRP-6.2.1.1-SPCV-07 (e). This plot covers the part of the transient used to establish steady-state initial conditions

2) Is the minimum service metal temperature of -18.5 °F in the AP1000 DCD based on the steady state result or the additional transient scenario discussed in your response to RAI-SRP-6.2.1.1-SPCV-07?

Additional Question: (Revision 4)

DRAFT RAI-SRP3.8.2-CIB1-01, Revision 4, “Containment Min. Metal Service Temperature”

Based on your response (Revision 3) to RAI-SRP3.8.2-CIB1-01, in a letter dated February 17, 2010, the staff has the following supplemental requests for additional information, in order to determine that -18.5°F is the minimum service metal temperature of the steel containment, ensuring that the material will be tested to have adequate toughness for the design and environment the steel containment will experience. Adequate fracture toughness ensures that the material used meets the requirements of GDCs 1, 2 and 16.

1. Your response to RAI-SRP3.8.2-CIB1-01, states that the -30° F external temperature case was used to evaluate the containment shell temperature because wind speed at -30°F is recorded to be faster than at -40°F resulting in a higher velocity through the annulus between the containment and air baffle and therefore greater heat transfer. The NRC staff notes that Westinghouse Document APP-MV50-ZOC-039, Revision 0 used minimum temperatures and corresponding wind speeds from Duluth, Minnesota.

   Since temperatures between -40 °F -30 °F, -20 °F, etc. were not used, and a sensitivity study was not performed to show that other temperatures with a higher associated wind speed would not produce a lower calculated minimum service metal temperature, the minimum service metal temperature calculated in Westinghouse Document APP-MV50-ZOC-039, Revision 0 is not bounding. Therefore, in order to complete our evaluation of this issue, we require that WEC either:

   a. perform a bounding calculation using an outside temperature of -40 °F and a maximum wind speed of 48 mph, used in previous calculations, or provide the following information:

      i. Justify the validity of this Duluth temperature/wind speed data.

      ii. Discuss the maximum wind speed corresponding to the appropriate temperatures.

      iii. Discuss why some other temperature with a greater wind speed would not produce a lower service metal temperature.

      iv. Provide a sensitivity study.

2. In a letter dated February 17, 2010, your response to RAI-SRP3.8.2-CIB1-01 states that the minimum service metal temperature is -0.61° F. Discuss why the minimum service metal temperature of -0.61° F occurs during the start of the steady state run and not at the transient for the inadvertent activation of the fan coolers.

3. Discuss why loss of AC (LOAC) transient runs specified in your RAI response to RAI TR09-008, Revision 4 were performed using an external temperature of -40° F, but an external temperature of -30° F has the lower service metal temperature based on your response to RAI-SRP3.8.2-CIB1-01 and Westinghouse Document APP-MV50-ZOC-039, Revision 0.

4. Westinghouse Document APP-MV50-ZOC-039, Revision 0 states that the minimum service metal temperature is calculated at TC230 level. Confirm that this location is near the bottom of the air baffle plate, and provide the elevation as shown in Figure 3.8.4-1 of the DCD.

5. Since this is a new analysis (Westinghouse Document APP-MV50-ZOC-039, Revision 0), discuss which parts of your responses (Revisions 0, 1 and 2) to RAI-SRP3.8.2-CIB1-01 are still valid and applicable. For areas that are no longer valid, please provide an update to these areas, such as conservatisms used for WGOTHIC versus previous calculations, etc.

Additional Question: (Revision 5)

The NRC staff notes that in a letter dated May 10, 2010, Westinghouse's provided a response to RAI-SRP3.8.2-CIB1-01, Revision 4, which provided a bounding calculation using -40°F, and wind speed of 48 mph, in lieu of justifying the current data in Document APP-MV50-ZOC-039, Revision 0. However, Westinghouse did not revise Document APP-MV50-ZOC-039, Revision 0, to reflect this bounding calculation, and assumes that the results depicted in Document APP-MV50-ZOC-039, Revision 0, are the result of record for the AP1000 DCD. The NRC staff requests that Westinghouse revise Document APP-MV50-ZOC-039, Revision 0, to reference this bounding calculation, since the bounding case was provided in lieu of justifying the current data in APP-MV50-ZOC-039, Revision 0.

Westinghouse Response: (Revision 0)

An evaluation of AP1000 containment vessel, in the vicinity of large penetrations, was performed by Westinghouse to meet the requirements of COL Information Item 3.8-1. During this evaluation an additional scenario was postulated for the containment vessel shell analysis. The AP1000 plant is designed for sites that can have cold weather conditions with a minimum atmospheric temperature of -40 °F. Therefore, an SSE event was postulated to occur in conjunction with extreme cold weather condition (-40 °F outside temperature) and inadvertent actuation of active containment cooling. The analyses results were documented in an AP1000 calculation. The analyses determined that during this event, the containment vessel will be subjected to an external pressure of 0.9 psid and a 'Service Metal Temperature' of -18.5 °F.

Westinghouse Technical Report APP-GW-GLR-005 submitted to the NRC described these analyses in subsection 2.4.1 of the report. Also, in Table 3.8.2-1 'Load Combinations', at the end of the report, a reference was added for this event. This Table showed the external pressure of 0.9 psid, but inadvertently did not include the corresponding 'Service Metal Temperature' of -18.5 °F.

This change will be incorporated in the next revision of the DCD.

Additional Response (Revision 1):

The Revision 0 change indicated was made in DCD Rev 17.

The additional information required to verify the minimum service metal temperature is provided in Westinghouse document APP-MV50-Z0C-020. Rev 0. This document is made available for review in the Twinbrook office, and provides support for the Lowest Service Metal Temperature of -18.5 °F, corresponding to -40 degree F outside temperature.

Additional Response (Revision 2)

The original calculation supporting a minimum shell temperature of -15 °F represented a simple radial heat balance. The model is shown below:

q" = h-in * (Tcont – Twall-in) (1)

q" = k/x * (Twall-in – Twall-out) (2)

q" = h-out * (Twall-out – Tamb) (3)

where	q"	is the average heat flux through the shell wall
	h-in	is the average heat transfer coefficient between the containment atmosphere and the inside wall of the shell
	Tcont	is the average containment atmosphere temperature
	Twall-in	is the average temperature of the shell inside surface
	Twall-out	is the average temperature of the shell outside surface
	k	is the steel shell thermal conductivity
	x	is the thickness of the steel shell
	h-out	is the average heat transfer coefficient between the outside surface of the containment shell and the air in the annulus
and	Tamb	is the average temperature of the air in the annulus

For this calculation, the following values were used:

h-in =	1.0 Btu/hr/ft^2/°F	based on free convection
Tcont =	50 °F	lower containment limit
k =	30 Btu/hr/ft/°F	carbon steel thermal conductivity
x =	1.75 in	containment average thickness
h-out =	2.6 Btu/hr/ft^2/°F	based on mixed forced/free convection (Ref. 1)

Solving equations 1-3 simultaneously,

Twall-in = -14.7 °F

Twall-out = -15.1 °F

This is the basis for the -15 °F shell temperature reported previously.

For the more detailed calculation, the WGOTHIC computer code was used. The correlations used to calculate the heat transfer coefficients on the shell surfaces were slightly different than those used in the simplified model. Essentially, the free/forced convection model used on the outside surface resulted in a slightly higher heat transfer coefficient which, in turn, resulted in a lower shell temperature. WGOTHIC calculates a heat transfer coefficient of

h-out = 3.18 Btu/hr/ft^2/F

The radial heat balance performed by WGOTHIC results in an average outside shell temperature of -18 °F

References:

1. Holman, J.P., *Heat Transfer*, 4th Ed, McGraw-Hill, 1976.

The conservatisms used for the WGOTHIC calculation are those inherent in the WGOTHIC code and not necessarily those in the March 13, 2003 letter. The conservative factors described in the Westinghouse letter dated March 13, 2003 apply to the manual calculation method and do not apply to the method using WGOTHIC.

Additional Response (Revision 3)

1. There is one transient type that challenges the minimum service metal temperature requirement of -18.5 F. These transients are an inadvertent actuation of the active containment cooling system (VCS). These transients are discussed in depth in RAI-TR09-008. Figure 1 depicts the inadvertent fan cooler operation case at the minimum safety analysis temperature of -40°F, and an additional case at -30 °F. The WGOTHIC computer code was used to analyze these transients. Figure1 shows the minimum service metal temperature for the inadvertent fan cooler case. The transient was completely contained in one case. The case was allowed to equilibrate for 35000s before transient initiation. Operator action is assumed to occur within 60 minutes to shut off the fan coolers and return the transient to normal conditions. Figure 2 depicts the inadvertent fan cooler case at -30°F. This case is evaluated for containment shell temperature because wind speed at -30°F ambient condition is recorded to be faster than at -40°F resulting in a higher velocity through the annulus between the containment and air baffle

and therefore greater heat transfer. The increased heat transfer results in a lower shell temperature. For Figures 1 and 2 the minimum service metal temperature is 7.18°F for the -40°F case and -0.61°F for the -30°F case. The transient cases along with the entire spectrum of analyses considering the external pressure and minimum service metal temperature can be found in APP-MV50-Z0C-039 Rev. 0.

Figure 1: Inadvertent Fan Cooler Case at T = -40 F

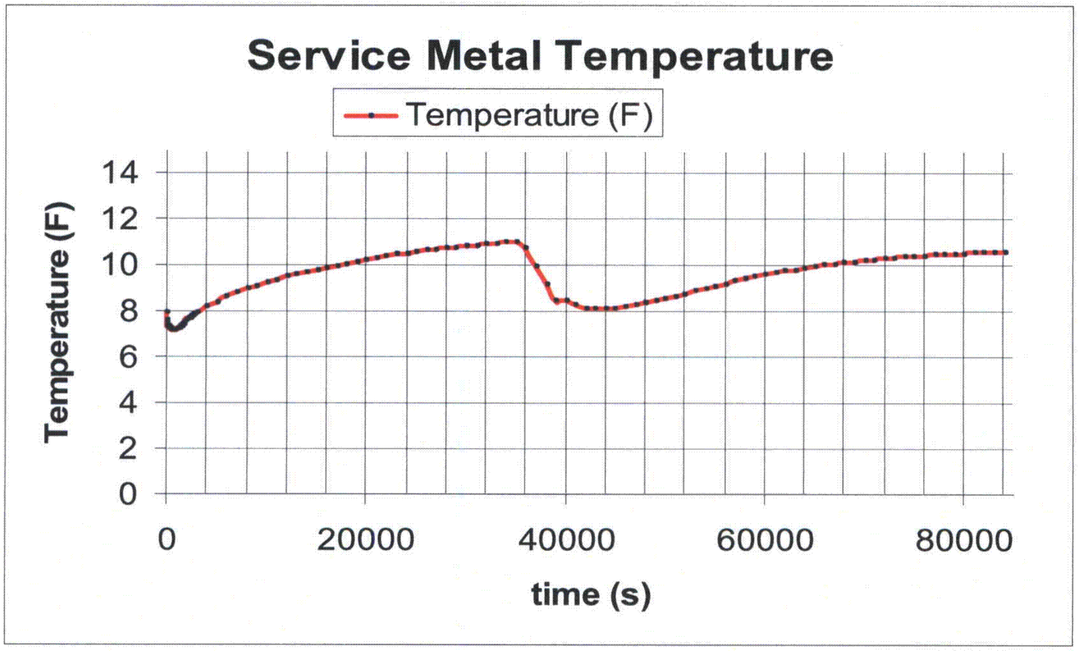

Figure 2: Inadvertent Fan Cooler Case at T= -30 F

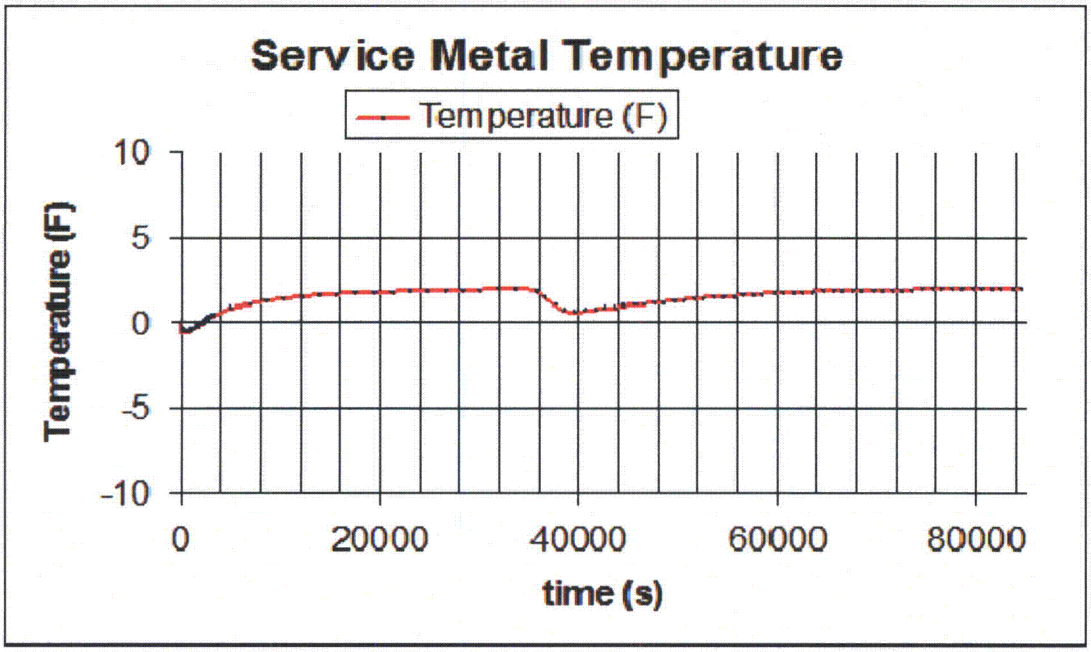

Additional Response (Revision 4)

1. To facilitate the staff's closure of this RAI, a bounding case was analyzed to provide an indication of the margin to acceptance criteria associated with the minimum allowable service metal temperature for the AP1000 Containment Vessel. From APP-MV50-Z0C-039 Rev. 0, the LOAC transient (Case 11) at -40°F yielded the lowest service metal temperature of 7.32 °F (Note this was the lowest service metal temperature for the -40 °F transients). For this reason, Case 11 was used as a representative transient to develop a bounding scenario to demonstrate the associated margin to acceptance criteria.

   The wind speed for Case 11 was adjusted to achieve 25 ft/s, which corresponds to a 48 mph outside wind speed. The outlet pressure of Boundary Condition (BC) 1 of the Case 11 WGOTHIC base deck was changed to 14.37 psia, to adjust the ΔP magnitude to achieve the 25 ft/s riser velocity. The heat transfer coefficient was recalculated according to the increased velocity in the riser region, and is depicted in Table 1 along with the associated thermophysical properties of air at -40 °F. The HTC was calculated according to the same methodology (application of Dittus-Boelter for turbulent flow in a fluid channel) contained in APP-MV50-Z0C-039 Rev. 0. Figure 3 shows the containment pressure response. It is slightly greater in magnitude (~0.25 psid) than that depicted for Case 11 from APP-SSAR-GSC-039 Rev. 0, but is still within the -0.9 psid constraint.

The associated containment temperature reduction is displayed in Figure 4. Figure 5 displays the velocity in the containment riser region to confirm that the riser velocity was adequately accounted for in the analysis (the actual riser velocity from the raw data was 24.90 ft/s). Note the slight anomaly in the velocity trend. This slight decrease (~0.05 ft/s) is due to the temperature reduction in containment resulting from the LOAC transient. This reduction in temperature actually slows the flow down slightly due to the free convection component of the velocity. This reduction is insignificant to the analysis results and is only explained to facilitate the understanding of the results. The observed minimum service metal temperatures will be discussed and conveyed as a part of the answer to Item 4 of this RAI. For the bounding sensitivity performed to answer this RAI the containment response is still within the service limits depicted in DCD Table 3.8.2-1.

Table 1: HTC for LOAC Transient at -40 F and 25 ft/s.

Dh (ft)	Density (lbm/ft^3)	Kinematic Viscosity (ft^2/s)	Thermal Conductivity (Btu/hr-ft-F)	Thermal Diffusivity(ft^2/s)	Reynolds Number	Prandtl Number	Nussult Number (Dittus-Boelter)	HTC (BTU/hr-ft^2-F)
2	0.1239402	0.000127742	0.012991811	1.915018E-04	391412.8	0.667056	582.7747	4.732062

† *The positive 25% uncertainty associated with application of Dittus-Boelter was applied to the calculated value of the HTC to conservatively bound the minimum service metal temperature reported in Revision 4 of this RAI.*

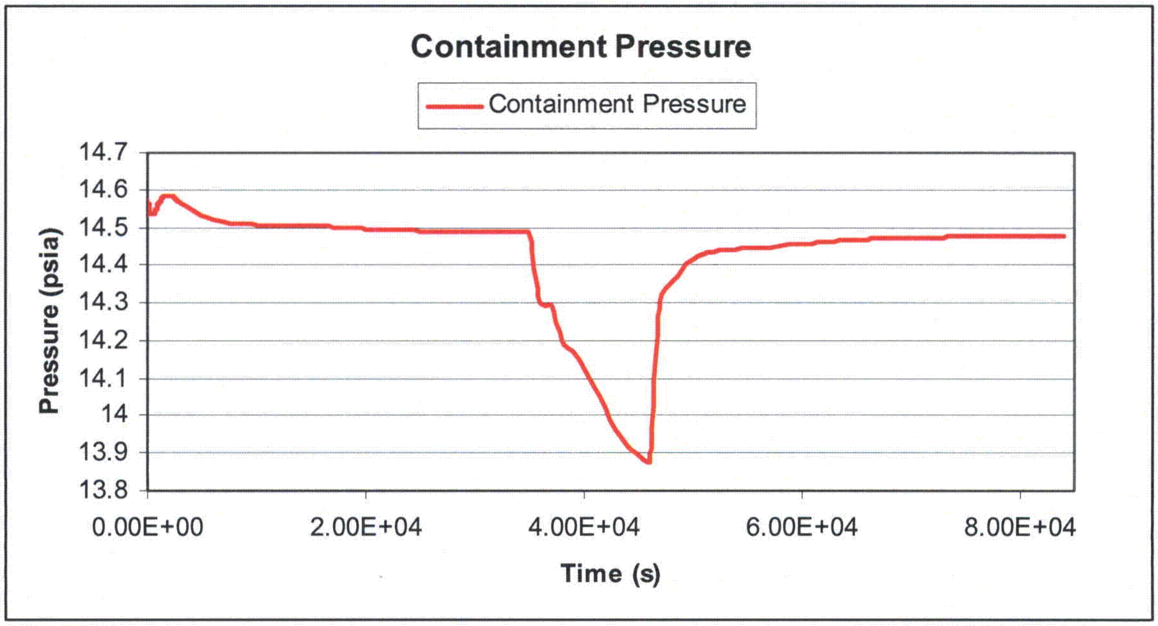

Figure 3: Containment Pressure for LOAC transient at -40 F and 25 ft/s.

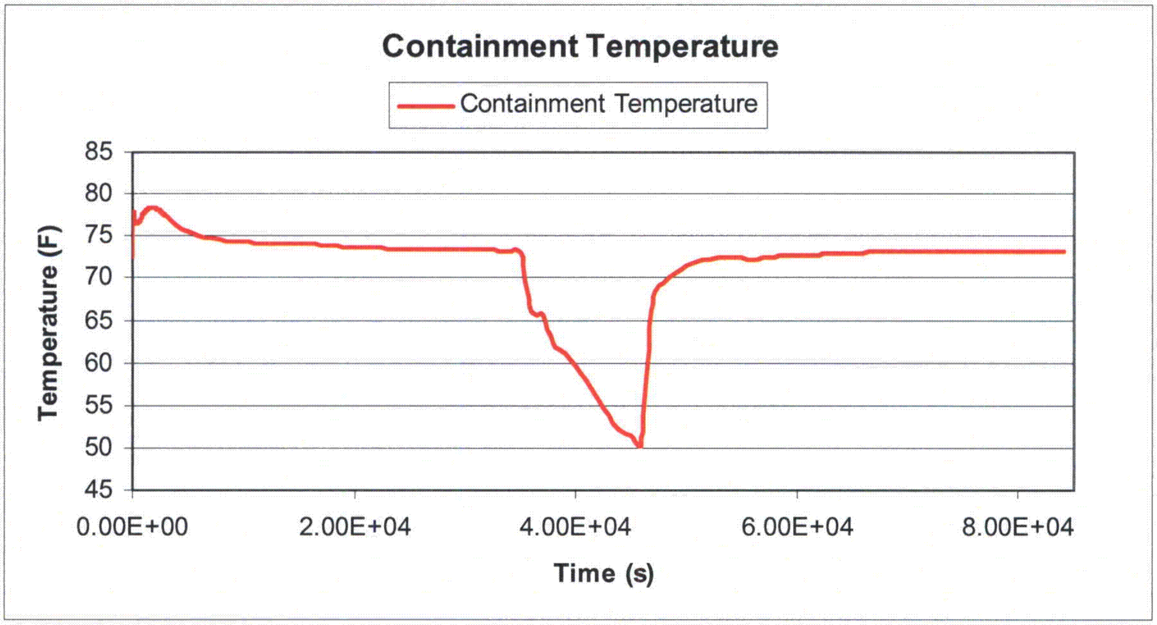

Figure 4: Containment Temperature for LOAC transient at -40 F and 25 ft/s.

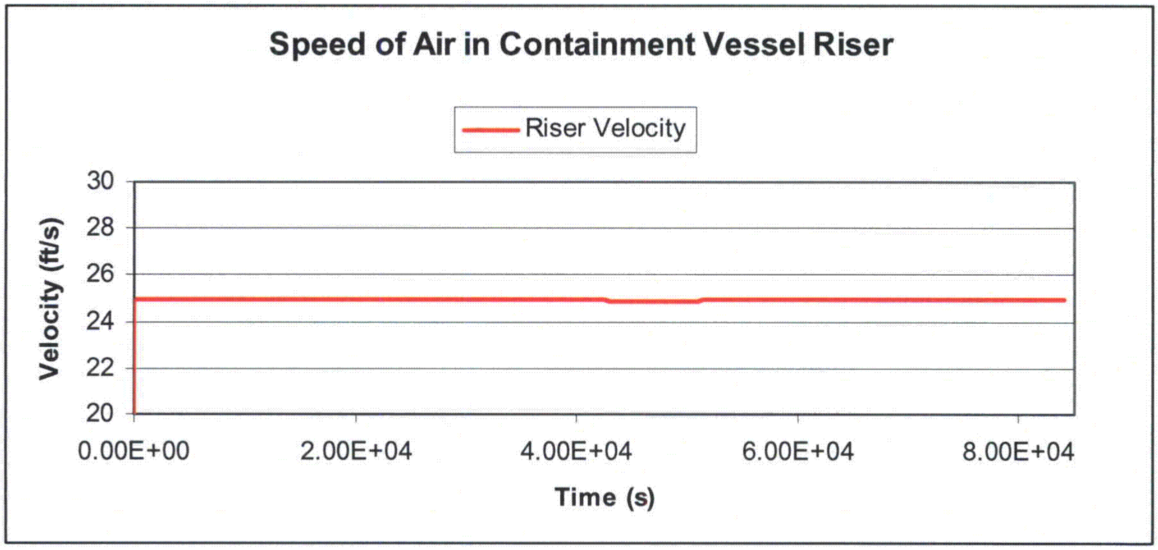

Figure 5: Containment Riser Velocity for LOAC transient at -40 F and 25 ft/s.

2. During performance of APP-MV50-Z0C-039 Rev. 0, it was necessary to run several iterations of each case to dial in the initial conditions accordingly, so that equilibrium conditions could be adequately demonstrated prior to transient initiation. The initial conditions for TC230 were set slightly lower than the equilibrium value, which resulted in the minimum service metal temperature occurring at the beginning of the transient. This inconsistency will be corrected as part of item 5 of this response.

3. The staff had asked for various types of transients to be performed. The inadvertent fan cooler cases were performed to develop meaningful relationships between the source terms of the analysis (humidity, internal temperature, external temperature, wind speed…etc.). Once the relationship of the various source terms was identified, the inadvertent PCS and LOAC cases were strategically chosen to minimize the amount of additional runs required to complete the analysis. While it is quite possible the -30 °F LOAC case could have resulted in a lower service metal temperature, it was Westinghouse's decision to perform the -40 °F LOAC case, because we believed that to be the case for which the staff would be most interested in viewing the results. Additionally, the difference between the -40 °F and -30 °F fan cooler cases was (8.45 °F-0.67 °F) = 7.78 °F. Applying this delta to the -40 °F LOAC case to determine a predicted -30 °F LOAC case would result in (7.32 °F – 7.78 °F) = -0.46 °F, which is less than 1 °F lower. However, it does not in any,way challenge the allowable minimum service metal temperature of -18.5 °F.

4. From the WGOTHIC model, TC230 spans control volume (CV) 49 from the 135.25' elevation to the 153.0' elevation. From Figure 6, below it is seen that the 135.25

elevation is below the bottom of the air baffle plate, and the upper elevation of 153.0' is above the air baffle plate, so TC230 spans the region just above the external stiffener to above the bottom of the air baffle plate which is at the 142.0' elevation.

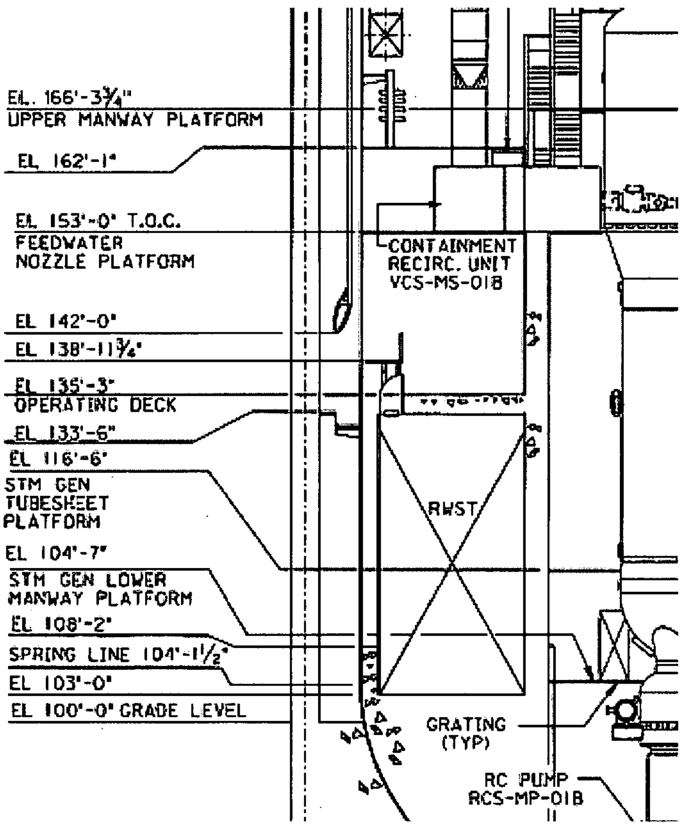

Figure 6: Elevation of Air Baffle and External Stiffener in relation to TC230 span

Figure 7 reports the service metal temperatures for TC230 and TC229. TC229 is included to show that the temperature distribution is fairly uniform from the 135.25' elevation to the 170.0' elevation (top of TC229). This makes sense, as due to the velocity of 25 ft/s a particle of air traveling within the uniform velocity streamline in the constant velocity riser region would only take approximately 34.25ft/(25ft/s) = 1.39 seconds to transport above the top elevation of TC229. Analysis of the raw data shows that the maximum temperature difference between TC229 and TC230 is just less than 1.3 °F for the duration of the transient. Application of this temperature difference to the raw data as an uncertainty in the temperature reported for TC230, would yield a minimum service metal temperature of -15.78 °F + -1.13 °F = -16.91 °F. This is still greater than the DCD minimum required service metal temperature of -18.5 °F.

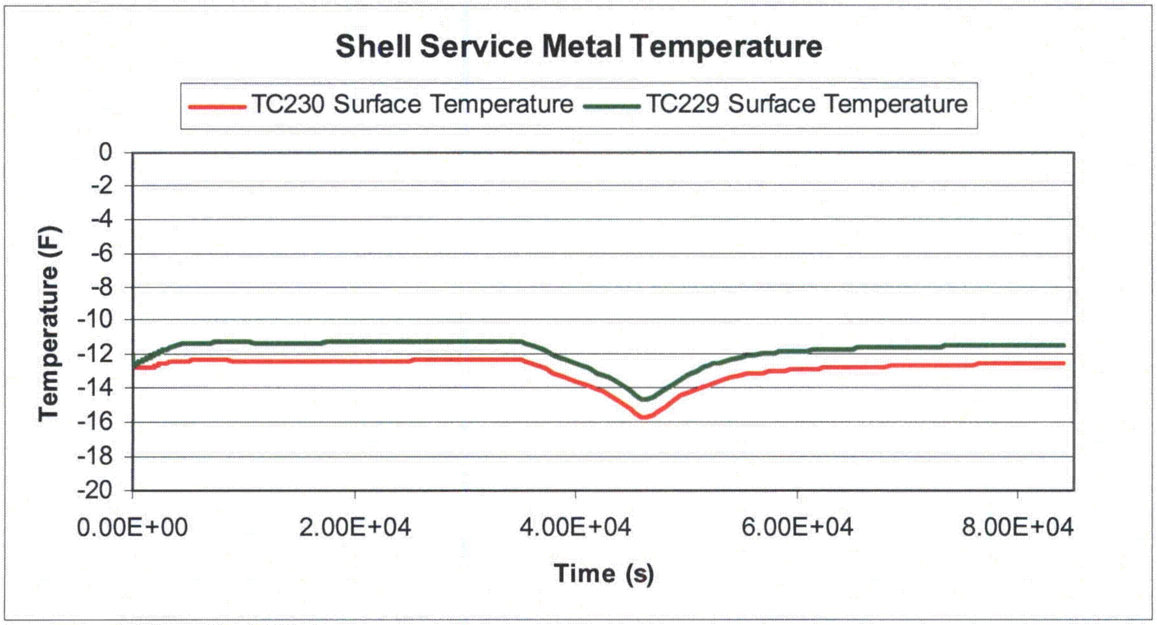

Figure 7: Containment Shell minimum service metal temperature for LOAC transient at -40 F and 25 ft/s.

5. The response to item 5 will assume that the results depicted in APP-MV50-Z0C-039 Rev. 0 are the results of record, to satisfy the service limits specified in Chapter 3 of the AP1000 DCD Rev. 17. The results depicted in Item 1 through 4 were strictly conveyed to demonstrate the margin to acceptance criteria, to facilitate the staff's review and acceptance of this RAI and of the adequacy of the CV design.

Revision 0:

Revision 0 of this RAI is still applicable with regards to the bounding limits (-0.9 psid and -18.5 °F) previously transmitted. However, please note that the analysis to determine this now comes from APP-MV50-Z0C-039 Rev. 0. The referenced calculation was performed to ensure that the CV service limits were bounded for a wide spectrum of transient initial and faulted conditions. This was accomplished by analyzing three different types of transients:

i. Inadvertent Actuation of the VCS (Fan Coolers)
ii. LOAC
iii. Inadvertent PCS

The results of the spectrum of transients performed can be found in APP-MV50-Z0C-039 Rev. 0. The results of the transients do not exceed the structural design limits bounded by the conditions associated with the -0.9 psid and the -18.5 °F transient results conveyed in Rev. 0 of this response.

Revision 1:

Below includes the applicable changes to Revision 1 of this response.

The Revision 0 change indicated was made in DCD Rev 17.

The additional information required to verify the minimum service metal temperature is provided in Westinghouse document APP-MV50-Z0C-039, Rev 0. This document is available for review in the Twinbrook office, and provides support for the bounding Lowest Service Metal Temperature of -18.5 °F, corresponding to -40 degree °F outside temperature.

Revision 2:

The calculation of the HTC from Revision 2 is no longer viable, and is superseded by the Dittus-Boelter correlation applied in APP-MV50-Z0C-039 Rev. 0. The Dittus-Boelter correlation was chosen because it yielded the greatest HTC for a given velocity of air in the containment riser region. For ease of review, the excerpt from the above mentioned calculation conveying the Dittus-Boelter application is displayed below in Figure 8.

Calculation of the HTC's for the WGOTHIC model shell and baffle thermal conductors in the constant velocity region were developed through implementation of the Dittus-Boelter correlation. For the 8.0 ft/s cases the following example calculation displays the application of Dittus-Boelter to the containment annulus region:

D_h = hydraulic diameter of square channel. From Reference 16 the hydraulic diameter of a channel D_h = 2h where h is the channel width. For the riser region the width of the channel is 1ft. so D_h = 2 ft.

$$\mathrm{Re}_D = \frac{V \times D}{\nu}$$

For air at -40°F
Where V = fluid velocity = 8.0ft/s
D = Characteristic Length or Hydraulic Diameter = 2 ft
ν = kinematic viscosity = 0.00012774 ft²/s

$$\mathrm{Re}_D = \frac{8.0 ft/s \times 2 ft}{0.00012774 ft^2/s} = 125{,}252$$

$\mathrm{Pr} = \nu / \alpha$ where α is the thermal diffusivity of air = 0.000192ft²/s, and υ is previously defined as the kinematic viscosity.

$$\mathrm{Pr} = \frac{0.00012774 ft^2/s}{0.0001915 ft^2/s} = 0.67$$

$$Nu_D = 0.023 \times 125252^{4/5} \times 0.67^{0.4} = 234.6$$

$$h = \frac{Nu \times k}{D_h} = \frac{234.6 \times 0.012991811 (BTU/hr - ft^2 - F)}{2 ft} = 1.52 BTU/hr - ft^2 - F$$

Figure 8: Application of the Dittus-Boelter Correlation for use with WGOTHIC

Further demonstration of the conservatism associated with this calculation of the HTC can be conveyed, by comparing the value of the HTC in Rev. 4, Table 1 of this response with that calculated in Revision 2 of this response. For clarification, a higher HTC will result in a lower calculated service metal temperature.

Revision 3:

Revision 3 should be superseded by the response to Item 4 of Revision 4 of this RAI. The sensitivity performed for Revision 4 of this RAI bounds all scenarios depicted in APP-MV50-Z0C-039 Rev. 0.

It is pertinent at this time to discuss the differences in the performance of APP-MV50-Z0C-039 Rev. 0 as compared to that of APP-MV50-Z0C-020 Rev. 0:

Since no LOAC transients were performed for APP-MV50-Z0C-020 Rev. 0, the discussion will be fairly limited to the comparison of the inadvertent fan cooler cases. However, one major difference in the analyses was that APP-MV50-Z0C-039 Rev. 0 assumed an 8.0 ft/s riser velocity for the -40 °F cases. The use of 8.0 ft/s corresponded to the actual meteorological data taken in Duluth, MN over a 44 year period, for the maximum external wind speeds associated with an external temperature of -40 °F. APP-MV50-Z0C-020 Rev. 0 used the fastest wind speed observed at cold temperatures (-25 °F) to bound all transients. This was not representative of the meteorological data, but was used to bound all conditions.

For the fan cooler cases there were three main differences in the analysis methodology:

1. APP-MV50-Z0C-020 Rev. 0 ramped the fan cooler performance curves from 32 °F, and APP-MV50-Z0C-039 Rev. 0 ramped from 40 °F. The minimum chilled water temperature is 40 °F (APP-VWS-M3-001 Rev. C). Evaluating the fan cooler performance curves from 32 °F is conservative as it allows for greater heat removal at lower temperatures, increasing the calculated ΔT and thus increasing the calculated external pressure.

2. As mentioned previously, APP-MV50-Z0C-039 Rev. 0 used the Dittus-Boelter correlation coupled with a 25% bias to conservatively calculate the HTC. This minimized the minimum service metal temperature and associated external pressure.

3. APP-MV50-Z0C-039 Rev. 0 performed the transient in one case. APP-MV50-Z0C-020 Rev. 0 performed the transient in two cases. One case was performed to establish the initial conditions, and one to depict the associated transient. WGOTHIC is very sensitive to initial conditions, as demonstrated in the plots for Revision 4 of this RAI. The initial conditions must be specified with a low degree of uncertainty and with a steady state condition, to avoid coupling equilibration and transient effects. Allowing the containment to equilibrate for an adequate length of time (~35000 seconds), the transient effects on containment response were more accurately depicted. Additionally, the distributed parameter WGOTHIC model used for these analyses contains approximately 126 volumes, 313 flow paths, and 270 thermal conductors. The task of setting the initial conditions for these parameters with a low degree of uncertainty given the complexity of the model would be extremely difficult. Performance of the transients into one case removes any possible errors associated with incorrectly setting the initial conditions, and provides a true containment response to the transients. This change in methodology is believed to have the greatest impact on the differences in the results depicted in the two calculations.

Additional Response (Revision 5)

1. Westinghouse will revise APP-MV50-Z0C-039 Rev. 0 to incorporate the bounding case presented in Revision 4 of this response.

Design Control Document (DCD) Revision: (Revision 0)

None

PRA Revision:
None

Technical Report (TR) Revision: (Revision 0)

Technical Report APP-GW-GLR-005 (TR 9) will be revised as follows:

Note 6 will be added in Table 3.8.2-1 and will read:

> The 'Lowest Service Metal Temperature' corresponding to -40 degree F outside temperature is -18.5 degree F.